

NASA Technical Memorandum 78308

**Skylab Orbital Lifetime
Prediction and Decay Analysis**

**P. E. Dreher, R. P. Little,
and G. Wittenstein**
*George C. Marshall Space Flight Center
Marshall Space Flight Center, Alabama*



**National Aeronautics
and Space Administration**

**Scientific and Technical
Information Branch**

1980

SKYLAB ORBITAL LIFETIME PREDICTION AND DECAY ANALYSIS

Table of Contents

| | <u>Page</u> |
|-------------------------------------------------------|-------------|
| LIST OF TABLES | iv |
| LIST OF FIGURES | v |
| INTRODUCTION | ix |
| 1. PREFLIGHT LIFETIME PREDICTIONS | 1-1 |
| 1.1 DENSITY MODEL | 1-1 |
| 1.2 AERODYNAMICS | 1-4 |
| 1.3 SOLAR ACTIVITY PREDICTIONS | 1-8 |
| 1.4 PREFLIGHT LIFETIME PREDICTIONS | 1-10 |
| 2. ORBITAL DECAY DURING THE MANNED MISSION | 2-1 |
| 3. ORBITAL DECAY DURING THE PASSIVE PERIOD | 3-1 |
| 4. ORBITAL DECAY DURING THE REACTIVATED SKYLAB PERIOD | 4-1 |
| 4.1 ORBITAL DECAY DURING THE EOVV PERIOD | 4-3 |
| 4.2 ORBITAL DECAY DURING THE SI PERIOD | 4-20 |
| 4.3 ORBITAL DECAY DURING THE TEA PERIOD | 4-35 |
| 5. SKYLAB REENTRY | 5-1 |
| 5.1 DRAG MODULATION TO CONTROL REENTRY | 5-1 |
| 5.1.1 PROCEDURES | 5-1 |
| 5.1.2 RESULTS | 5-4 |
| 5.2 POSTFLIGHT ANALYSIS | 5-8 |
| 5.2.1 RECONSTRUCTION PROCEDURES | 5-8 |
| 5.2.2 RECONSTRUCTION ANALYSIS | 5-9 |
| 5.3 IMPACT FOOTPRINT ANALYSIS | 5-14 |
| 6. SUMMARY AND CONCLUSIONS | 6-1 |
| ACRONYMS | 7-1 |
| REFERENCES | 8-1 |

SKYLAB ORBITAL LIFETIME PREDICTION AND DECAY ANALYSIS

List of Tables

| <u>TABLE</u> | <u>TITLE</u> | <u>PAGE</u> |
|--------------|---------------------------------------------------------------------------------------------------------------|-------------|
| 1.4-1 | Mission Description for Cluster Configuration - Mode A | 1-11 |
| 1.4-2 | Mission Description for Cluster Configuration - Modes B, B ₁ , B ₂ , and B ₃ | 1-12 |
| 1.4-3 | Mission Description for Cluster Configuration and Lifetime Prediction | 1-21 |
| 3-1 | Skylab Lifetime (Impact) Predictions During the Passive Period | 3-2 |
| 4.1-1 | Attitude History During Low Drag Period | 4-4 |
| 4.1-2 | Lifetime Predictions While in EOVV | 4-5 |
| 4.2-1 | Predicted Impact Dates for Constant BC | 4-24 |
| 4.2-2 | Predicted Impact Dates for SI and TEA Attitudes | 4-25 |
| 4.3-1 | Predicted Impact Dates Using SI, 121P and Tumble BC | 4-41 |
| 5-1 | Impact Predictions for July 11, 1979 | 5-5 |

SKYLAB ORBITAL LIFETIME PREDICTION AND DECAY ANALYSIS

List of Figures

| <u>FIGURE</u> | <u>TITLE</u> | <u>PAGE</u> |
|---------------|-----------------------------------------------------------------------------------------------|-------------|
| 1-1 | Orbit Lifetime Predictions Procedure | 1-2 |
| 1.2-1 | Preflight Skylab Mass History | 1-5 |
| 1.2-2 | Skylab Configuration with the Solar Arrays Extended | 1-6 |
| 1.2-3 | Final Preflight Aerodynamic Data | 1-7 |
| 1.3-1 | Predicted Solar Activity | 1-9 |
| 1.4-1 | Cluster Lifetime Versus Launch Date for Discrete Altitudes - Referenced to Launch of Workshop | 1-14 |
| 1.4-2 | Lifetime Vs. Altitude for Mode A | 1-16 |
| 1.4-3 | Lifetime Vs. Altitude for Mode B | 1-16 |
| 1.4-4 | Orbital Decay for 230 NMI Circular Orbit Launch Date January 1, 1970, Cluster Mission Mode B | 1-17 |
| 1.4-5 | Orbital Decay for 230 NMI Circular Orbit Launch Date July 1, 1970, Cluster Mission Mode B | 1-18 |
| 1.4-6 | Nominal and $\pm 2\sigma$ Lifetimes for Various Elliptic Orbits Cluster Mission Mode B | 1-19 |
| 2-1 | Drag Coefficient Vs. Roll Angle | 2-4 |
| 2-2 | Actual and Predicted Solar Flux During the Manned Period | 2-5 |
| 2-3 | Solar Flux Comparison | 2-6 |
| 2-4 | Skylab Altitude History During the Manned Period | 2-7 |
| 2-5 | Skylab Actual and Predicted Decay Comparison | 2-8 |
| 3-1 | Skylab Lifetime Predictions During Passive Period | 3-7 |
| 3-2 | Actual and Predicted Decay Comparison | 3-8 |

| <u>FIGURE</u> | <u>TITLE</u> | <u>PAGE</u> |
|---------------|----------------------------------------------------------------------|-------------|
| 3-3 | Actual and Predicted Solar Flux | 3-9 |
| 3-4 | Actual and Predicted Solar Flux | 3-10 |
| 3-5 | Actual Solar Activity Data | 3-11 |
| 3-6 | Skylab Actual and Predicted Decay Comparison | 3-12 |
| 3-7 | Predicted and Actual Decay | 3-13 |
| 3-8 | Predicted and Actual Decay Rates | 3-14 |
| 3-9 | In Orbit Aerodynamic Data | 3-15 |
| 3-10 | Roll Moment Coefficient Vs. Roll Angle | 3-16 |
| 3-11 | Atmospheric Density During the Passive Period | 3-17 |
| 4.1-1 | Skylab Orbital Decay from Launch to Impact | 4-6 |
| 4.1-2 | Comparison of Predicted and Actual Solar Flux | 4-7 |
| 4.1-3 | Actual Solar Activity Data | 4-8 |
| 4.1-4 | EOVV Decay Comparison for Averaged Ballistic Coefficient | 4-9 |
| 4.1-5 | Beta Angle During the EOVV Period (June 9, 1978 to January 25, 1979) | 4-11 |
| 4.1-6 | Ballistic Coefficient from June 9, 1978 to January 25, 1979 | 4-12 |
| 4.1-7 | EOVV Decay Comparison | 4-13 |
| 4.1-8 | Solar Activity - Actual and Predicted | 4-14 |
| 4.1-9 | EOVV Decay Comparison Using Theoretical BC | 4-15 |
| 4.1-10 | EOVV Predicted and Actual Decay Rates Using Theoretical BC | 4-16 |
| 4.1-11 | Predicted and Actual Decay Rates During EOVV Using Theoretical BC | 4-17 |

| <u>FIGURE</u> | <u>TITLE</u> | <u>PAGE</u> |
|---------------|------------------------------------------------------------------------------------------|-------------|
| 4.1-12 | Ratio of Actual to Predicted (No Bias) Decay Rate During EOVV Using Theoretical BC | 4-18 |
| 4.1-13 | Ratio of Actual to Predicted (6% Bias) Decay Rate During EOVV Using Theoretical BC | 4-19 |
| 4.2-1 | Beta Angle Vs. Date | 4-21 |
| 4.2-2 | Ballistic Coefficient Vs. Date During SI Attitude | 4-22 |
| 4.2-3 | Decay Comparisons During SI Attitude | 4-26 |
| 4.2-4 | Predicted and Actual Decay Rates During SI Attitude | 4-27 |
| 4.2-5 | Ratio of Actual to Predicted (18% Bias) Decay Rate | 4-28 |
| 4.2-6 | Actual Solar Activity Data | 4-30 |
| 4.2-7 | Decay Comparison During SI Attitude | 4-31 |
| 4.2-8 | Predicted and Actual Decay Rates During SI Attitude | 4-32 |
| 4.2-9 | Ratio of Actual to Predicted (6% Bias) Decay Rate | 4-33 |
| 4.2-10 | Solar Activity Data | 4-34 |
| 4.3-1 | Constraints for TEA Attitude | 4-37 |
| 4.3-2 | Tl21 Ballistic Coefficient Vs. Date | 4-38 |
| 4.3-3 | Predicted and Actual Decay | 4-39 |
| 4.3-4 | Predicted and Actual Decay | 4-40 |
| 5-1 | Transition Aerodynamics | 5-3 |
| 5-2 | Population Hazard (And Predicted Longitude of Ascending Nodes) | 5-6 |
| 5-3 | Map of Real Time Results of Impact Prediction | 5-7 |

| <u>FIGURE</u> | <u>TITLE</u> | <u>PAGE</u> |
|---------------|-------------------------------------------------|-------------|
| 5-4 | Drag/Attitude Timeline | 5-10 |
| 5-5 | Map of Postflight Results Reconstructed Impacts | 5-11 |
| 5-6 | Reconstructed Altitude Profile | 5-13 |
| 5-7 | Map of Footprint | 5-15 |
| 5-8 | Detailed Map of Footprint | 5-16 |

SKYLAB ORBITAL LIFETIME PREDICTION AND DECAY ANALYSIS

INTRODUCTION

This report partially summarizes chronologically the events and decisions that affected Skylab's orbital decay and lifetime predictions. It was written to satisfy a number of objectives but primarily to provide a complete record of Skylab's orbital lifetime predictions, its actual decay, and analysis thereof. Since the objectives and activities regarding lifetime were different for various stages of the Skylab mission, it was convenient to discuss the lifetime for five periods (preflight, manned, passive, reactivated, and reentry).

Skylab was launched on May 14, 1973, at 17:30 GMT and reentered the earth's atmosphere on July 11, 1979, at 16:37 GMT. While Skylab was in orbit, it was visited by three different astronaut crews; and at the end of the last visit, Skylab was left in a passive mode. On March 6, 1978, the Skylab reactivation began. Skylab was brought under active control in June, 1978, and remained in that status (except for a two-week period) until approximately 12 hours prior to reentry. On July 11 at 7:45 GMT, Skylab was commanded to maneuver to a tumble attitude, at which time active control of Skylab ended. This action was taken in order to shift the most probable Skylab impact footprint away from the east coast of the United States and Canada.

During the preflight and other phases of the Skylab orbital life, a great deal of data was generated and knowledge gained on orbital decay. Also, considerable capability and experience in lifetime prediction was accumulated. This capability will greatly benefit future missions. The actual procedures and related activities that went into predicting the Skylab orbital decay, impact time, and reentry point are contained in this report.

1. PREFLIGHT LIFETIME PREDICTIONS (PRIOR TO MAY 1973)

Discussion of the preflight period was included to provide an understanding of the design decisions made in the early mission planning that affected the Skylab lifetime. Some discussion of the technical aspects of lifetime prediction and techniques are also included. Since numerous design iterations were made for Skylab, this section provides an appreciation of the sensitivity of a satellite's orbital lifetime to various parameters.

A vast amount of orbital lifetime data was generated during the mission planning phase of Skylab. The parameters influencing orbital lifetime which varied the most were launch date, predicted $F_{10.7}$, initial altitude, size of the workshop solar array, weight, orbital array orientation, and mode of operation (schedule of events). Aerodynamic characteristics also varied since they were dependent on other parameters which changed.

Preflight lifetime predictions are based on several key factors (See Figure 1-1): A sound mathematical formulation of the decay of the semimajor axis, a description of the atmospheric density, a description of how the variation in solar activity affects this density, a prediction of the variation in solar activities, and the physical characteristics of the satellite; i.e., its aerodynamic characteristics. Each of these factors are then modeled in a computer program (Reference 1 and 2), developed at and for the Marshall Space Flight Center, called Orbital Lifetime Program (LTIME). The following paragraphs will describe these models, as well as summarize the preflight lifetime predictions.

1.1 DENSITY MODEL

Prior to 1970, the density model used in LTIME was a "Special" 1962 U. S. Standard Atmosphere. The 1962 U. S. Standard Atmosphere is a static model compiled by the United States Committee on Extension to the Standard Atmosphere (Reference 3). This model provided density as a function of altitude. The "Special" atmosphere used the density tables from the static model but modified the density to correct for solar activity and diurnal effects.

The diurnal effect is the day to night variation in nearly all atmospheric parameters that is caused by the rotation of the earth. A slight bulge in the daylight portion of the atmosphere is caused by atmospheric heating. The center of the bulge follows the sun, lagging by two hours. The maximum density occurs at the center of the bulge.

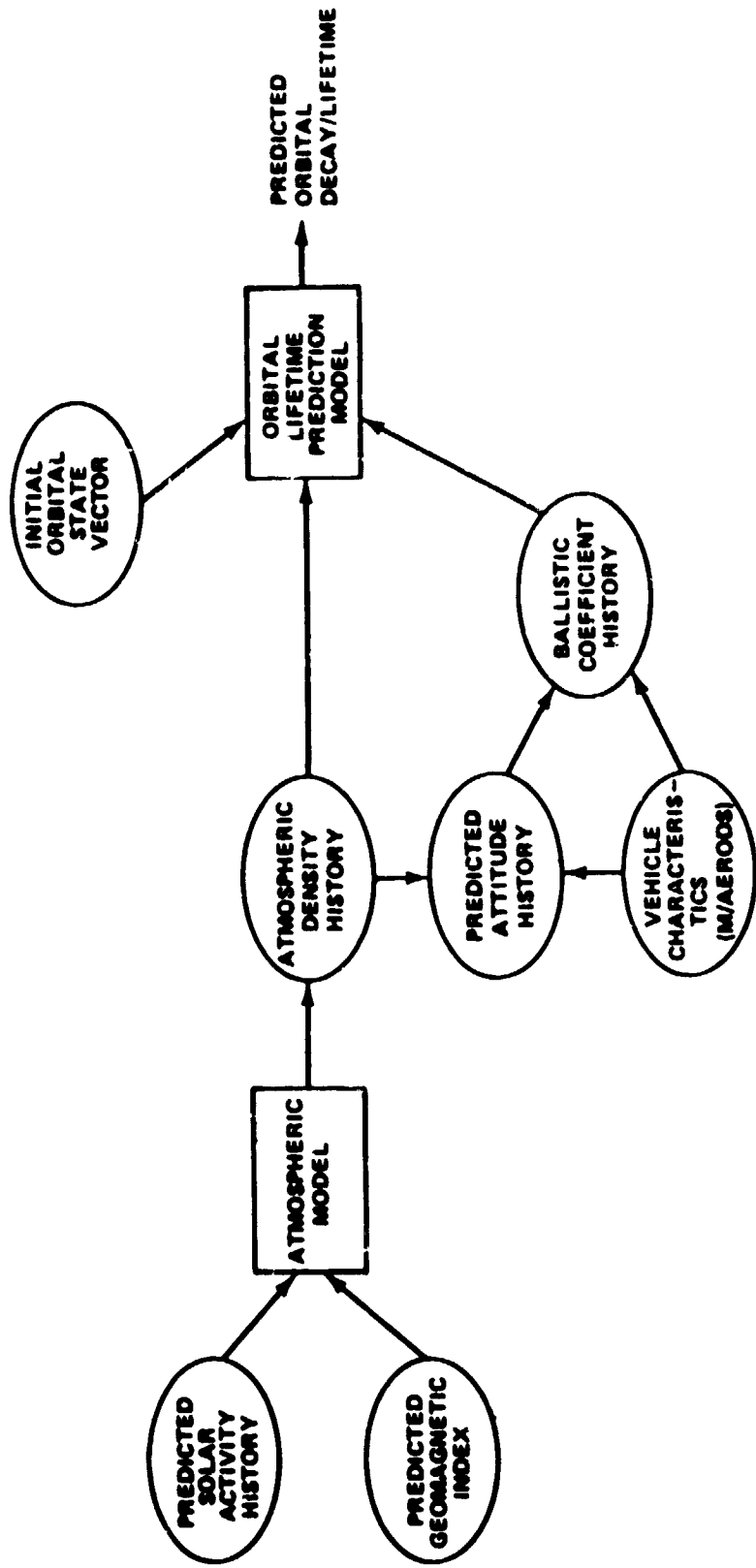


FIGURE 1-1-1 ORBIT LIFETIME PREDICTIONS PROCEDURE

There are three parameters included in the term "solar activity." They are: the daily 10.7 cm solar flux ($F_{10.7}$), an average of the daily solar flux over some time interval ($\bar{F}_{10.7}$), and the geomagnetic activity index (A_p). Predicted values for $\bar{F}_{10.7}$ are generated at MSFC by the Space Sciences Laboratory. Long-range predictions of $F_{10.7}$ cannot be made, so for lifetime predictions it is assumed that $F_{10.7} = \bar{F}_{10.7}$. Prior to February, 1978, the value of A_p was determined based on the value of $\bar{F}_{10.7}$. Space Sciences Laboratory started making long-range predictions of A_p just prior to the end of the passive phase of the Skylab mission. LTIME was then modified to use the predicted A_p data.

Since 1970, the Jacchia density model (Reference 4) has been used in LTIME. This density model was developed by Dr. L. G. Jacchia (and others) at the Smithsonian Astrophysical Observatory (SAO). The basic theory for the Jacchia density model was published in 1964 and updated in 1966, 1967, and 1970. This model included the solar activity effects and the diurnal effects along with a semiannual variation and seasonal-latitudinal variations and is based on additional study of the earth's atmosphere, especially with respect to solar effects on density. The model as used in LTIME is documented in Reference 5.

The amplitude of the semiannual variation depends on $\bar{F}_{10.7}$. Maxima occur in April and October, and minima occur in January and July. Orbital decay and lifetime are dependent on the inclination of the orbit because of the latitudinal variation of density. Orbital decay and lifetime are also dependent on launch date because atmospheric density is a function of the solar activity since it varies with time.

1.2 AERODYNAMICS

An important parameter in lifetime prediction is the ballistic coefficient, $M/C_D A$, where M is the mass in kg, C_D is the coefficient of drag, and A is the reference area in m^2 . During the preflight period, all these parameters varied. Numerous mass and configuration changes (size and shape) were made, which resulted in changes in the C_D and the ballistic coefficient. From 1967 to 1972, the mass of the workshop increased from 35,600 kg to 74,558 kg (See Figure 1.2-1).

Thus, preflight aerodynamic data were updated to reflect changes in the configuration. Aerodynamic data sets were generated for the orbital configuration of the Orbital Workshop (OWS) with the docked LM/ATM and OWS solar panels extended for an altitude of 190 nmi (Reference 6), for the Skylab cluster configuration with the OWS and ATM solar array extended for a 235 nmi altitude (Reference 7), and finally once more for the configuration changes (Reference 8).

There was no further update of the aerodynamic data until after launch. The angle of attack (α) is the angle between the velocity vector (\bar{v}) and the positive x-axis (See Figure 1.2-2). The roll angle (ϕ) is the angle between the plane formed by \bar{v} and the x-axis and the plane formed by the x and z axis. Figure 1.2-3 shows some of this data, the drag coefficient, C_D , as a function of the roll angle, ϕ , for two angles of attack, α , of 90° and 0° and also averaged over the range of α from 0° to 360° . Using the projected mass at the end of the manned mission of 74,558 kg, the ballistic coefficient can be determined. The resulting BC scale is shown on Figure 1.2-3. The BC of 122 kg/m^2 was the value used in the final preflight lifetime memorandum.

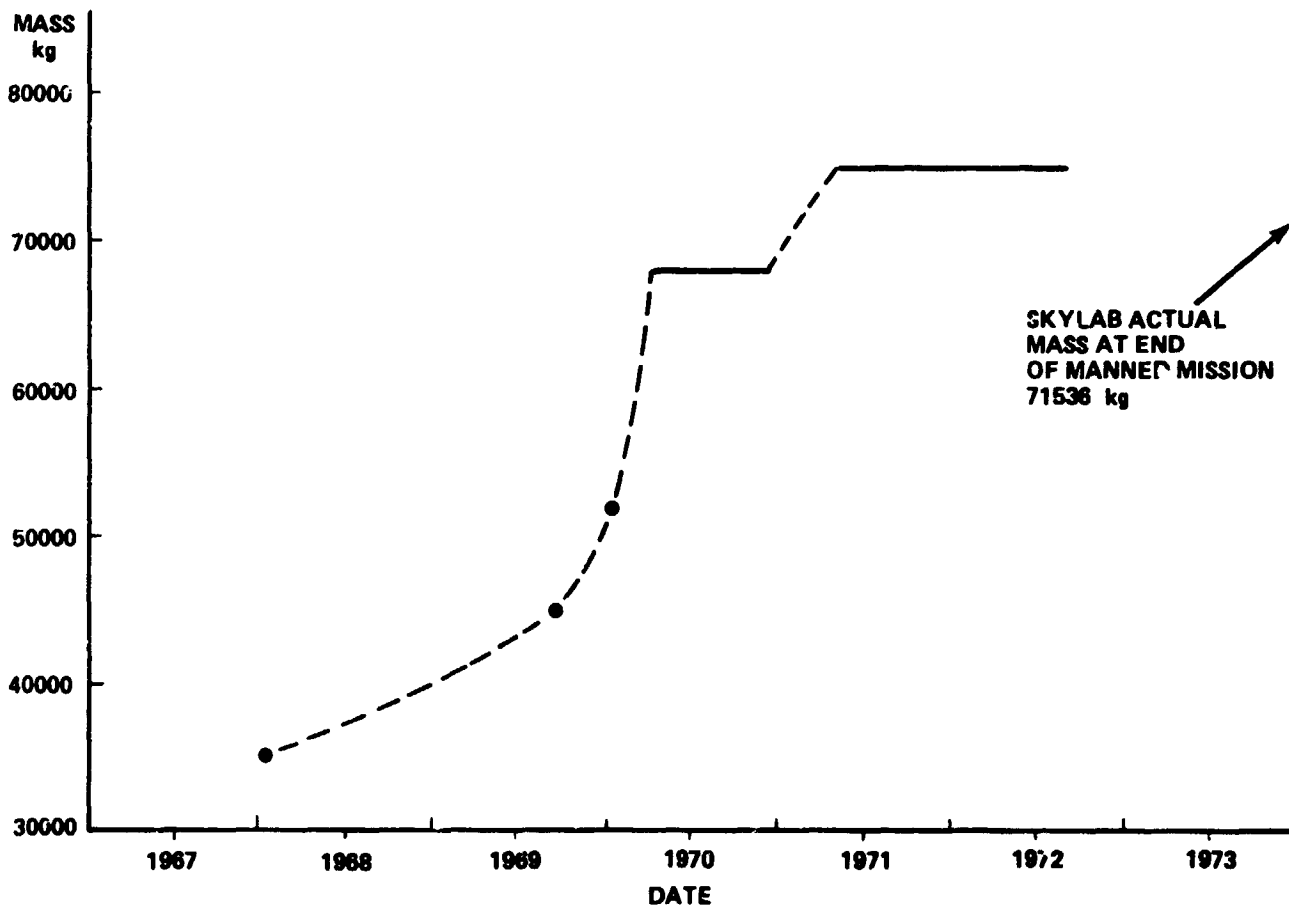
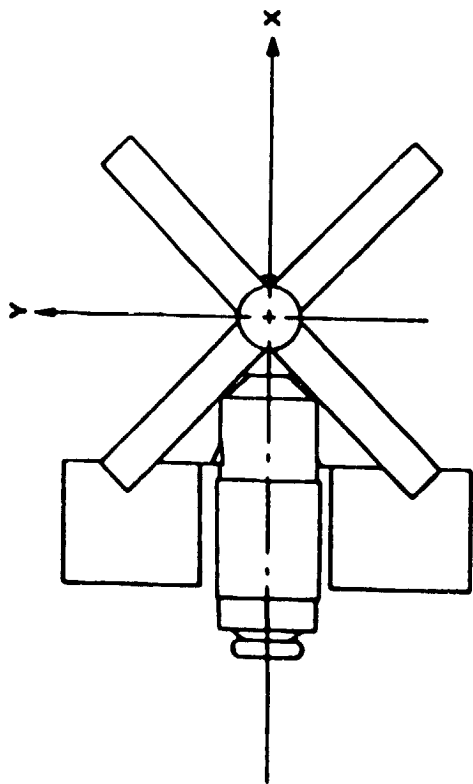


FIGURE 1.2-1 PREFLIGHT SKYLAB MASS HISTORY



NOTE REFERENCE 8

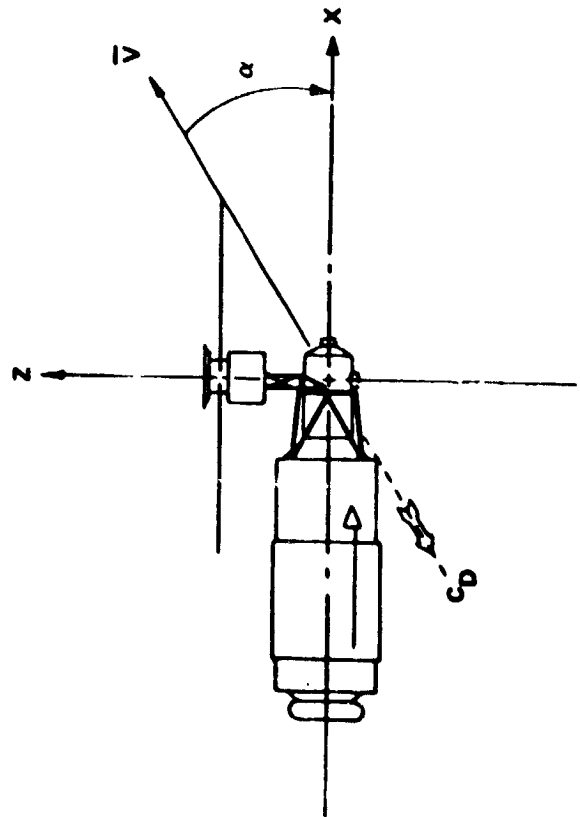
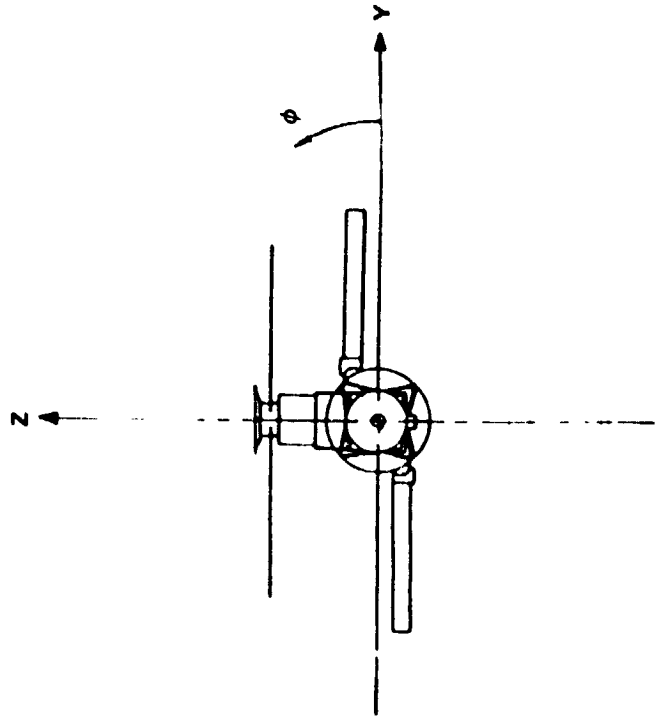


FIGURE 1.2-2 SKYLAB CONFIGURATION WITH THE SOLAR ARRAYS EXTENDED

REFERENCE AREA = 79.46 m²

SKYLAB CONFIGURATION WITH SOLAR ARRAYS EXTENDED
REFERENCE 8

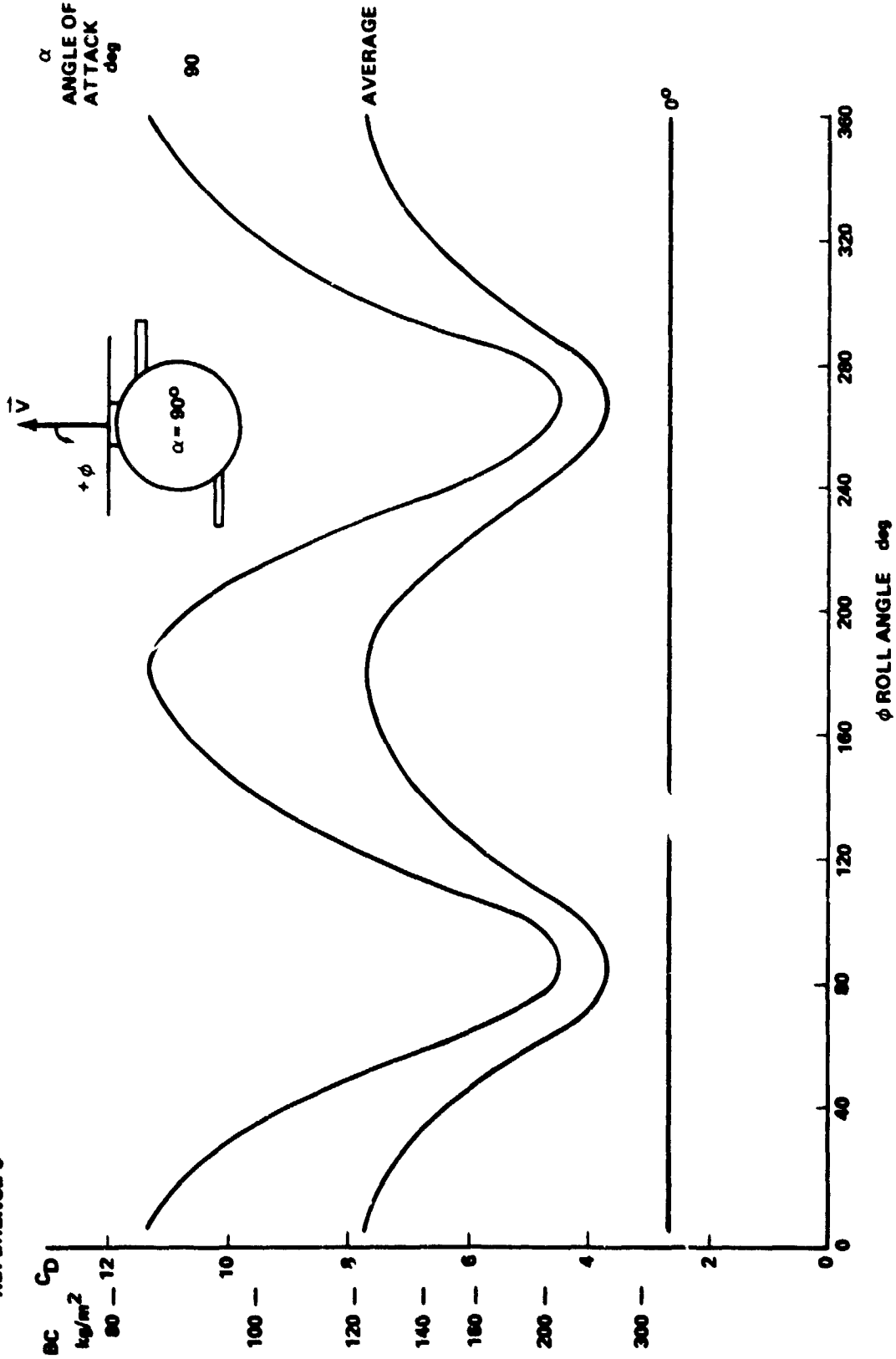


FIGURE 1.2-3 FINAL PRE-FLIGHT AERODYNAMIC DATA

1.3 SOLAR ACTIVITY PREDICTIONS

Orbital lifetime is highly dependent on launch date due to solar activity. The atmospheric density is a function of solar activity which heats the atmosphere. The higher the solar activity, the denser the atmosphere will be and the greater the orbit decay. The largest contributor to the heating of the atmosphere is the averaged solar flux $\bar{F}_{10.7}$, with the daily solar flux $F_{10.7}$ and geomagnetic index \bar{A}_p contributing much less. Predictions of $\bar{F}_{10.7}$ are generated on a monthly basis. Figure 1.3-1 shows the predicted $\bar{F}_{10.7}$. Predictions shown are January, 1969, corresponding to the earliest launch date considered; July, 1972, which was the prediction used for the final prelaunch lifetime prediction memo; and May, 1973, which was the current prediction at the time of launch. Both the nominal and the $+2\sigma$ predictions are shown. The nominal prediction is the best estimate of what the solar activity will be and the $+2\sigma$ prediction is the associated statistical upper bound. The -2σ prediction, the statistical lower bound, was generated but not shown in Figure 1.3-1. The $+2\sigma$ $\bar{F}_{10.7}$ causes the most dense atmosphere and the shortest lifetime. Also shown is the 162-day average, which is based on actual solar activity data.

The solar activity varies in an approximate 11-year cycle. Figure 1.3-1 shows the predicted $\bar{F}_{10.7}$ from near the peak of cycle 20 to near the peak of cycle 21. A change in launch date meant that Skylab would have been in orbit during a different portion of the cycle which would mean a change in the predicted lifetime.

It should be noted that the orbital atmospheric density model used in MSFC's satellite lifetime prediction program was developed based on empirical relationships established between orbital density and the 162-day average $\bar{F}_{10.7}$, daily $F_{10.7}$, and daily A_p index (See Reference 4). None of these parameters can be predicted with any acceptable degree of confidence. Therefore, longer term smoothed value of $\bar{F}_{10.7}$ and \bar{A}_p are used in the statistical regression technique to estimate future nominal (50%) and $+2\sigma$ (95%) confidence band values. These $\bar{F}_{10.7}$ and \bar{A}_p values are used as inputs to the orbital atmospheric density model and, thereby, to the orbital lifetime prediction program. No universally accepted solar activity prediction technique exists in the scientific community and, therefore, statistical estimates and periodic updates thereof are necessary. Such was the practice during the preflight planning period and while Skylab was in orbit.

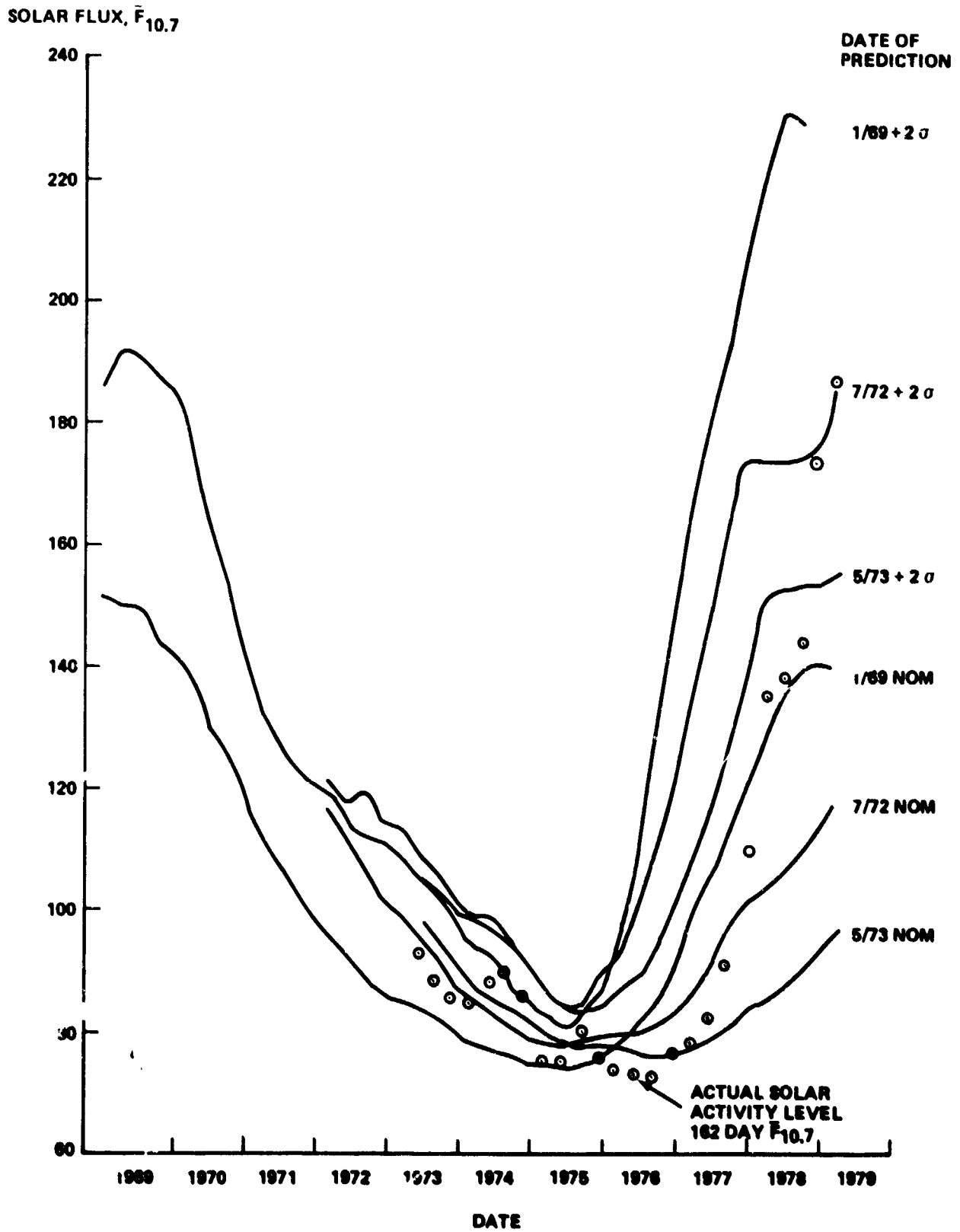


FIGURE 1.3-1 PREDICTED SOLAR ACTIVITY

1.4 PREFLIGHT LIFETIME PREDICTIONS

During the preflight mission planning phase of the Skylab program, many mission planning iterations were required that affected the Skylab lifetime predictions. A partial summary of these analyses is included to provide an understanding of how various early decisions (configuration, mass, initial orbit, attitude, etc.) affected the actual Skylab lifetime.

The planned sequence in 1967 for launching Skylab and the manned missions, AAP-1, AAP-2, AAP-3, and AAP-4, was as follows: The AAP-2 flight would place Skylab into orbit followed by the launch of AAP-1 which would place a CSM into orbit. At that point, the CSM would rendezvous and dock with the orbital workshop and perform its mission, after which the CSM would undock and the CM would deorbit. At some later time, the AAP-3 flight would place a CSM into orbit followed by the launch of AAP-4 with the LM/ATM. The AAP-3/CSM would rendezvous and dock with the LM/ATM. Maneuvers would be performed to dock the CSM-LM/ATM to the orbital workshop. The cluster configuration OWS-CSM-LT/ATM mission would then be performed after which the CSM would undock and the CM would return to earth. The OWS and the LM/ATM would remain docked in orbit.

Tables 1.4-1 and 1.4-2 present mission descriptions for two basic modes that were considered for performing the Skylab mission and some of the iterations performed on each of those basic modes. Modes were distinguished by mission and attitude timeline. Table 1.4-1 presents the mission description for Mode A and ballistic coefficients $M/C_D A$ for orbital workshop solar arrays of 850 sq.ft.; 1,180 sq.ft.; 1,466 sq.ft.; and 1,588 sq.ft. As can be seen from the table, there was no significant difference in the $M/C_D A$ values for solar arrays of 1,180; 1,466; and 1,588 sq.ft.. This was due primarily to the fact that for an increase in area there was also an increase in mass, such that the ratio remained essentially the same.

For the Mode A configuration, phases one through five broke the mission into distinct time intervals for performing each phase of the mission. Associated with each phase and time interval was a particular orbital configuration and a proposed orbital attitude for the cluster vehicle. Although the mass and surface area associated with each phase also changed, in this instance this was a secondary affect. The attitude of an elongated vehicle with large solar panels, such as Skylab, is very critical in orbital lifetime prediction. Nose-on attitude implies the longitudinal axis of the orbital workshop is parallel to the velocity vector. Broadside implies the

TABLE 1.4-1 MISSION DESCRIPTION FOR CLUSTER CONFIGURATION - MODE A

| PHASE | CONFIGURATION | TIME (days) | ATTITUDE | SOLAR ARRAY SIZE | | | |
|-------|-----------------------|----------------|--------------|-------------------------|------------------------|------------------------|------------------------|
| | | | | 850 sq. ft. M/CDA | 1180 sq. ft. M/CDA | 1466 sq. ft. M/CDA | 1588 sq. ft. M/CDA |
| 1 | OWS | 0 - .29 | Nose-On | 223.5 kg/m ² | --- | --- | --- |
| | | | Broadside | 42.2 kg/m ² | 38.6 kg/m ² | 37.1 kg/m ² | |
| 2 | OWS + CSM | .29 - 28 | Broadside | 69.3 kg/m ² | 83.1 kg/m ² | 77.1 kg/m ² | 74.6 kg/m ² |
| | | | | | | | |
| 3 | OWS | 28 - 180 | Broadside | 50.4 kg/m ² | 83.1 kg/m ² | 82.9 kg/m ² | 83.0 kg/m ² |
| | | | | | | | |
| 4 | OWS + CSM + LM/ATM | 180 - 235 | Sun-Oriented | 89.6 kg/m ² | 81.2 kg/m ² | 77.0 kg/m ² | 75.1 kg/m ² |
| | | | | | | | |
| 5 | OWS + LM/ATM | 235 - Imp. | Broadside | 43.6 kg/m ² | 58.5 kg/m ² | 58.6 kg/m ² | 58.7 kg/m ² |
| | | | | | | | |
| | | | | | | | |
| | | | | | | | |

TABLE 1.4-2 MISSION DESCRIPTION FOR CLUSTER CONFIGURATION - MODES B, B₁, B₂, AND B₃

| PHASE | CONFIGURATION | TIME (days) | ATTITUDE | 1180 SQ. FT. ARRAY | | | |
|-------|-----------------------|-------------|--------------------------------------|------------------------|------------------------------|------------------------------|------------------------------|
| | | | | Mode B M/CDA | Mode B ₁ M/CDA | Mode B ₂ M/CDA | Mode B ₃ M/CDA |
| 1 | OWS | 0 - 1 | Broadside | 42.2 kg/m ² | 42.2 kg/m ² | 42.2 kg/m ² | 42.2 kg/m ² |
| 2 | OWS + CSM | 1 - 29 | Sun-Oriented Broadside (ASO**) | 83.1 kg/m ² | 77.5 kg/m ² | 83.1 kg/m ² | 77.5 kg/m ² |
| 3 | OWS | 29-119 | Broadside (AR*) | 83.1 kg/m ² | 83.1 kg/m ² | 83.1 kg/m ² | 83.1 kg/m ² |
| 4 | OWS + CSM + LM/ATM | 119 - 175 | Sun-Oriented | 81.2 kg/m ² | 81.2 kg/m ² | 81.2 kg/m ² | 81.2 kg/m ² |
| 5 | OWS + LM/ATM | 175 - 205 | Broadside (AR*) Sun-Oriented | 58.5 kg/m ² | 58.5 kg/m ² | 59.5 kg/m ² | 59.5 kg/m ² |
| 6 | OWS + CSM + LM/ATM | 205 - 261 | Sun-Oriented | 81.2 kg/m ² | 81.2 kg/m ² | 81.2 kg/m ² | 81.2 kg/m ² |
| 7 | OWS + LM/ATM | 261 - Imp | Broadside (AR*) | 58.5 kg/m ² | 58.5 kg/m ² | 58.5 kg/m ² | 58.5 kg/m ² |

*Array Rotated **Array Sun-Oriented

longitudinal axis of the vehicle is perpendicular to the velocity vector with the plane of the solar panels also broadside to the velocity vector causing maximum drag. Sun oriented implies that the plane of the solar panels are always perpendicular or broadside to the Earth - Sun vector.

Table 1.4-2 presents the mission description for Modes B, B₁, B₂, and B₃, which differ only in orbital attitude. The parameters of Table 1.4-2 hold the same connotation as those of Table 1.4-1; however, the term (ASO) associated with "Broadside" orientation implies that the workshop is continually broadside but that the solar array panels are sun oriented. Also, the term (AR) implies that the orbital workshop is again broadside but that the solar array panels have been rotated such that their planes are parallel to the velocity vector.

It should be reiterated that Modes B₁, B₂, and B₃ differ from Mode B only in attitude of the orbital vehicle during the first 28-day mission (Phase 2) and during the second 30-day storage period (Phase 5). It can be seen from Table 1.4-2 that those changes had very little affect on the ballistic coefficient $M/C_D A$. Therefore, since there was no significant difference in the $M/C_D A$ for those two phases and since the time period of those phases was only a small percent of the total orbital lifetime of the cluster mission, no significant difference was noted in the orbital lifetime prediction of the cluster mission for the Modes B, B₁, B₂, or B₃.

The cluster mission underwent a multitude of major and minor changes in its development from an early concept of the mission as presented in Table 1.4-1, Mode A, to the later concept presented in Table 1.4-2, Mode B₃. Some of the early assumptions for Mode A included: start of the cluster mission as early as 1969, an initial workshop altitude of 260 nmi to guarantee a one-year orbital lifetime ($+2\sigma$ probability atmospheric density), and an 850 sq.ft. array of solar panels on the orbital workshop.

Figure 1.4-1 presents nominal and $+2\sigma$ orbital lifetime predictions as a function of launch date for circular altitudes of 260, 240, 230, 220, and 200 nmi. This graph reflects the Mode A configuration assuming launch dates of 1969 through 1971 and a solar array of 850 sq.ft.. As can be seen from Figure 1.4-1, launch date is a very important parameter in orbital lifetime. Figure 1.3-1 shows the solar cycle peak around 1969, so a slip in launch date gave an increase in lifetime.

The size of the solar arrays proposed for the orbital workshop came under much discussion during the preflight planning

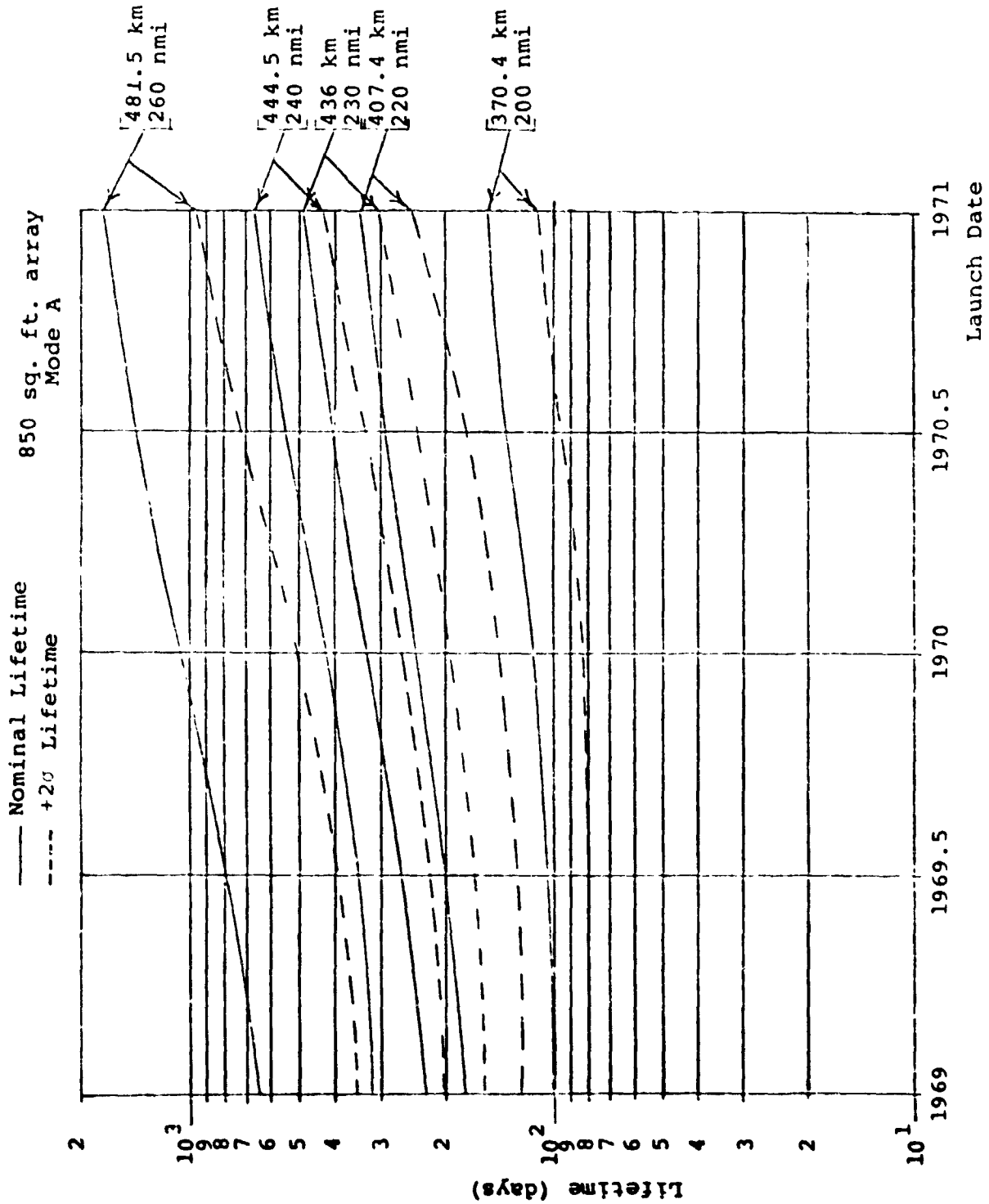


FIGURE 1.4-1 CLUSTER LIFETIME VERSUS LAUNCH DATE FOR DISCRETE ALTITUDES - REFERENCED TO LAUNCH OF WORKSHOP

Published 11/7/67

phase. The 850 sq.ft. solar array originally planned for the orbital workshop was found to be inadequate to meet the power requirement for the cluster mission. Three proposed array sizes (1,180 sq.ft.; 1,466 sq.ft.; and 1,588 sq.ft.) were investigated from the orbital lifetime standpoint. An analysis was performed for Modes A and B assuming 1970 and 1970.5 launch dates for each of the three proposed solar arrays. It was determined that there was no significant difference in the orbital lifetime between the solar array sizes investigated. The maximum difference noted was less than one percent of the total cluster lifetime. Therefore, Figures 1.4-2 and 1.4-3 could be used to determine the orbital lifetime versus altitude for Modes A and B, respectively, for any of these three array sizes.

By November, 1967, the mission planning process had selected the 1,180 sq.ft. solar array, an initial altitude for the orbital workshop of 230 nmi, and operating in Mode B₃ as defined in Table 1.4-2. Assuming those conditions, Figures 1.4-4 and 1.4-5 present a detailed decay history for the cluster mission for launch dates of 1970 and 1970.5, respectively.

At one point, it was planned that the orbital workshop would be placed into an initial 205X230 nmi elliptic orbit. The orbit would then be circularized to the desired 230 nmi through passivation of the S-IVB at the apogee point of the elliptic orbit. Nominal impulses obtained from this passivation would raise the perigee sufficiently to obtain a circular 230 nmi orbit. Should some other impulse other than nominal be obtained from passivation, the final orbit would not be circular. Figure 1.4-6 presents nominal and $\pm 2\sigma$ lifetimes for the cluster mission for a range of those possible orbits. The lifetimes were based on Mode B₃ with a 1,180 sq.ft. array and launch dates of 1970 and 1970.5.

By September, 1969, the initial altitude for the workshop was chosen to be 235 nmi with an inclination of 35°. By January, 1970, the inclination had been changed to 50°. The launch was scheduled for March 15, 1972; but the launch date continued to slip. The launch date was November 9, 1972 in December, 1970 and was April 30, 1973 in September, 1972.

The mode of operation also changed. By September, 1969, it had been decided to maintain a solar inertial attitude during the mission. The duration of the various phases of the mission continued to change. A summary of these changes is shown in Table 1.4-3. The continued increase in M/C_{pA} reflects the continued increase in the mass of the workshop, from 35600 kg in 1967 to 74558 in 1972. The different phases of the mission were very short compared to the total lifetime so a change in

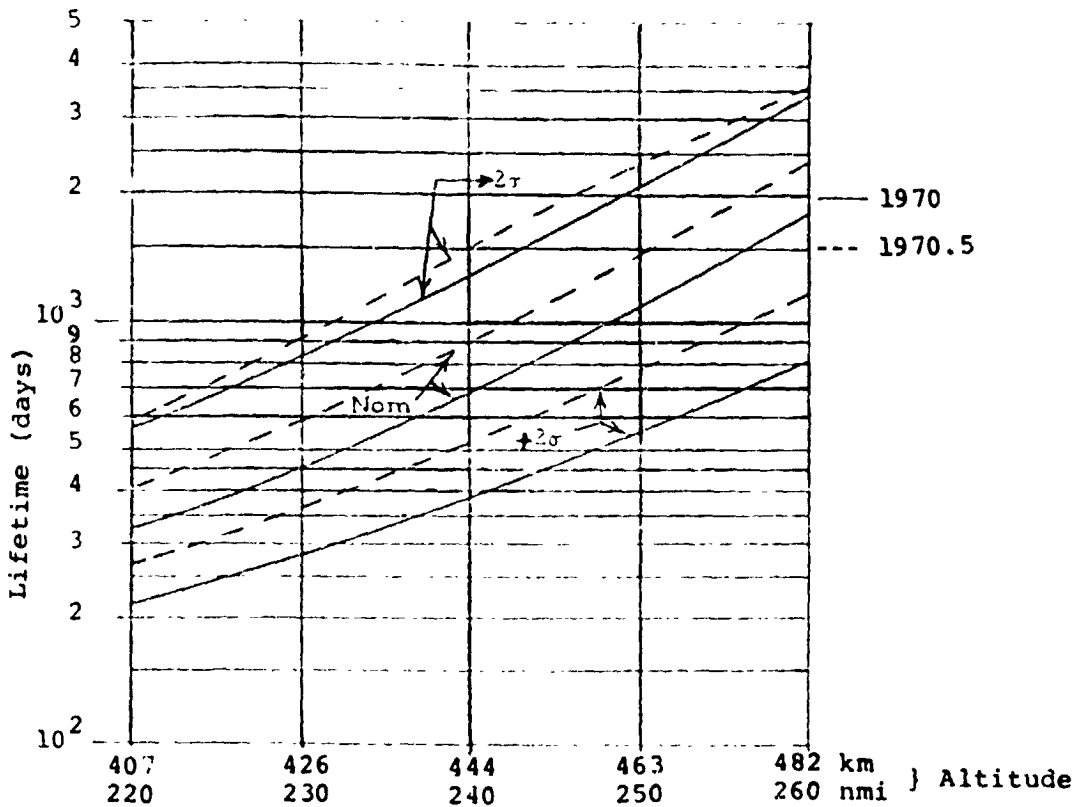


FIGURE 1.4-2 LIFETIME VS. ALTITUDE FOR MODE A 1970 AND 1970.5 LAUNCHES

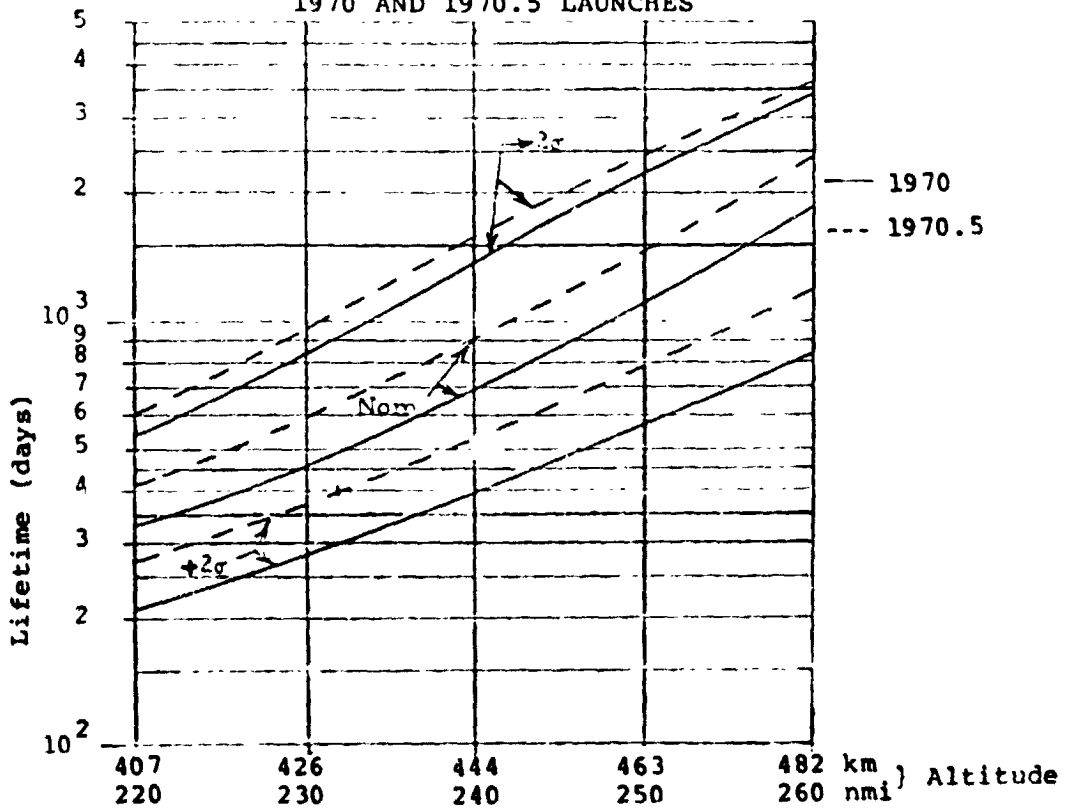


FIGURE 1.4-3 LIFETIME VS. ALTITUDE FOR MODE B 1970 AND 1970.5 LAUNCHES

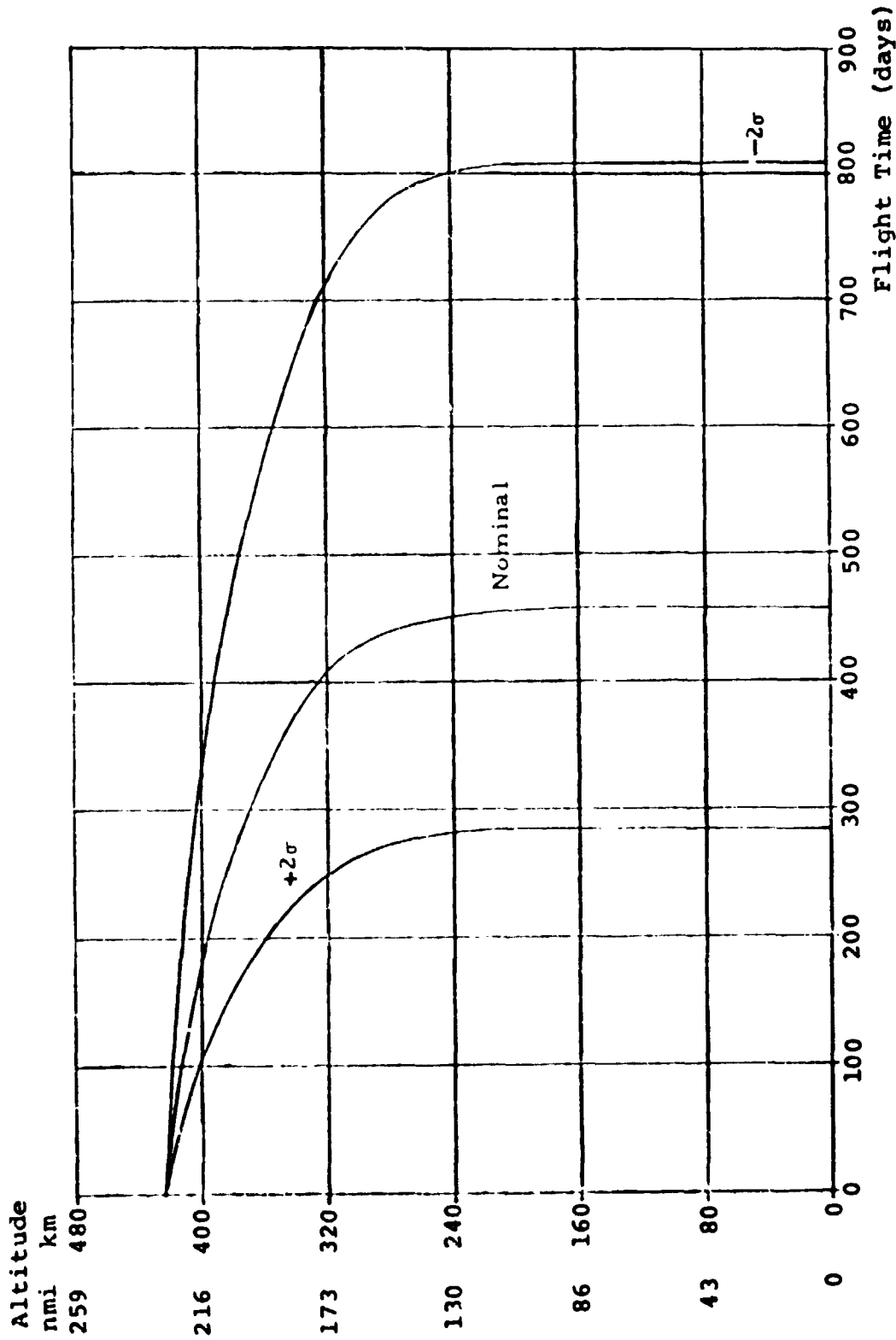


FIGURE 1.4-4 ORBITAL DECAY FOR 230 NMI CIRCULAR ORBIT LAUNCH DATE
JANUARY 1, 1970, CLUSTER MISSION MODE B

Published 11/7/67

Altitude
nmi km

259 480

216 400

173 320

130 240

86 160

43 80

0 0

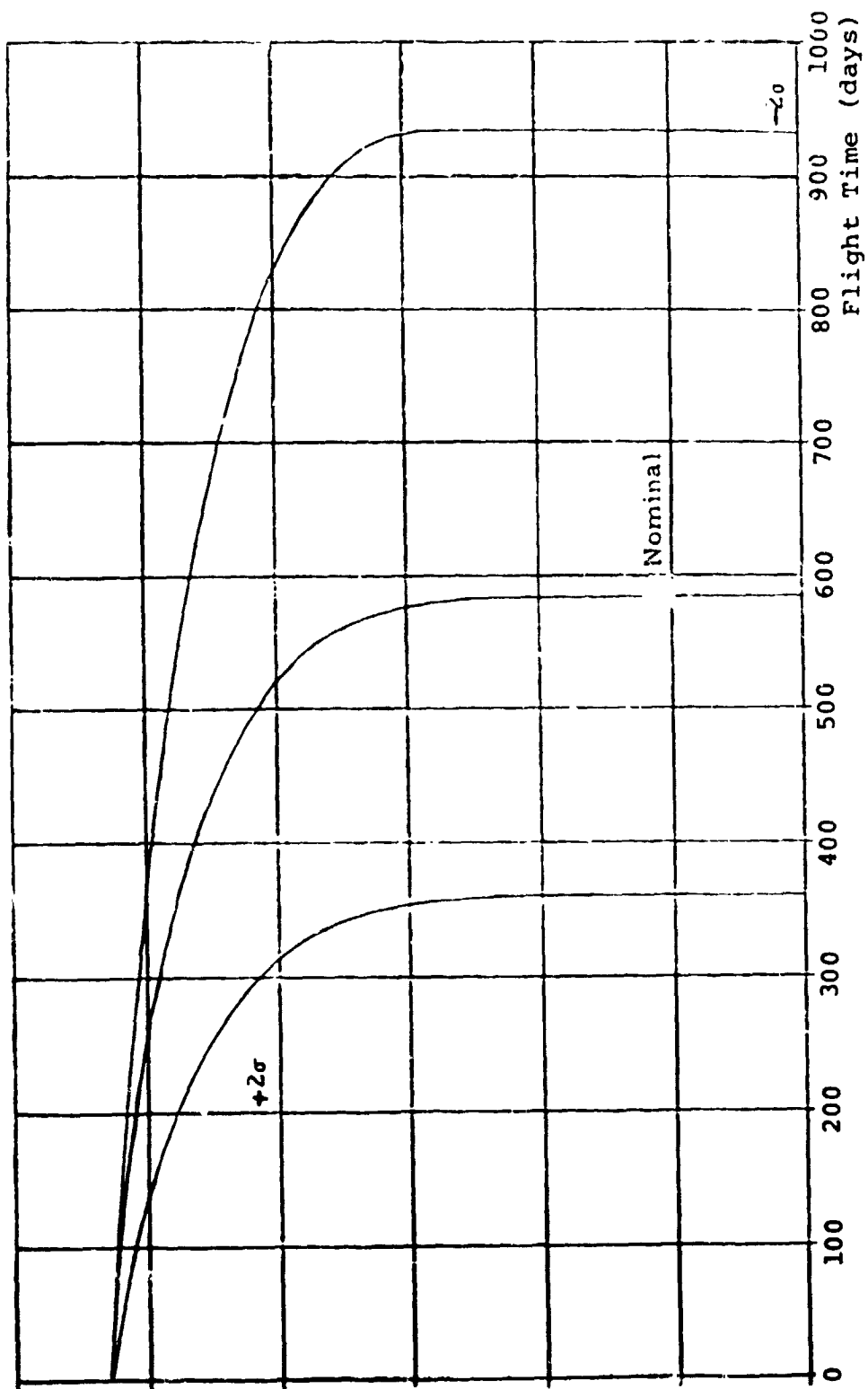


FIGURE 1. 4-5 ORBITAL DECAY FOR 230 NMI CIRCULAR ORBIT LAUNCH DATE JULY 1, 1970, CLUSTER MISSION MODE B

Published 11/7/67

----- 1970 Launch Date
 - - - - - 1970.5 Launch Date

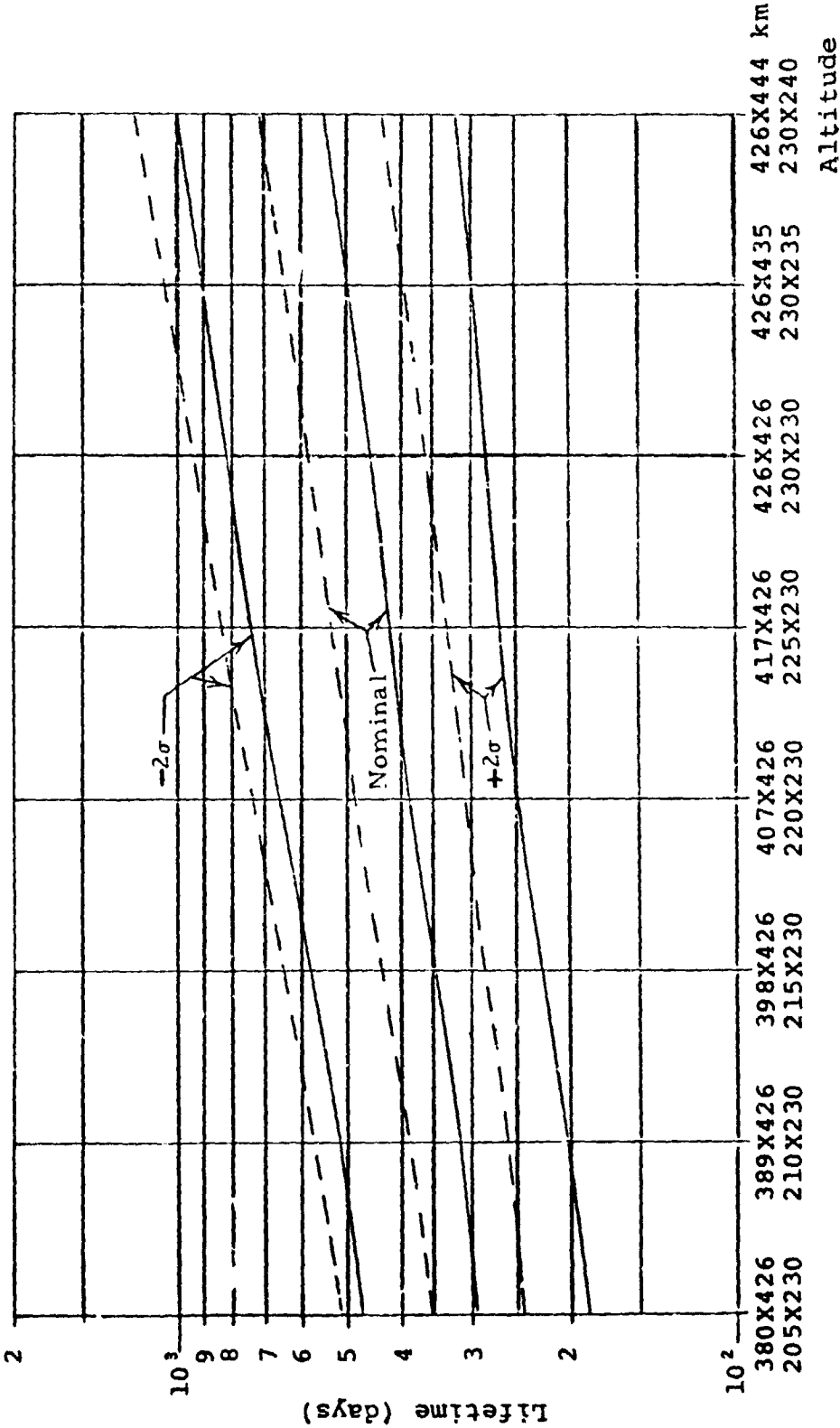


FIGURE 1. 4-6 NOMINAL AND $\pm 2\sigma$ LIFETIMES FOR VARIOUS ELLIPTIC ORBITS CLUSTER
 MISSION MODE B

Published 11/7/67

the duration of one or more phases caused no significant change in the predicted lifetime.

The last preflight lifetime prediction was published in September, 1972. The mode of operation for the mission was ignored because it was planned, in order to maintain a repeating ground track, to maintain the initial altitude for the entire mission. This made the mission duration a variable parameter but one with no significant affect on the predicted lifetime. The $M/C_D A$ at the end of the manned mission was 122 kg/m^2 . A summary of the lifetime predictions is included in Table 1.4-3. The final preflight prediction gave impact as early as November, 1977 for a $+2\sigma$ and as late as June, 1982 for -2σ (not shown) with the nominal October, 1979, which was only three months later than the actual impact.

TABLE 1.4-3

MISSION DESCRIPTION FOR CLUSTER CONFIGURATION AND LIFETIME PREDICTION

| Memorandum Date | 9/20/69 (MSFC) | 1/20/70 (MSFC) | 4/70 (LMSC) | 12/2/70 (MSFC) | 9/6/72 (MSFC) |
|-----------------------------|-----------------|-----------------------------------------|-----------------|-----------------------------------------|-----------------|
| Phase Configuration | Time (Days) | M/C _D A (kg/m ²) | Time (Days) | M/C _D A (kg/m ²) | Time (Days) |
| 1 WS | 0-2 | 89.33 | 0-2 | 101.6 | 0-1 |
| 2 WS + CSM | 2-30 | 106.42 | 2-29 | 115.2 | 1-29 |
| 3 WS | 30-90 | 87.10 | 29-85 | 99.3 | 29-71 |
| 4 WS + CSM | 90-146 | 103.18 | 85-140 | 111.5 | 71-127 |
| 5 WS | 146-180 | 82.32 | 140-190 | 95.0 | 127-173 |
| 6 WS + CSM | 180-236 | 98.84 | 190-245 | 107.4 | 173-229 |
| 7 WS | 236-Im- pact | 77.64 | 245-Im- pact | 90.6 | 229-Im- pact |
| Launch Date | 3/15/72 | 3/15/72 | 7/15/72 | 11/15/72 | 4/30/73 |
| Altitude (nmi) | 235 | 235 | 235 | 235 | 235 |
| Inclination (deg) | 35 | 50 | 50 | 50 | 50 |
| Mass (kg) at end of mission | 44826 | 52317 | 67962 | 67962 | 74558 |
| Predicted Lifetime | 1660 | 1760 | 2093 | 2074 | 2360 |
| Nominal - Days | 4.54 | 4.82 | 5.73 | 5.68 | 6.64 |
| +2σ - Days | 1120 | 1210 | 1442 | 1415 | 1650 |
| - Years | 3.07 | 3.32 | 3.95 | 3.87 | 4.52 |

1
2

2. ORBITAL DECAY DURING THE MANNED PERIOD (MAY 1973 - FEB. 1974)

During the actual manned mission period, which lasted from 5/23/73 until 2/8/74, Skylab was occupied by three different astronaut crews. The first crew occupied Skylab from 5/23/73 to 6/21/73. The second crew occupied Skylab from 7/28/73 to 9/25/73. The third crew occupied Skylab from 11/16/73 to 2/8/74.

As might be expected, the actual mission differed somewhat from the planning; however, the overall mission activity was close to planned, except for the loss of one of the OWS solar panels during the very earliest portions of flight (~63 seconds). This had a major effect on orbital lifetime considerations, and new aerodynamic data had to be generated to match this orbital configuration (See Reference 9).

The manned period provided an unusual opportunity to correlate theoretical aerodynamic data with derived data, using orbital decay methods, and aided in determining uncertainties (biases) in the atmospheric density model. The key factor which makes this period so unusual is the knowledge of the Skylab's attitude. For a known attitude, a theoretical ballistic coefficient based on the above mentioned aerodynamics could be calculated.

With knowledge of the actual solar activity and decay, a derived ballistic coefficient could also be determined. The ballistic coefficients resulting from the two methods were then compared to assess the quality of the theoretical aerodynamics and/or to determine biases in the density model.

To determine the ballistic coefficient, the known orbital decay is compared to the predicted decay, using the actual solar activity and an estimate for the ballistic coefficient. The ballistic coefficient is then varied until the actual decay is matched by the predicted decay. The resulting value of the ballistic coefficient is used for future lifetime predictions. Since orbital adjustments were made during the manned periods, the only time decay comparisons could be made was between the manned periods.

Between the manned missions, Skylab was held in Solar Inertial attitude. Using an estimate of the mass, 74525 kg, at the end of the first manned mission and C_D as a function of beta angle (i.e., roll), the theoretical ballistic coefficient could be calculated. An example of the theoretical aerodynamics data is shown in Figure 2-1. Here the drag coefficient is shown as a function of the roll angle, ϕ , and for three values

of the angle of attack, α , 90° , 0° , and averaged over the total range from 0° to 360° . Using a projected mass at the end of the first manned mission, the ballistic coefficient was determined and is shown on Figure 2-1. For the ballistic coefficient as a function of beta, the ballistic coefficient varied from 150 kg/m^2 to 235 kg/m^2 , with the average value being 173 kg/m^2 .

Concerning the solar activity, both the 10.7 cm solar flux ($F_{10.7}$) and the geomagnetic activity index (A_p) are available daily. Preliminary values of $F_{10.7}$ and A_p for a given date are generally available by mid-afternoon on that day from NOAA (National Oceanic and Atmospheric Administration). The preliminary value of $F_{10.7}$ is usually within 1 or 2 percent of the final value, but the preliminary value of A_p (which is a measurement from the Fredericksburg Observatory only) is usually not very close to the final value. The final value of A_p is an average from several observatories and could be as much as 50 percent different from the preliminary value. Final values are not available until 1 or 2 months later. The preliminary values of $F_{10.7}$ and A_p were used in real time LTIME decay comparisons. The Jacchia density model calls for these two parameters and additionally a 162-day average of the $F_{10.7}$, which is a midpoint 81 days prior to date of interest to 81 days after the date of interest. The daily values of $F_{10.7}$, the predicted nominal $\bar{F}_{10.7}$, the predicted $+2\sigma \bar{F}_{10.7}$, the actual 162-day average $\bar{F}_{10.7}$, and the actual 13-month average $\bar{F}_{10.7}$ are shown in Figure 2-2 covering the time span of the manned operation of Skylab. The 13-month average is a long-term smoothed value utilized in the statistical regression technique to estimate future solar activity and is consistent with solar activity records for several hundred years. A comparison of the various solar flux averages is shown in Figure 2-3.

Support was received from NORAD (North American Air Defense Command) on a regular basis. Part of this support was the calculation of the mean orbital elements. From the NORAD elements, the semimajor axis was calculated. This is shown in Figure 2-4 from initial insertion of the Skylab into orbit until the end of the manned mission period.

Now the actual orbital decay was compared to the decay predicted with the lifetime program. For this prediction, the "best" decay comparison resulted in a ballistic coefficient of 170 kg/m^2 . This decay comparison is shown in Figure 2-5. The total decay over this short time interval (36 days) was only 480 meters. Since there is some uncertainty in the NORAD orbital elements, the uncertainty in the BC is greater

for this short time interval than it would be over a longer interval with more decay. A 10% error in BC would cause a 48-meter error in decay. Lifetime predictions using this BC are discussed in Section 3 of this report. As can be seen, this compares extremely well with the theoretical average value of 173 kg/m^2 ; and at least for the Solar Inertial attitude, the theoretical aerodynamics was quite good. Analysis of the Skylab results has indicated that errors in the atmospheric density model are probably minimal at low levels of solar activity. Since the solar activity was low at this time, the delta is probably entirely due to uncertainties in the theoretical aerodynamics vs. the real world. Additional analysis of the aerodynamics and density bias will be included later in this report and in Reference 10.

During the third Skylab manned period, several altitude adjustments were made to compensate for the orbital decay. The altitude adjustments of approximately 10 km raised Skylab altitude approximately 3 nmi above its initial altitude. The altitude boost (7.6 km) at the end of the third manned mission gave a predicted lifetime increase of 259 days for nominal solar activity and 107 days for $+2\sigma$ solar activity.

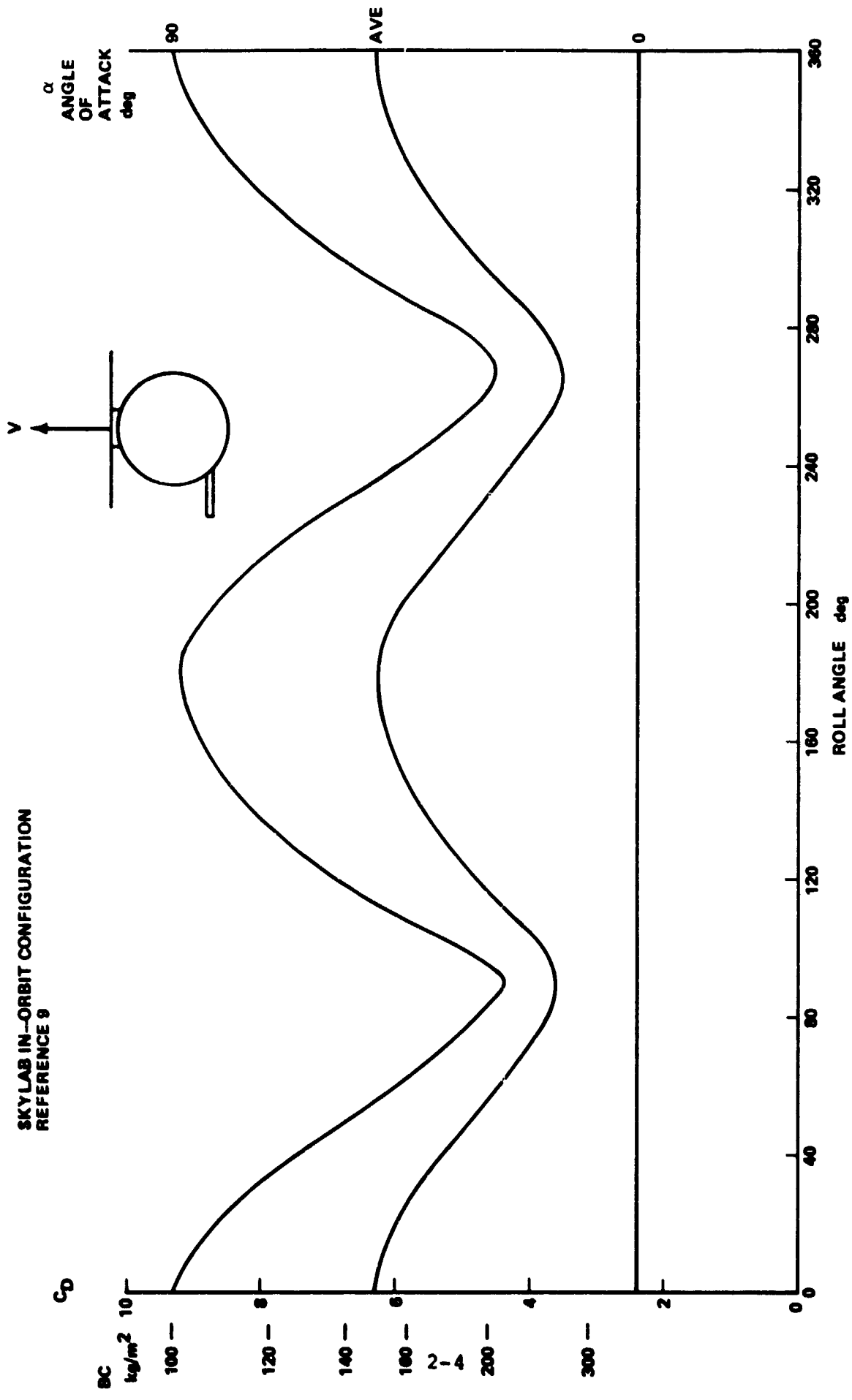


FIGURE 2-1 DRAG COEFFICIENT VS ROLL ANGLE

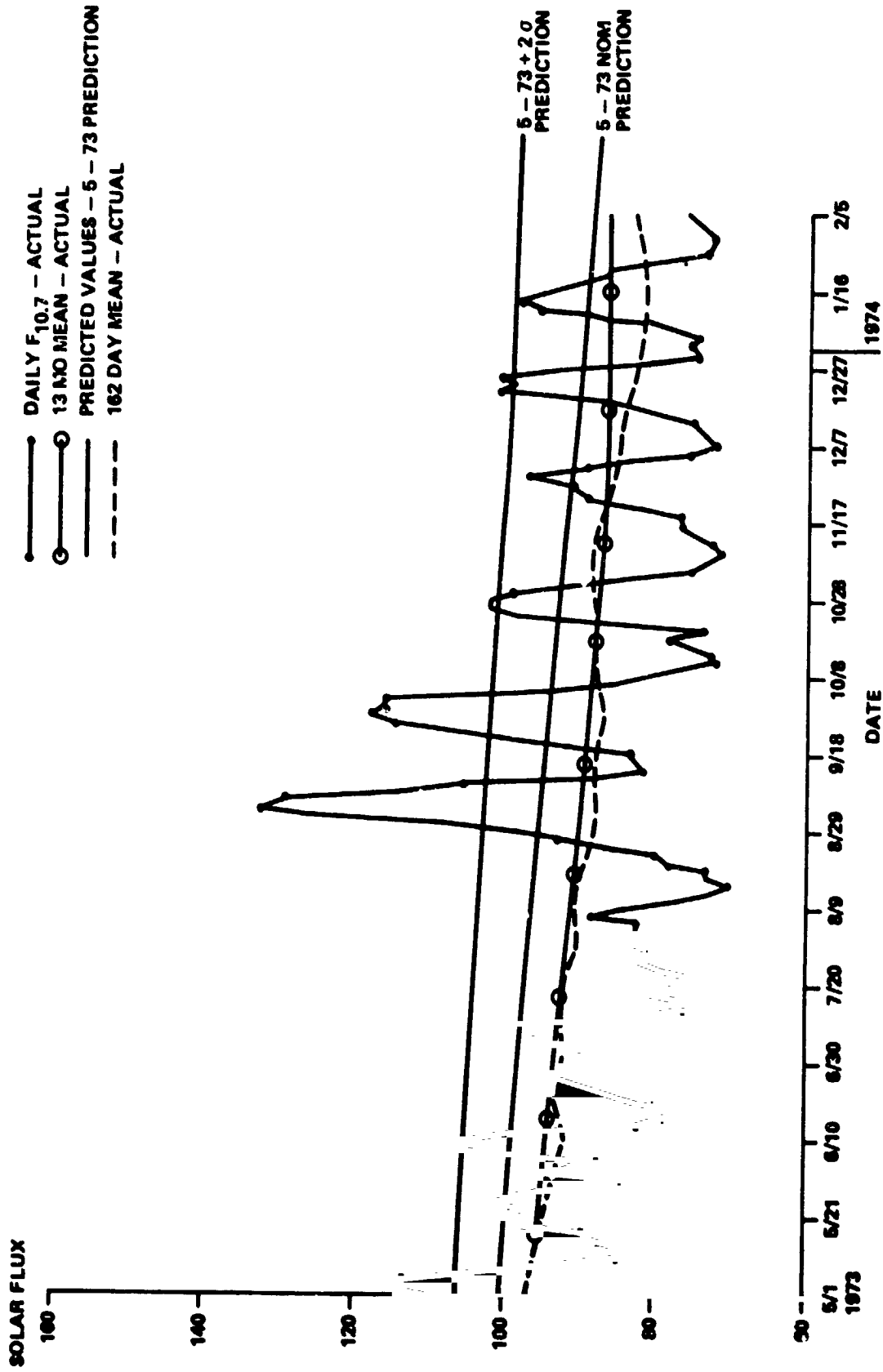


FIGURE 2-2 ACTUAL AND PREDICTED SOLAR FLUX DURING THE MANNED PERIOD

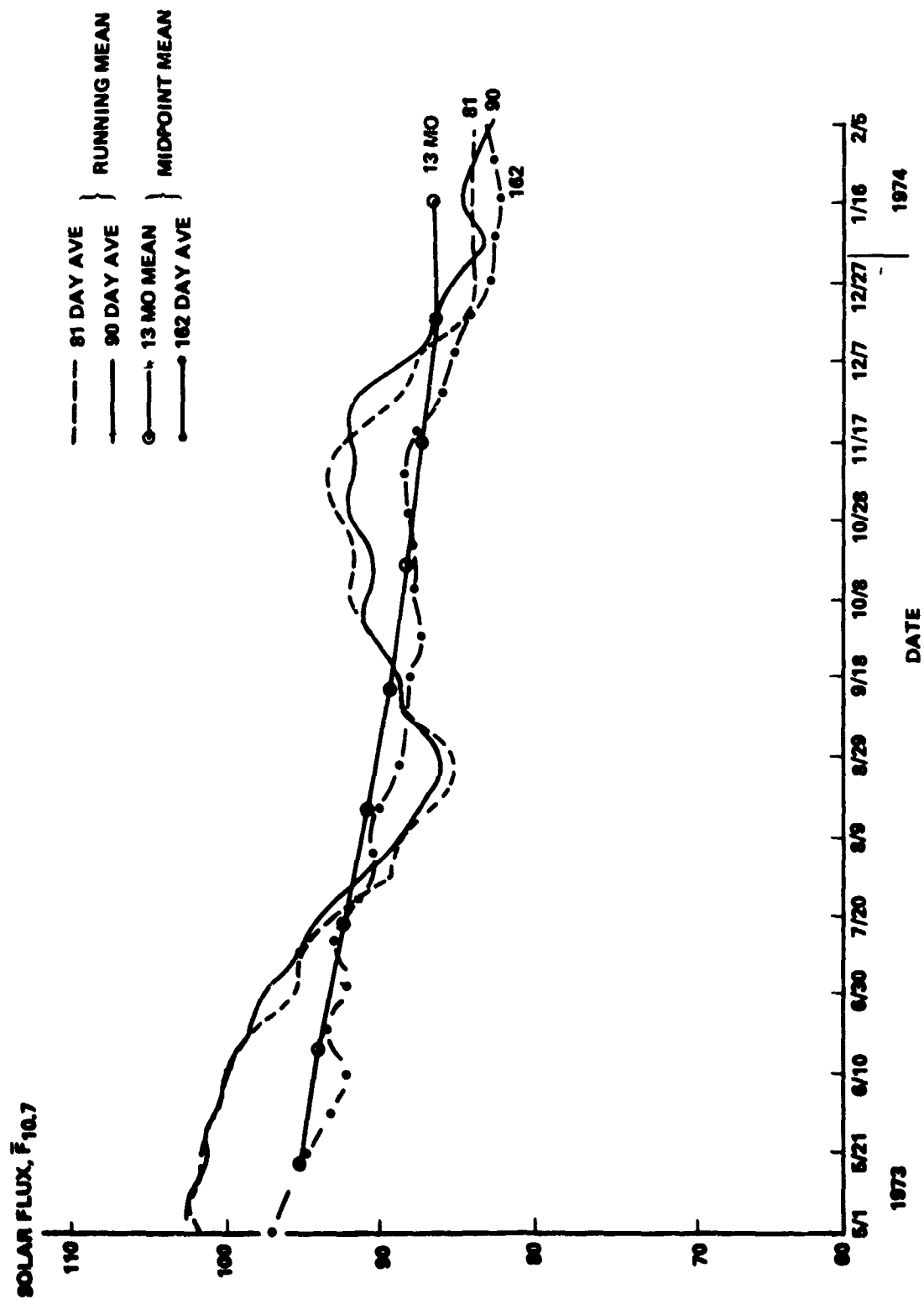


FIGURE 2-3 SOLAR FLUX COMPARISON

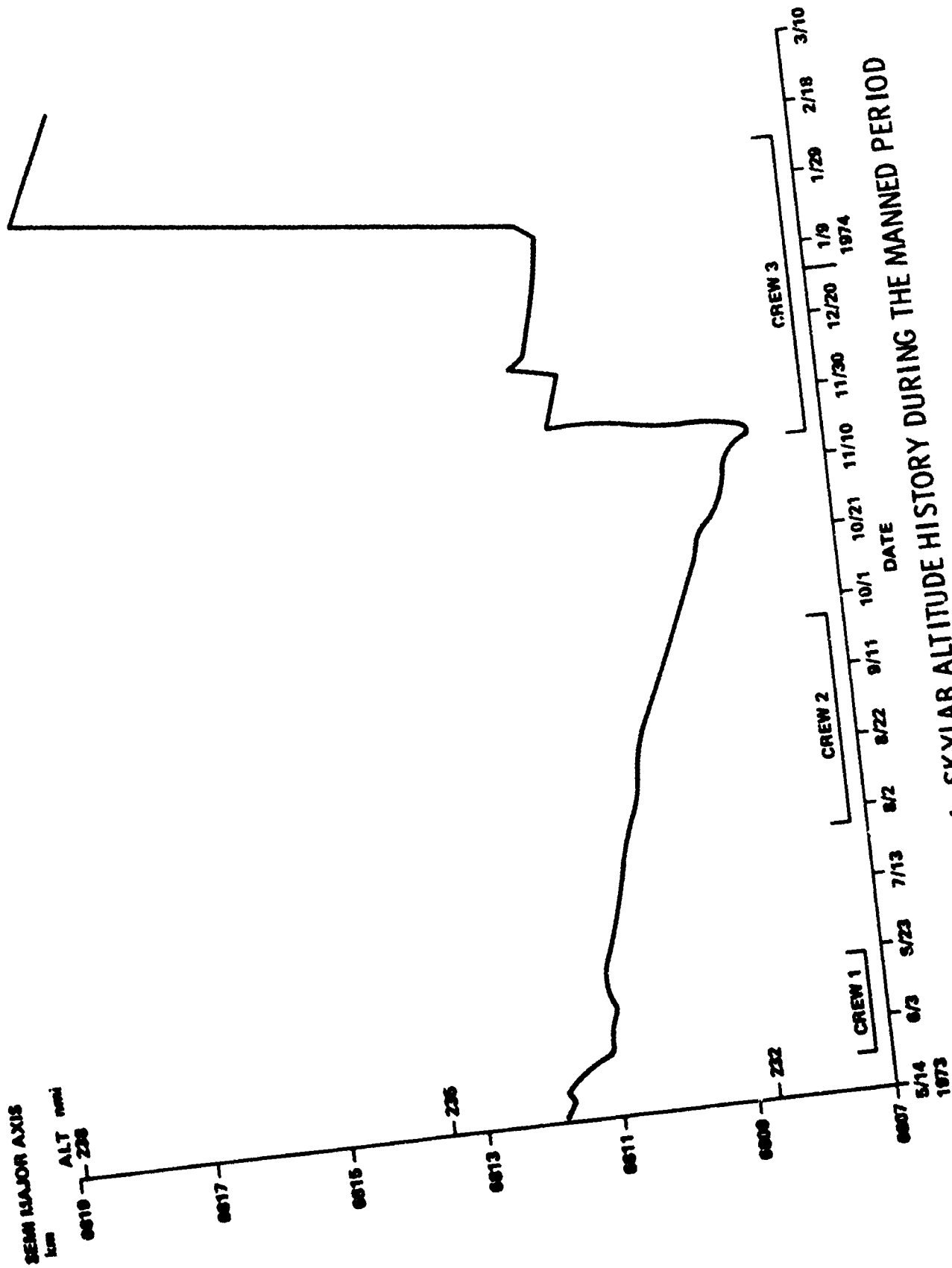


FIGURE 2-4 SKYLAB ALTITUDE HISTORY DURING THE MANNED PERIOD

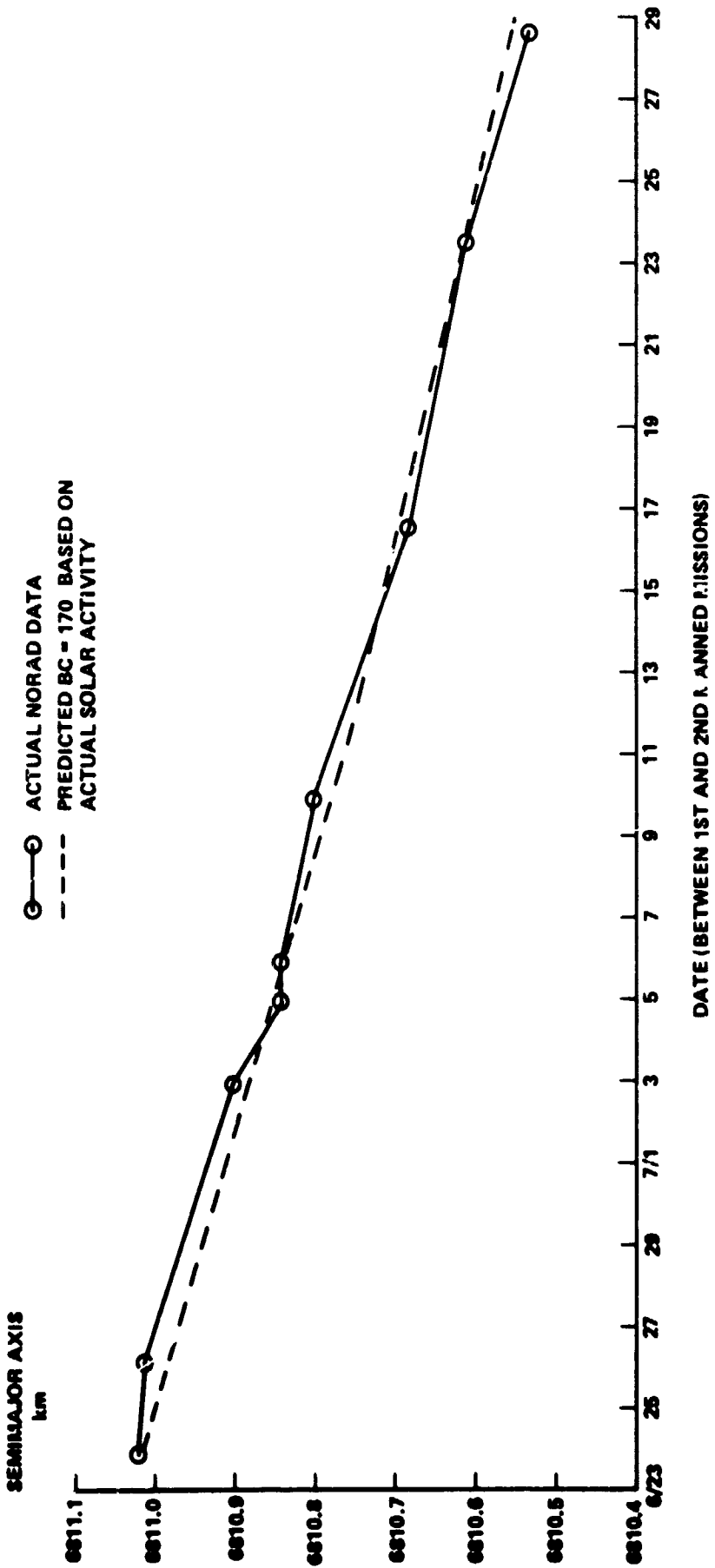


FIGURE 2-5 SKYLAB ACTUAL AND PREDICTED DECAY COMPARISON

3. ORBITAL DECAY DURING THE PASSIVE PERIOD (FEB. 1974 - JUNE 1978)

When the manned period was completed, Skylab was left in a gravity-gradient stabilized attitude (February 1974, to June 1978). This "gravitationally stable" attitude left Skylab exposed to the minimal forces that could cause tumbling. Skylab lifetime predictions were made on a regular basis during the first 2 years following deactivation. Then came a period of little interest in Skylab's expected lifetime. In 1977, when interest developed in a possible Skylab revisit, lifetime predictions were again made. These predictions are shown in Table 3-1 and graphically in Figure 3-1.

The first prediction shown assumed the solar inertial (SI) attitude to impact. A BC of 170 kg/m^2 was used, which was based upon the decay comparison between the first and second manned missions when Skylab was in a solar inertial attitude. (The fitting procedure was discussed in Section 2 of this report.) This BC gave a nominal predicted impact of July, 1981, and a $+2\sigma$ impact of September, 1978.

After the last crew left, Skylab was rotated to a gravity-gradient stabilized attitude with the docking adapter away from the earth. At that time, the OWS solar array was thought to be trailing the direction of flight. Using the theoretical aerodynamic data generated for the in-orbit Skylab configuration for α (angle of attack) and ϕ (roll angle) equal to 90° , gave a BC of 207 kg/m^2 (See Figure 2-1). This was used for the second lifetime prediction and gave a nominal impact of March, 1983, and a $+2\sigma$ impact of November, 1979. The increase in BC reflects the effect attitude has upon a satellite's lifetime. Preflight lifetime predictions assumed that Skylab would be left in the solar inertial attitude at the end of mission rather than the gravity-gradient attitude.

By the third prediction (September, 1974), enough actual decay data was available to determine the BC required to match the actual decay. Using the same procedures described in Section 2, a BC of 140 kg/m^2 was found to give a good decay comparison with the actual decay. Figure 3-2 shows the actual and predicted altitude decay from February 7, 1974 to August 26, 1974. Although not an exact fit, it is less than .2 km off. Using a BC of 140 kg/m^2 , the nominal impact was May, 1981; and the $+2\sigma$ impact was October, 1978.

Similarly, in 1975, the BC was determined to be 120 kg/m^2 to give the best comparison to the actual decay. Later, the BC value was determined to be 144 kg/m^2 . This value was

TABLE 3-1 SKYLAB LIFETIME (IMPACT) PREDICTIONS
DURING THE PASSIVE PERIOD

| Memo Date | Ballistic Coefficient (kg/m ²) | Predicted Impact (Mo/Yr or Mo/Day/Yr) | | |
|---------------|-----------------------------------------------|------------------------------------------|---------|-------|
| | | Nominal | +2σ | -2σ |
| Aug. 1, 1973 | 170 | 7/81 | 9/78 | 10/85 |
| Mar. 11, 1974 | 207 | 3/83 | 11/79 | 6/92 |
| Sep. 3, 1974 | 140 | 5/81 | 10/78 | 10/84 |
| Nov. 27, 1974 | 140 | 4/81 | 10/78 | 6/84 |
| Dec. 12, 1974 | 140 | 4/81 | 10/78 | 6/84 |
| Feb. 20, 1975 | 120 | 1/81 | 9/78 | 1/83 |
| May 20, 1975 | 120 | 12/80 | 9/78 | 11/82 |
| Jul. 27, 1977 | 144 | 12/2/80 | 8/21/79 | |
| Aug. 16, 1977 | 144 | 12/7/80 | 8/23/79 | |
| Oct. 15, 1977 | 144 | 4/16/80 | 5/31/79 | |
| Nov. 18, 1977 | 144 | 3/23/80 | 5/14/79 | |
| Dec. 18, 1977 | 144 | 3/14/80 | 5/22/79 | |
| Feb. 9, 1978 | 144 | 12/21/79 | 5/3/79 | |
| Apr. 10, 1973 | 144 | 8/29/79 | 4/13/79 | |

used for lifetime predictions until Skylab was reactivated in June, 1978. The 144 kg/m^2 became the official baseline for many comparison studies, which is the reason it was not changed for such a long period.

Figure 3-1 graphically illustrates the lifetime predictions that were previously discussed and summarized in Table 3-1. The 50% or nominal and 97.7% or $+2\sigma$ level predictions are shown. Note that for most of the passive period, the actual impact was bounded by the nominal and $+2\sigma$ predictions. For most of this period, the 2σ predictions were more accurate than the nominal; but as the solar activity predictions increased in magnitude, the nominal prediction moved closer to the actual impact. At the end of the passive period, the nominal prediction was more accurate than the $+2\sigma$ prediction.

The predicted solar activity data used for lifetime predictions did not vary much from 1973 to 1977. Figure 3-3 shows the nominal and 95% confidence level $F_{10.7}$ for three typical predictions. The nominal and 95% confidence level maximum were approximately 120 and 170, respectively. For comparison, the actual 162-day average $F_{10.7}$ is shown. The actual $F_{10.7}$ started increasing rapidly in 1977, and the later solar activity predictions reflected this increase (See Figure 3-4). By the middle of 1978, the predicted nominal solar flux maximum was almost as high as earlier 95% levels and the 95% confidence level had increased to greater than 200. Figure 3-5 shows the actual daily $F_{10.7}$, the actual 162-day average $F_{10.7}$, and the actual A_p for the time period 1974-1978. The 162-day average $F_{10.7}$ was below 80 until April, 1977. Then in July, 1977, there was a marked increase in $F_{10.7}$ and in November, 1977, an even greater increase. The solar activity predictions reflected this increased solar activity by increasing, and the lifetime predictions reflected the increase by decreasing.

Obviously there are some questions which needed to be answered concerning the variation in the BC derived from actual data. Several avenues of study were followed. A detailed look was taken at the daily solar activity and how it differed from the 13-month predicted data and how this affected the orbital decay. An extensive study was made of the atmospheric model used in LTIME. The theoretical aerodynamic data were used to determine if there was a correlation between expected attitudes and the derived BC.

A decay reconstruction analysis was made "after the fact" to find a constant BC to fit the Skylab decay for the entire passive period February 1974, to June 1978. Figure 3-6 shows the actual Skylab semimajor axis and the predicted decay for

three different ballistic coefficients, using the actual solar activity data as input to the atmospheric density model. The "best" decay comparison was found utilizing a ballistic coefficient of 130 kg/m^2 . For more detail on this comparison, Figures 3-7 and 3-8 are included, showing the predicted and the actual altitude decay and the decay rates during the passive period. The actual and predicted decay matched very well until the middle of 1976 when the predicted decay began to slightly exceed the actual decay. By the end of 1977, the actual decay was exceeding the predicted decay. Over the entire passive period, the actual and predicted altitudes differed no more than 1 km.

The anticipated (207) BC corresponding to the "as left" gravity-gradient (GG) attitude was much larger than the derived. As additional attitude information became available, analysis of the theoretical aerodynamics indicated a much smaller BC. Figures 3-9 and 3-10 show these aerodynamic data. The drag coefficient, C_D and the BC are shown as a function of the roll angle, ϕ , for angles of attack, α , of 80° , 90° , and 100° . In GG $\alpha = 90^\circ$, so 80° and 100° are also shown to give the variation. Similarly, in Figure 3-10, the roll moment coefficient is shown as a function of ϕ for the same α 's. Thus, considering only aerodynamic forces the Skylab would attempt to trim out at a ϕ of 137° . This would yield a BC of approximately 114 kg/m^2 , whereas 207 kg/m^2 corresponds to a $\phi = 90^\circ$, well away from this value. The much smaller BC derived from the decay comparison indicated that the Skylab OWS array was not exactly trailing as had originally been expected. In fact, further investigation revealed that Skylab had actually been left with the ATM trailing rather than the OWS solar array trailing. The BC for the ATM trailing attitude was 96 kg/m^2 . Thus, the gravity-gradient stabilized attitude of Skylab was not with the ATM or OWS solar array exactly trailing the direction of orbital motion.

Since this "preliminary analysis" considered only aerodynamic forces, a dynamics analysis was performed considering aerodynamic and gravity gradient forces (Reference 11). This analysis indicated that an equilibrium condition existed at a mean ϕ of 192° during the major portion of the passive period. This ϕ would yield a BC of 101 kg/m^2 . Initially, the vehicle's motion would have consisted of only small amplitude oscillations about the local vertical. However, instability is produced when a gravity gradient stabilized body is subjected to a torque (aerodynamic force) which forces it slightly away from the true gravity gradient equilibrium position. Given this instability, it was inevitable that large amplitude motion would build up. Because of the asymmetric OWS solar array configuration of Skylab, the

aerodynamic moments were unbalanced, producing a tendency to spin up about the long axis. An independent decay comparison was done at the Smithsonian Astrophysical Observatory (SAO) by some people involved in the development of the Jacchia density model. The SAO fit was a long-term fit over the entire passive period and resulted in a BC of 121 kg/m². These data (BC = 121 and 130) are in good agreement with the BC (101 to 114) derived from the dynamics simulation.

There are several possible explanations for the ballistic coefficient changes required to match the actual decay and the remaining differences. Primarily, the density model may not have sufficiently modeled the solar activity effects. Secondly, Skylab's attitude could have been changing. Finally, uncertainties in the actual orbital decay and solar data contribute to the bias. These effects are under further study and will be addressed later in a more detailed report (Reference 10) which will deal with this phenomena for Skylab and other satellites. In this report, this phenomena will be treated as a bias term required to cause the actual and predicted decay to match. However a brief summary of the scenario that Skylab might have undergone is given here to give the reader a brief explanation of the remaining differences.

Postflight analytical dynamics studies and actual flight experience indicated that there is no actual trim point, but the GG forces would predominate at low atmospheric density (higher altitudes and/or low solar activity), but aerodynamics would also influence the motion at higher atmospheric density (lower altitudes and/or high solar activity). This is also somewhat confirmed via data received from NORAD as to their analysis on the Skylab attitude, both right after the last crew left it and during the period of high interest prior to activation. This is further confirmed by the data gleaned via telemetry, right after activation and during the 10-day period after loss of attitude reference (Reference 12). While the atmospheric density is low, any motion would probably be small and the period of oscillation long, as the density increased the period would become smaller. This was confirmed by NORAD reports of their analysis of the Skylab attitude from 1974 to 1978. For the bulk of this time, August 1974 to January 1977, Skylab was near GG with little or no discernible motion. This was probably true through July 1977. At this time, the solar activity began to increase and the atmospheric density at Skylab's altitude showed a significant change (See Figure 3-11). The combination of aerodynamic forces and the increased solar activity caused an increase in Skylab's motion. From November 1977, until January 1978, information available indicated that Skylab went from a barely discernible to a very noticeable motion, finally breaking out of the near GG attitude. Data received via telemetry after activation

showed Skylab spinning with rates near $1^\circ/\text{s}$ and increasing. Data received in July of 1977 during the time following the loss of attitude reference show rates building up very rapidly to spin rates almost double that of the activation data.

Additionally, as mentioned above, the atmospheric density model has a bias. This bias tends to vary with changes in solar activity. The reconstructed BC to fit observed decay appears lower as the solar activity goes up, and higher as it decreases. Over a short term effect, these biases can be quite high (>20%), but over the long haul is about 10%. This was all identified as a result of the study of the atmospheric density model used in LTIME.

Two items were modified in LTIME, both input data items. More data points were added to the density tables in the atmospheric density model, and it was determined that the average $F_{10.7}$ cm flux, $\bar{F}_{10.7}$, should be a 162-day (± 81 days) average rather than an 81-day running mean (-81 days).

Thus, the apparent sequence of events was that Skylab was left in a near GG (only longitudinal or X axis GG), with the Solar Array Systems left broadside. Since this is not a trim from either GG or aerodynamic consideration, it rolled towards a roll trim point and started a slow, very slow initially, oscillation about the 192° roll trim mentioned earlier and stayed this way until around July, 1977. At that time, the solar activity began increasing significantly with a corresponding increase in atmospheric density (See Figures 3-4 and 3-11). The BC appeared to change, and indeed the motion probably began increasing. As these trends continued, the vehicle finally broke out of the near GG attitude it had been in for such a long time and began a "random" tumble, probably by November or December, 1977. Later dynamics analysis using theoretical aerodynamics indicated a BC range from 135 to 160 kg/m^2 with the most likely value for this tumble of 150 kg/m^2 .

With the increased motion of Skylab, the theoretical ballistic coefficient was expected to increase toward that of a random tumble. However, toward the end of 1977, as the solar activity began to increase, the decay comparisons indicated that a smaller ballistic coefficient was required. This unexpected behavior was determined to be a density model bias which was due to the model overcompensating the density for sharp increases in the solar activity (phenomena discussed further in Section 4 of this report). These are the factors that caused the inconsistencies in the ballistic coefficient.

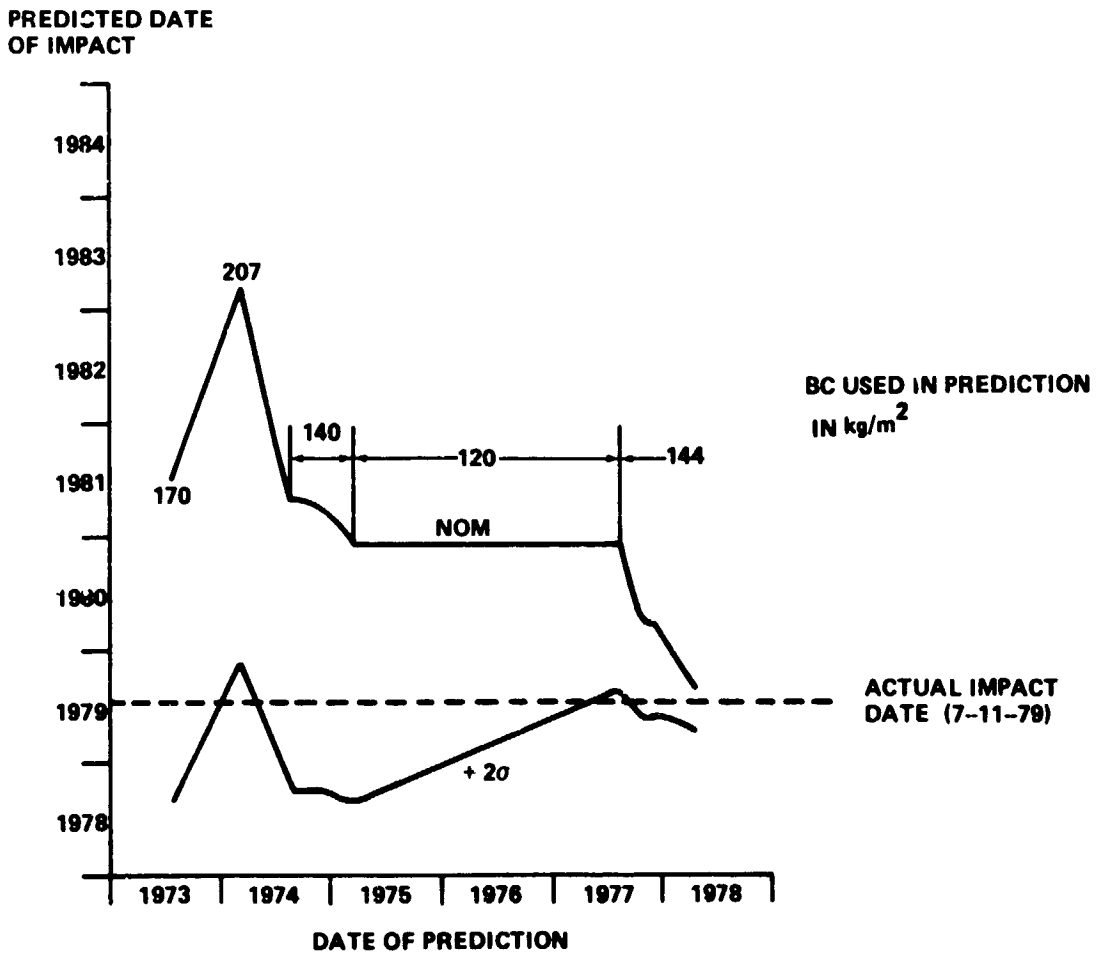


FIGURE 3-1 SKYLAB LIFETIME PREDICTIONS DURING THE PASSIVE PERIOD

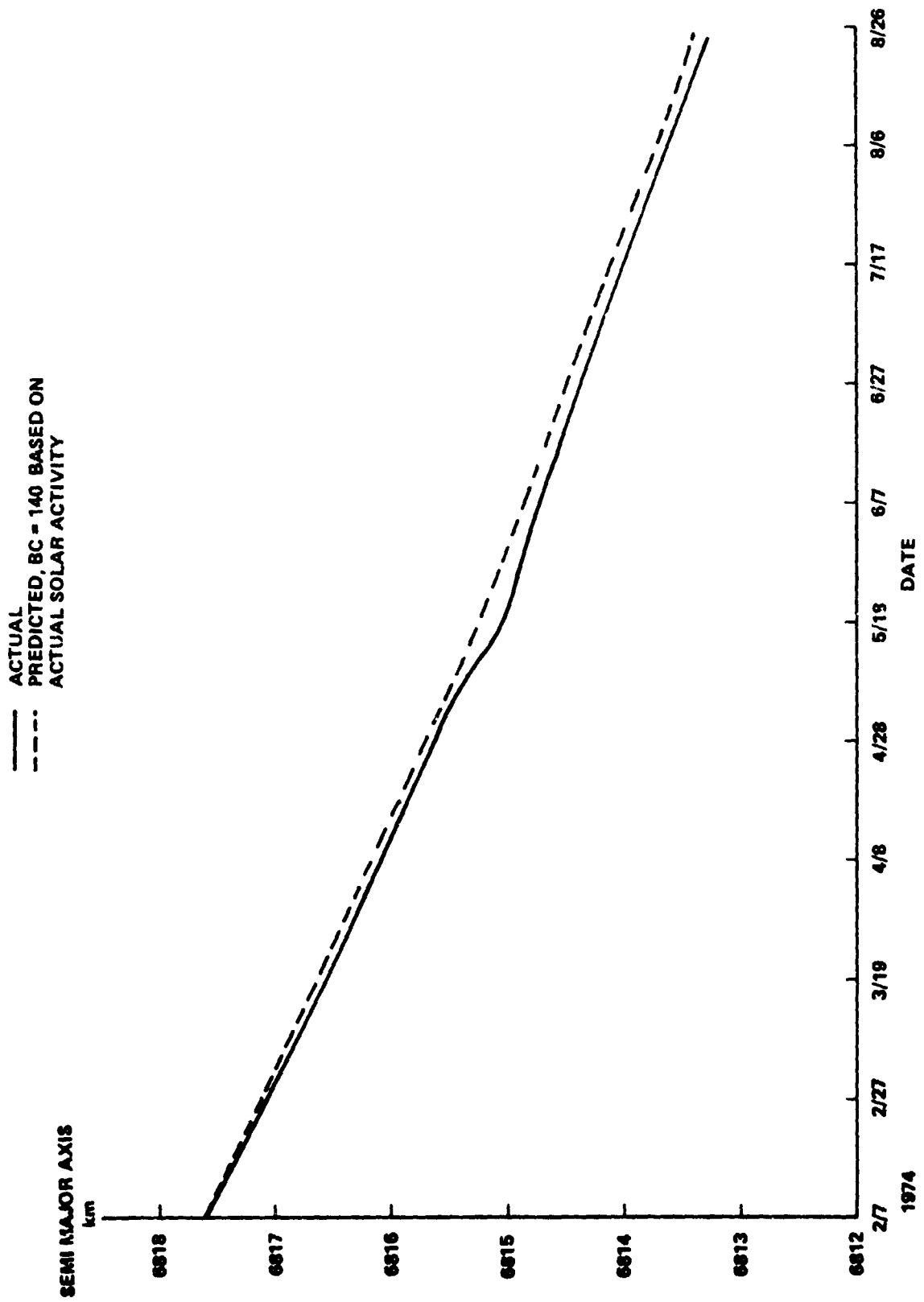


FIGURE 3-2 ACTUAL AND PREDICTED DECAY COMPARISON

SOLAR FLUX, $\bar{F}_{10.7}$

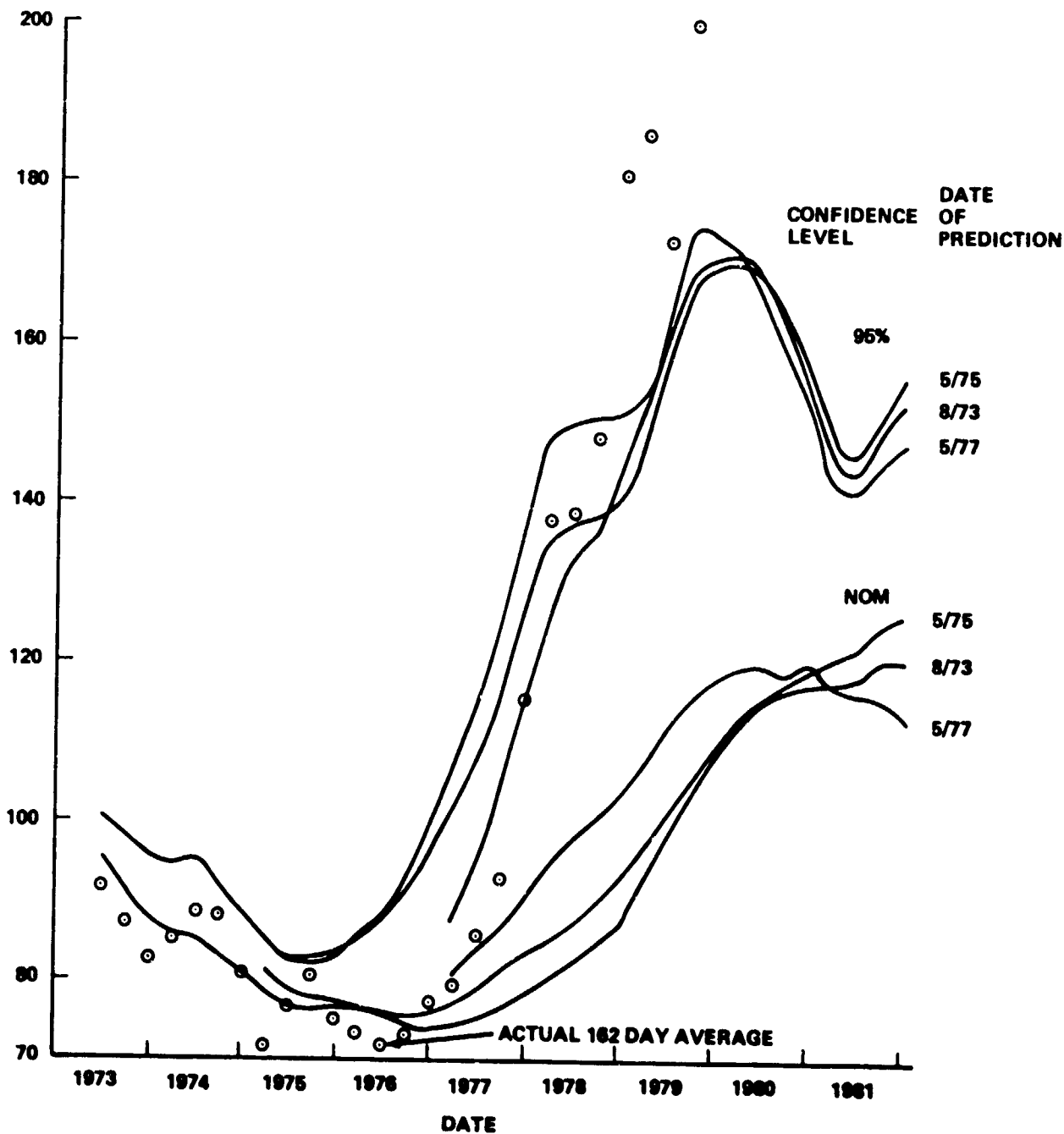


FIGURE 3-3 ACTUAL AND PREDICTED SOLAR FLUX

SOLAR FLUX, $\bar{F}_{10.7}$

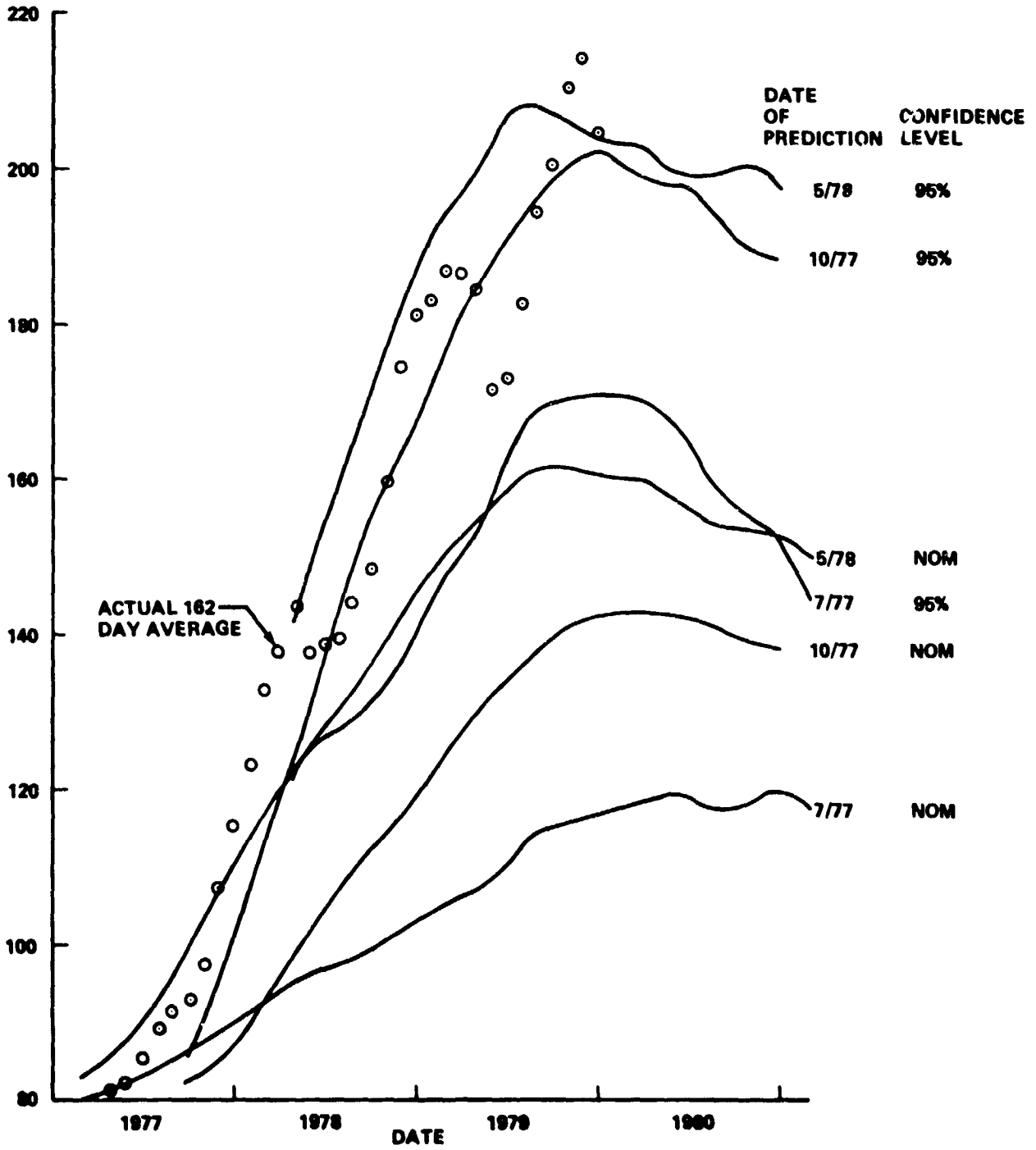


FIGURE 3-4 ACTUAL AND PREDICTED SOLAR FLUX

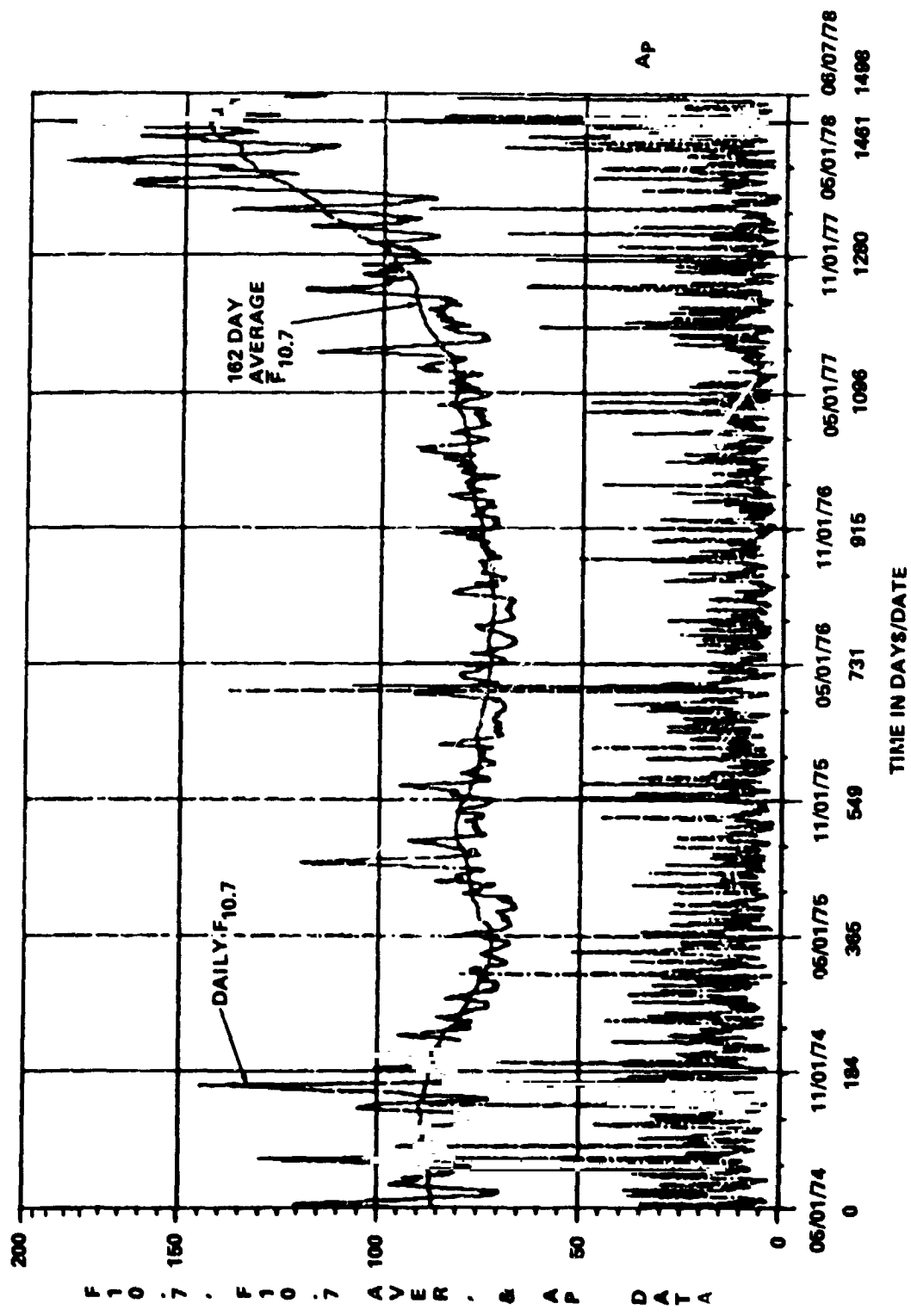


FIGURE 3-5 ACTUAL SOLAR ACTIVITY DATA

SEMI-MAJOR AXIS
km

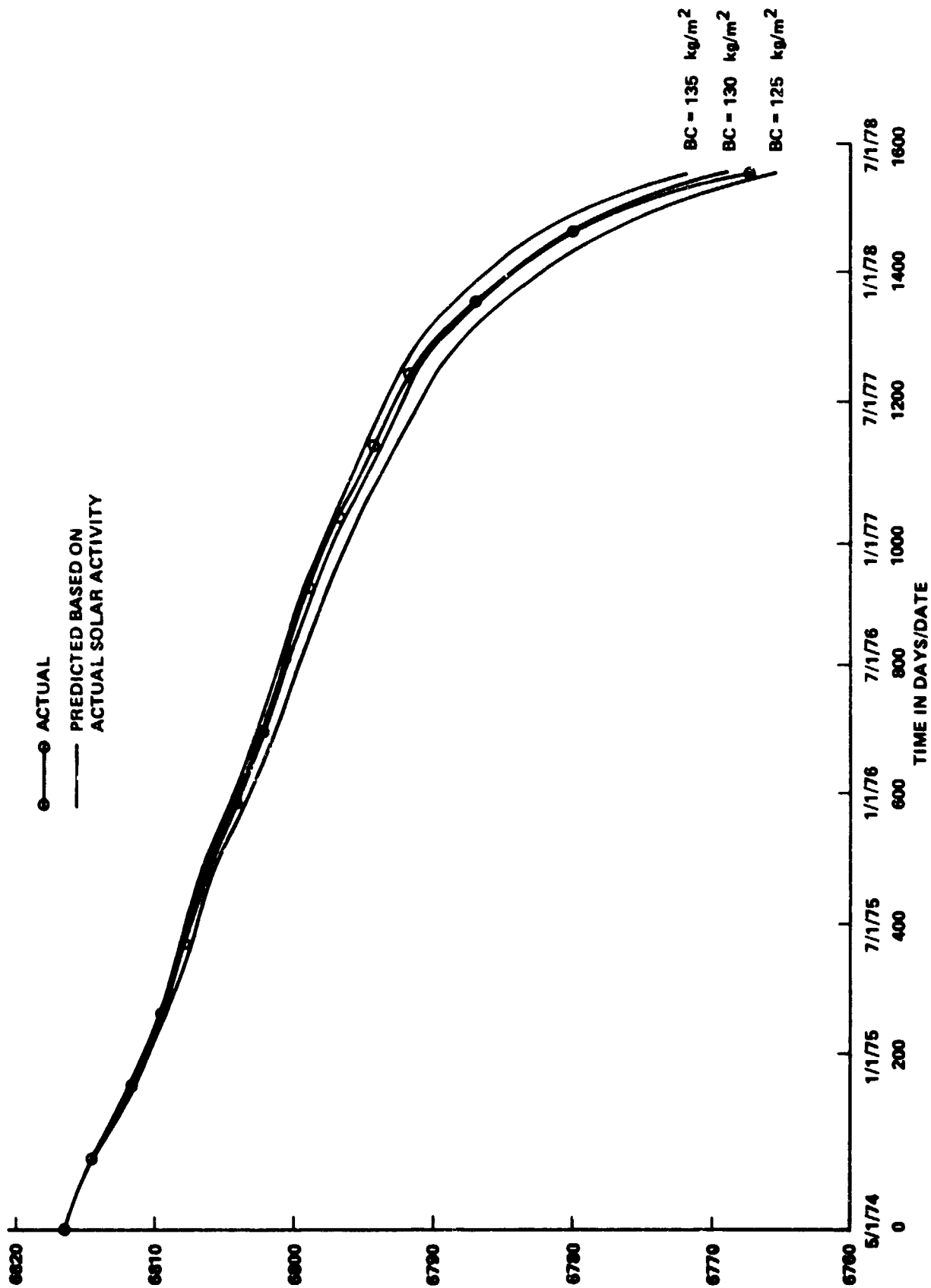


FIGURE 3-6 SKYLAB ACTUAL AND PREDICTED DECAY COMPARISON

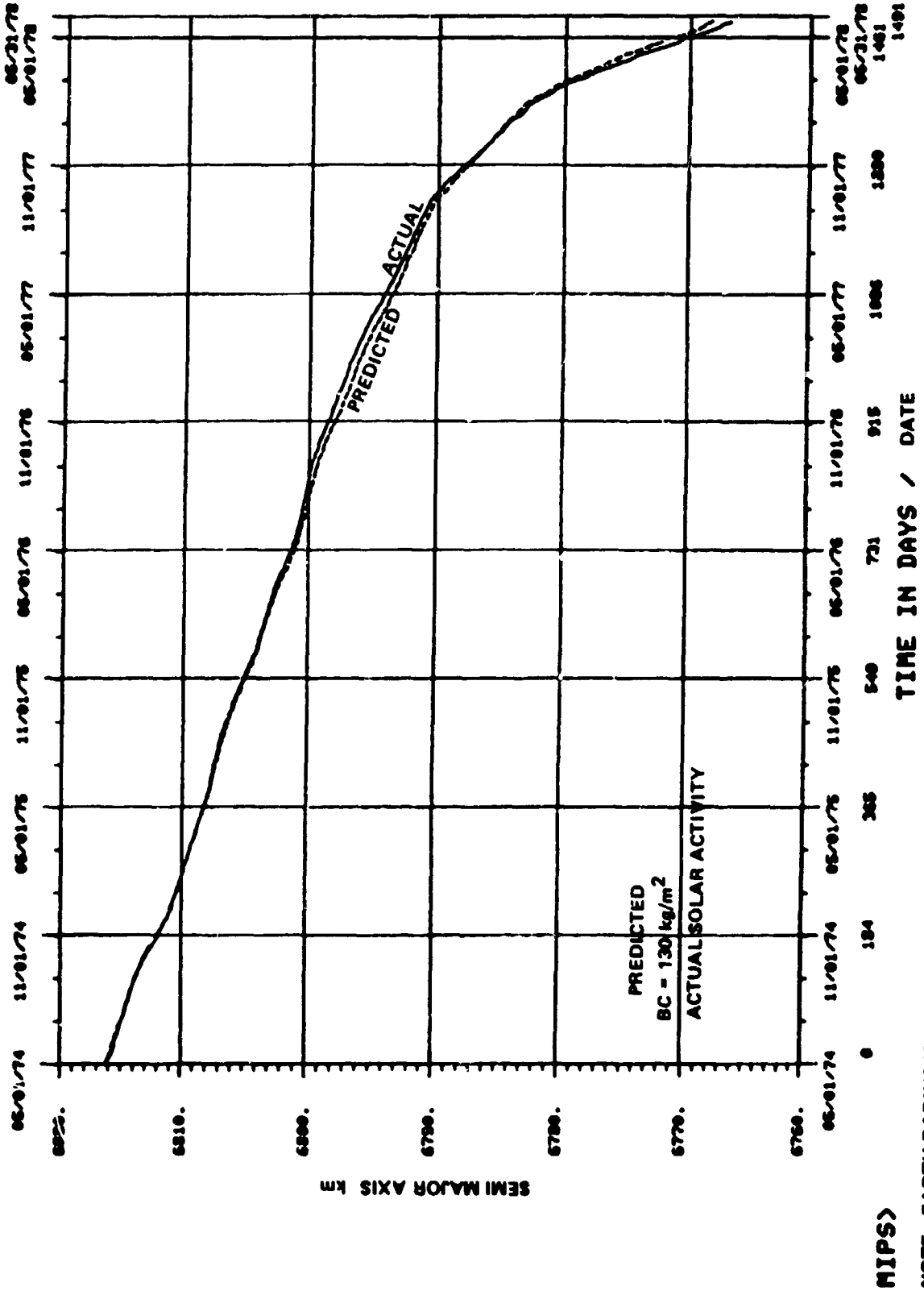
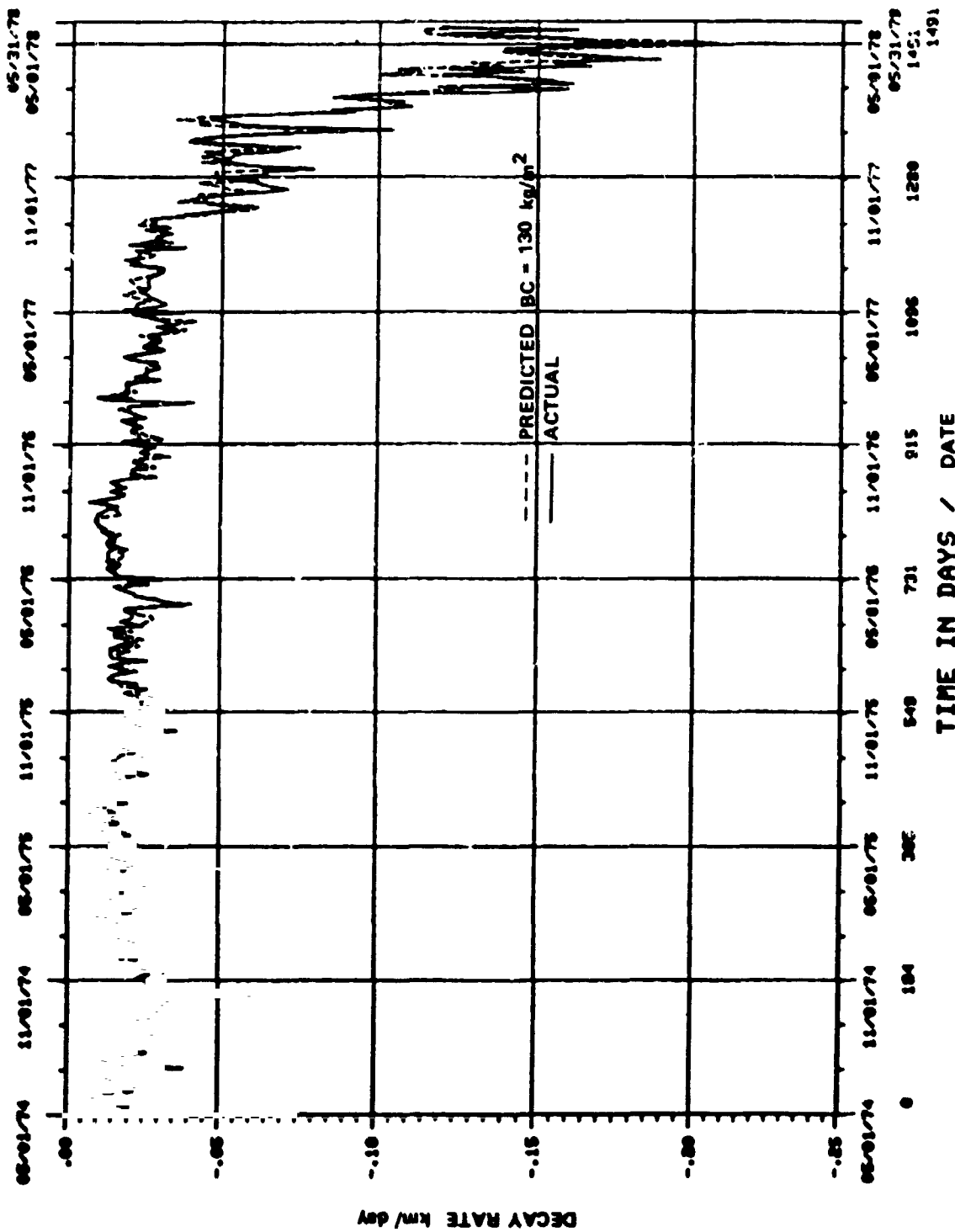


FIGURE 3-7 PREDICTED AND ACTUAL DECAY

NOTE: EARTH RADIUS IS ~ 6378 km



MIPS>

FIGURE 3-8 PREDICTED AND ACTUAL DECAY RATES

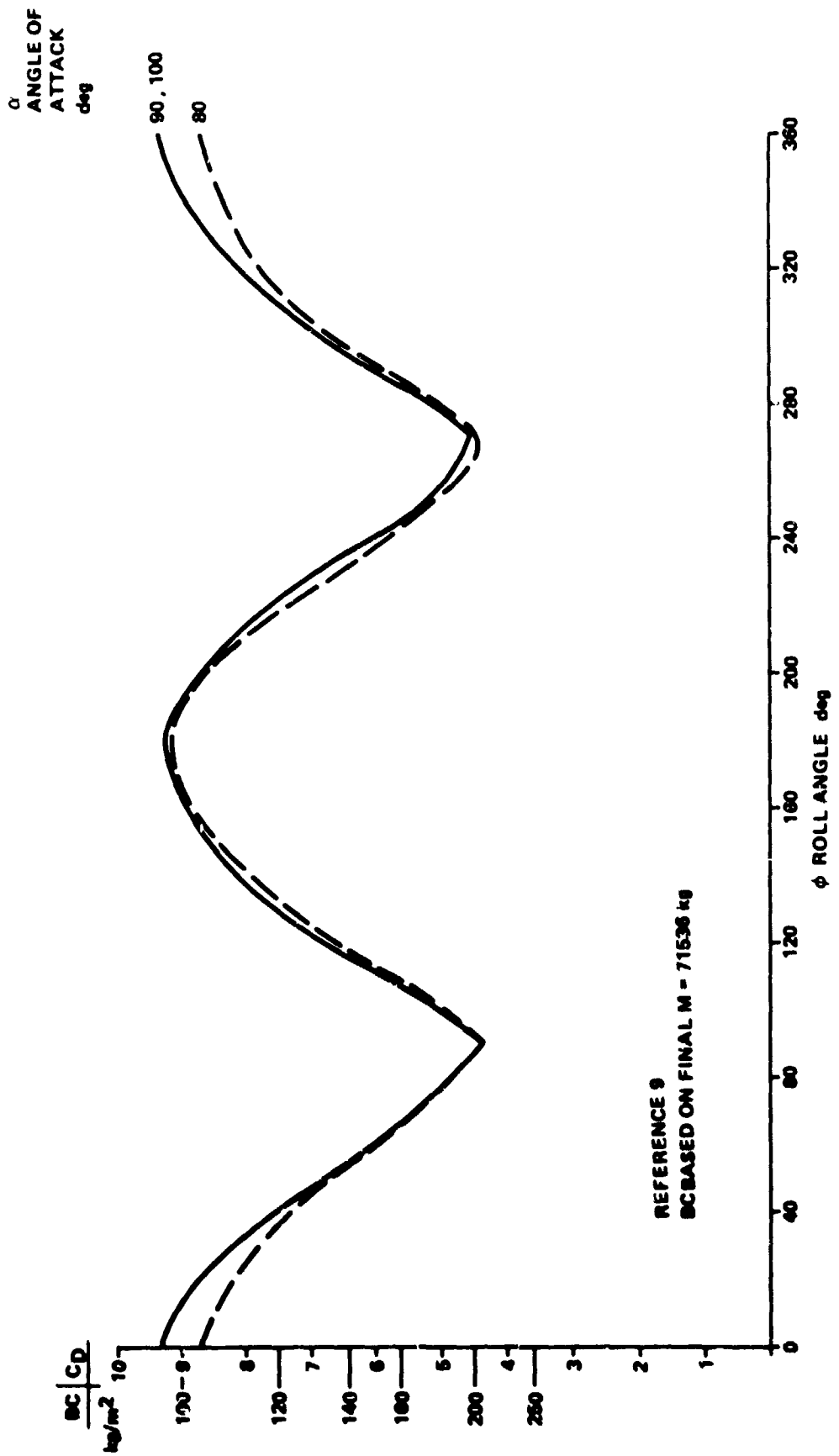


FIGURE 3-9 IN ORBIT AERODYNAMIC DATA

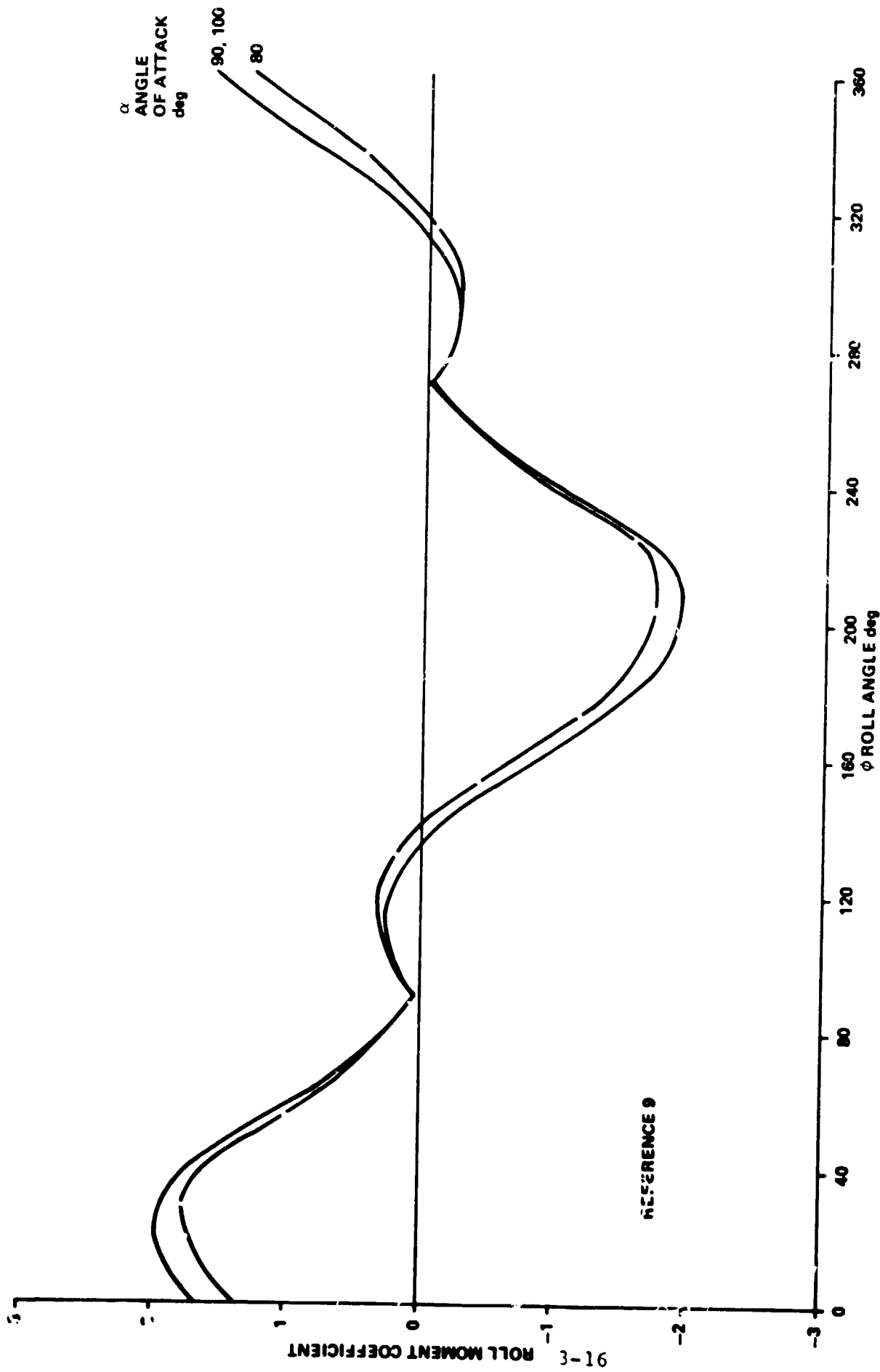
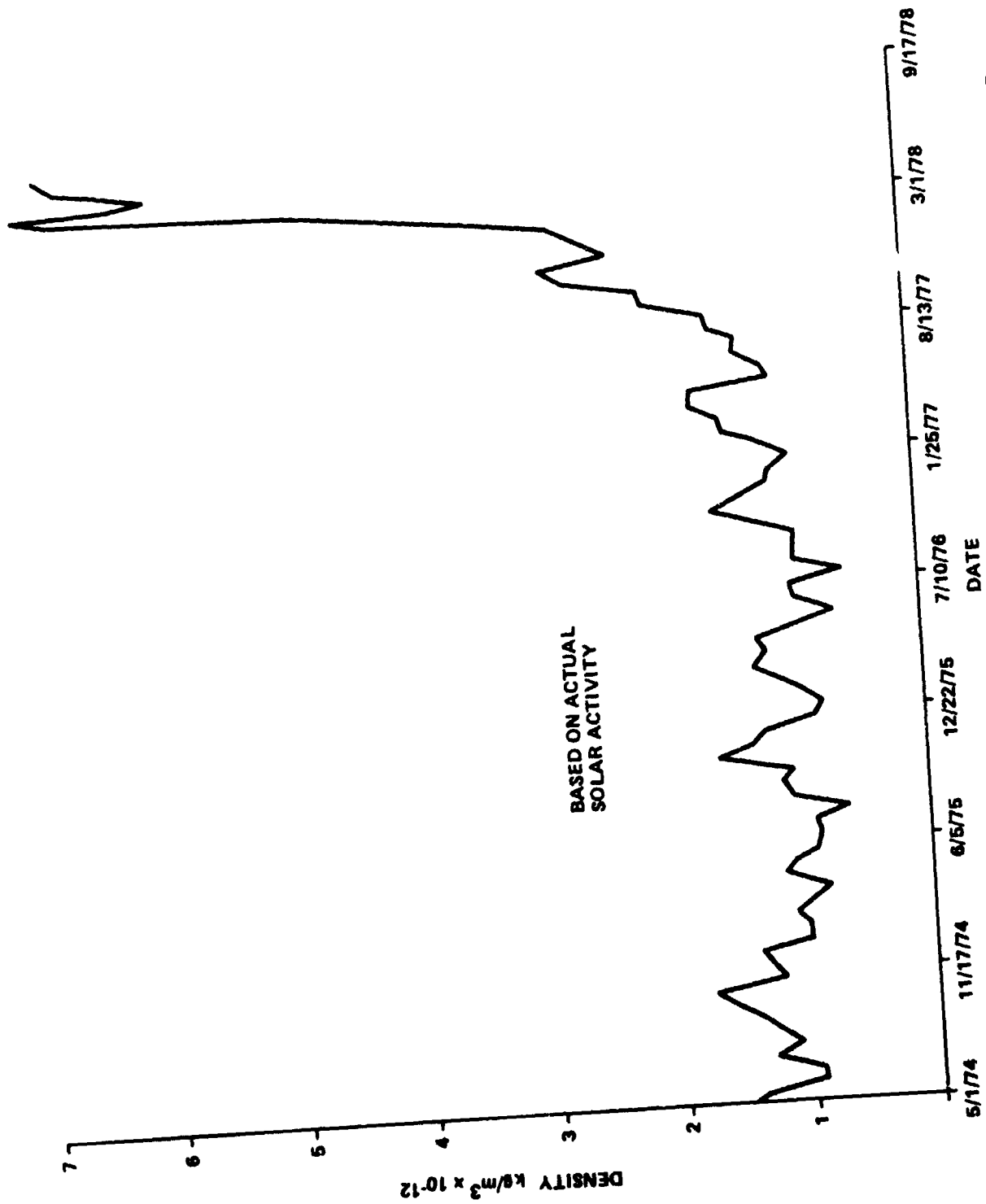


FIGURE 3-10 ROLL MOMENT COEFFICIENT VS ROLL ANGLE



BASED ON ACTUAL
 SOLAR ACTIVITY

FIGURE 3-11 ATMOSPHERIC DENSITY DURING THE PASSIVE PERIOD

4. ORBITAL DECAY DURING THE REACTIVATED SKYLAB PERIOD (JUNE 1978 - JULY 1979)

At the end of the manned period, Skylab was expected to remain in orbit between 5½ and 9 years (November 1979, to March 1983). This prediction was based on the March, 1974 prediction of solar cycle 21, a theoretical ballistic coefficient of 207 kg/m² and the assumption that Skylab would remain in a "gravity gradient" attitude with the ATM forward until impact. By the fall of 1977, it was apparent that Skylab had experienced a significant increase in orbital decay due to the unexpected sharp increase in the solar activity at the beginning of Cycle 21, which further reduced Skylab's expected lifetime. Skylab was then predicted to reenter the earth's atmosphere in late 1978 or early 1979 unless something was done to reduce the drag forces acting upon it.

It was necessary to make a decision to either accept an early uncontrolled reentry of Skylab or to attempt to actively control Skylab in a lower drag attitude, thereby extending its orbital lifetime until a Shuttle mission could effect a boost or deorbit maneuver with Skylab. From the fall of 1977 on, it became increasingly important to accurately determine the remaining lifetime of Skylab in order to ascertain which of several options might be available to NASA in regard to the disposition of Skylab. As the planning progressed and the various options were selected, their effect on mission lifetime was continually monitored.

Recontact was established with Skylab March 6-13, 1978. Systems reactivation took place from April 24 - June 8, 1978. Skylab was maintained in several different operating modes during the reactivated period. The solar inertial (SI) mode had been the major operating mode during the manned missions. When initial plans were made to extend the orbital lifetime of Skylab, the end-on-velocity-vector (EOVV) mode was developed to utilize its near minimum drag characteristics. After plans for a reboost/deorbit mission were abandoned, the torque equilibrium attitude (TEA) mode was developed to control the vehicle as the orbit decayed to the lower altitudes toward reentry with the resultant increased aerodynamic torques.

Following systems reactivation, Skylab was maneuvered into the EOVV attitude for the purpose of extending its orbital lifetime. This began on July 11, 1978, and lasted until January 25, 1979. Skylab was then returned to the SI attitude. The SI mode was primarily a low maintenance

holding pattern mode for vehicle control and maximum electrical power, while preparations were made for entering the TEA mode. The high drag TEA mode was used from June 20, 1979 until the vehicle was tumbled just prior to reentry on July 11, 1979. The maneuver to effect a tumble was initiated at 7:45 GMT on July 11, 1979. The official NORAD-determined impact occurred at 16:37:28 on July 11, 1979.

4.1 ORBITAL DECAY DURING THE EOVV PERIOD (JUNE 1979 - JANUARY 1979)

The EOVV mode was a near minimum drag attitude with the relatively small surface areas of the front or back ends of Skylab being pointed approximately along the velocity vector. The vehicle was then rolled so that its solar arrays pointed toward the sun at orbital noon. The sequence of events during the low drag attitude management is shown in Table 4.1-1.

The EOVV mode was utilized in the first part of the Skylab Reactivation period to reduce the Skylab decay rate. It was desired to extend the orbital life of Skylab until a reboost/deorbit mission by the Space Shuttle could be accomplished. The effect of the EOVV mode on the decay rate is illustrated by the altitude profile in Figure 4.1-1. There was a noticeable decrease in orbit decay rate (from 128 m/day to 51 m/day average) when Skylab was first maneuvered into the EOVV attitude in June, 1978. Likewise, an increase in the orbit decay rate (from 144 m/day to 385 m/day average) occurred when Skylab was maneuvered from the EOVV attitude to the Solar Inertial attitude in January, 1979. The average theoretical BC in the EOVV mode was originally estimated to be 325 kg/m². Lifetime predictions using this BC are shown in Table 4.1-2. For these predictions EOVV attitude was assumed to be held until impact.

On a regular basis, decay comparisons were made to determine the BC necessary to fit the actual decay. Daily values are available for $F_{10.7}$ and A_p , but there is a problem for $\bar{F}_{10.7}$. Since $\bar{F}_{10.7}$ is supposed to be a 162-day average (81 days prior to the date and 81 days past the date) in the atmospheric model, the most recent known value of $\bar{F}_{10.7}$ is 81 days old. For the 81 days in the future, predicted $\bar{F}_{10.7}$ values were used with $F_{10.7} = \bar{F}_{10.7}$. This introduces an uncertainty into the procedure. To reduce this uncertainty, a 55-day average was used for $\bar{F}_{10.7}$ in some runs. This required only 27 days of future $F_{10.7}$ values, which is one solar rotation. The 27-day predictions of $F_{10.7}$ are available from NOAA but are not very reliable, as illustrated in Figure 4.1-2. Thus, the predicted nominal values of $\bar{F}_{10.7}$ were generally used.

In December, 1978, a decay comparison was made to determine the BC. The starting date for this comparison was August 2 so that the abrupt BC changes between June 9 and July 26 would not have to be modeled. Figure 4.1-3 shows the daily $F_{10.7}$, the 55-day average $\bar{F}_{10.7}$, and A_p . Figure 4.1-4 shows the actual decay and the predicted decay for a BC of

TABLE 4.1-1 ATTITUDE HISTORY DURING LOW DRAG PERIOD

| <u>Date</u> | <u>Event</u> |
|------------------|-------------------------------------|
| June 9, 1978 | Initial SI Acquired |
| June 11, 1978 | Initial EOVV Acquired |
| June 28, 1978 | Retreat to SI |
| July 6, 1978 | Second EOVV Acquired |
| July 9, 1978 | Loss of Attitude Reference |
| July 19, 1978 | SI Acquired |
| July 25, 1978 | Third EOVV Acquired |
| January 25, 1979 | End of Low Drag Attitude Management |

TABLE 4.1-2 LIFETIME PREDICTIONS WHILE IN EOVV

| Vector Date | Date of MSFC Solar Activity Prediction | Predicted Date To Reach | | | |
|-------------|----------------------------------------|-------------------------|----------|---------|---------|
| | | 150 nmi | | Impact | |
| | | NOM* | +2σ * | NOM* | +2σ * |
| 7/4/78 | July, 1978 | 4/13/80 | 11/6/79 | 6/26/80 | 1/3/80 |
| 7/25/78 | August, 1978 | 3/28/80 | 11/4/79 | 6/18/80 | 1/1/80 |
| 8/21/78 | September, 1978 | 4/13/80 | 11/22/79 | 6/27/80 | 1/22/80 |
| 9/6/78 | September, 1978 | 4/10/80 | 11/23/79 | 6/24/80 | 1/23/80 |
| 9/29/78 | September, 1978 | 4/9/80 | 11/25/79 | 6/23/80 | 1/25/80 |
| 9/29/78 | October, 1978 | 4/5/80 | 12/2/79 | 6/18/80 | 2/3/80 |
| 10/27/78 | October, 1978 | 3/31/80 | 12/4/79 | 6/12/80 | 2/4/80 |
| 11/2/78 | November, 1978 | 3/8/80 | 11/24/79 | 5/16/80 | 1/24/80 |
| 11/27/78 | November, 1978 | 3/3/80 | 11/25/80 | 5/11/80 | 1/25/80 |
| 12/3/78 | December, 1978 | 2/22/80 | 11/25/80 | 4/30/80 | 1/23/80 |
| 1/1/79 | December, 1978 | 2/18/80 | 11/26/80 | 4/26/80 | 1/24/80 |
| 1/1/79 | January, 1979 | 2/9/80 | 11/20/79 | 4/17/80 | 1/18/80 |

*Solar Activity Probability Levels
 Nominal = 50%
 +2σ = 97.7%

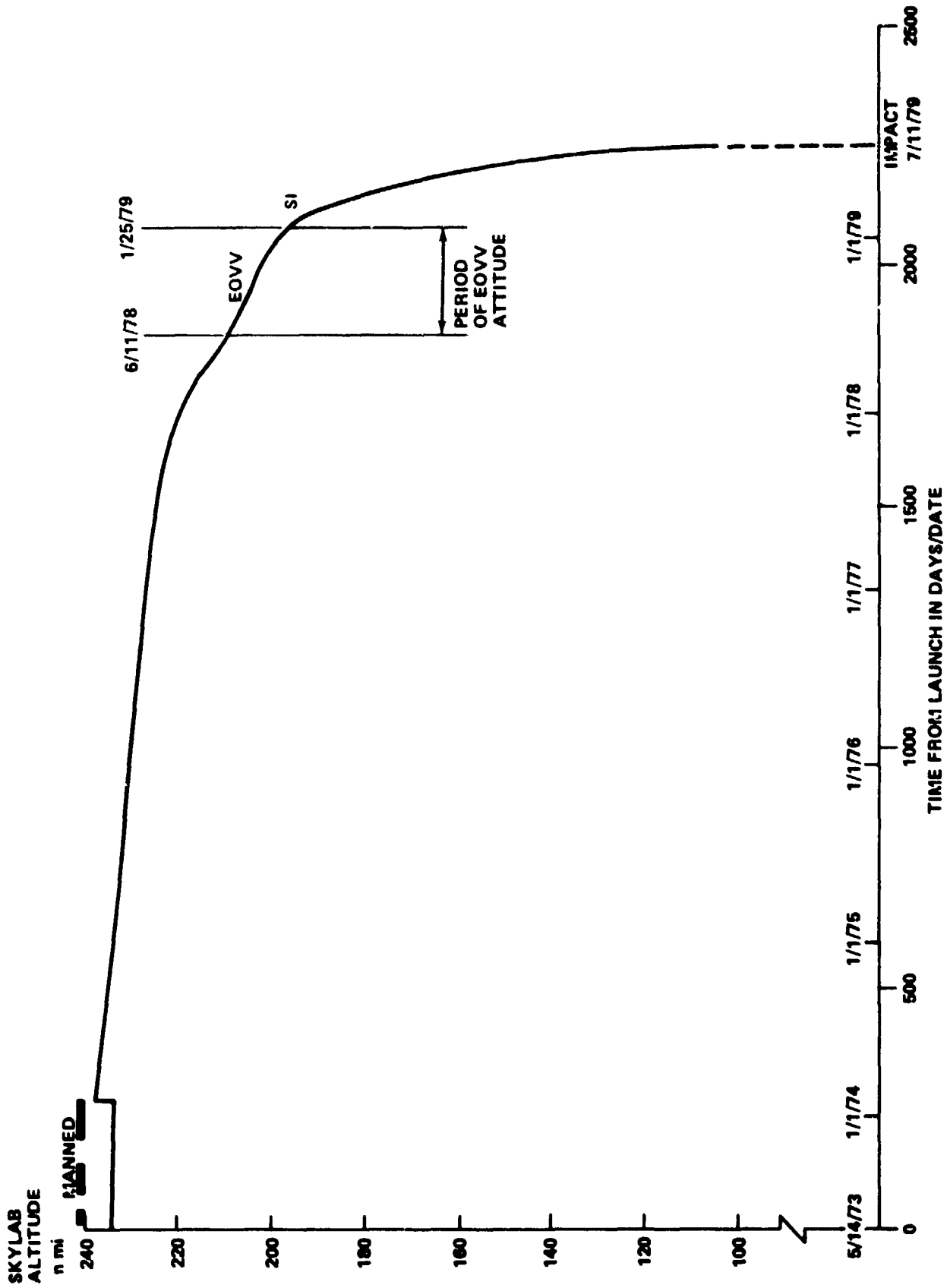


FIGURE 4.1-1 SKYLAB ORBITAL DECAY FROM LAUNCH TO IMPACT

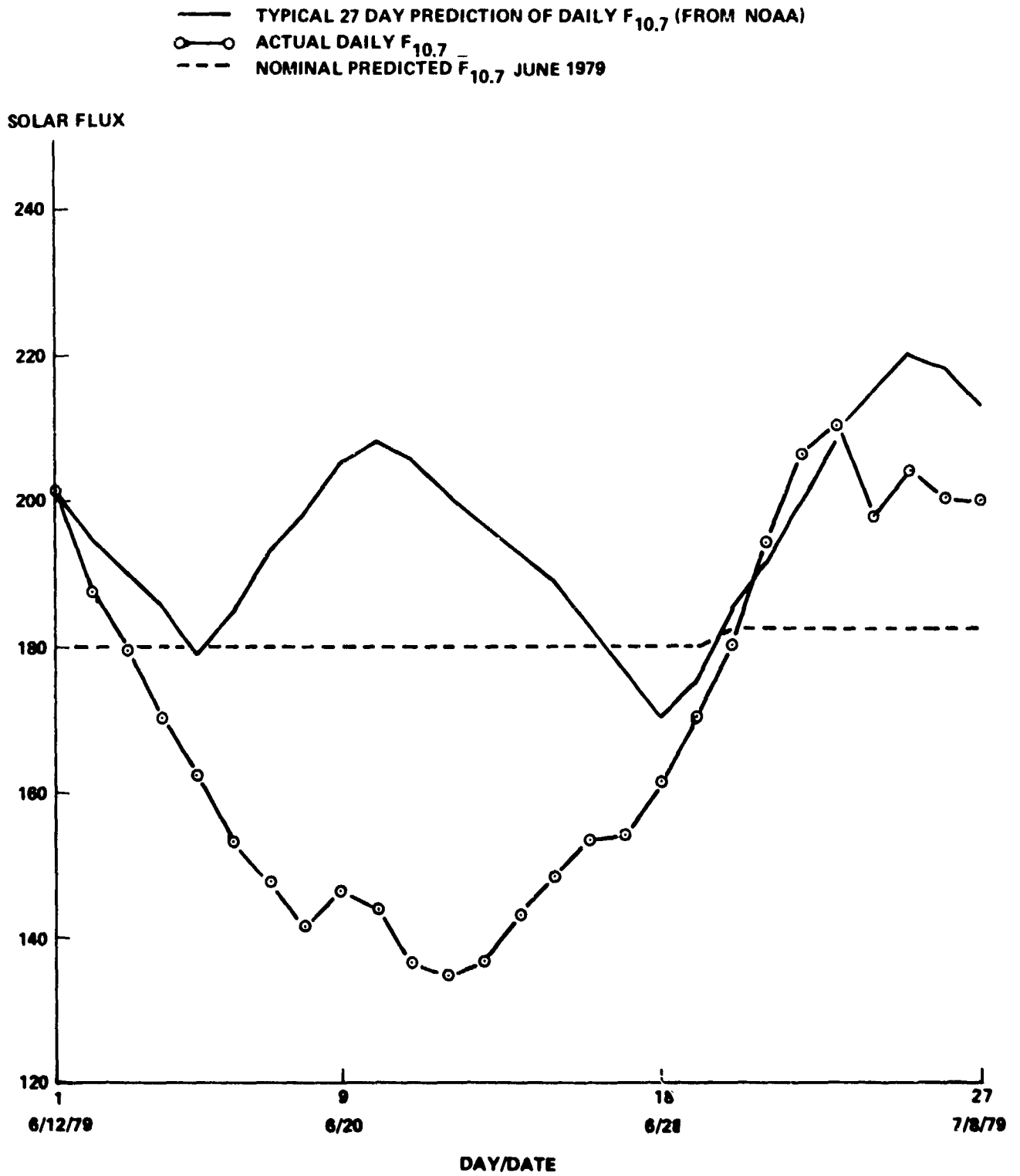


FIGURE 4.1-2 COMPARISON OF PREDICTED AND ACTUAL SOLAR FLUX

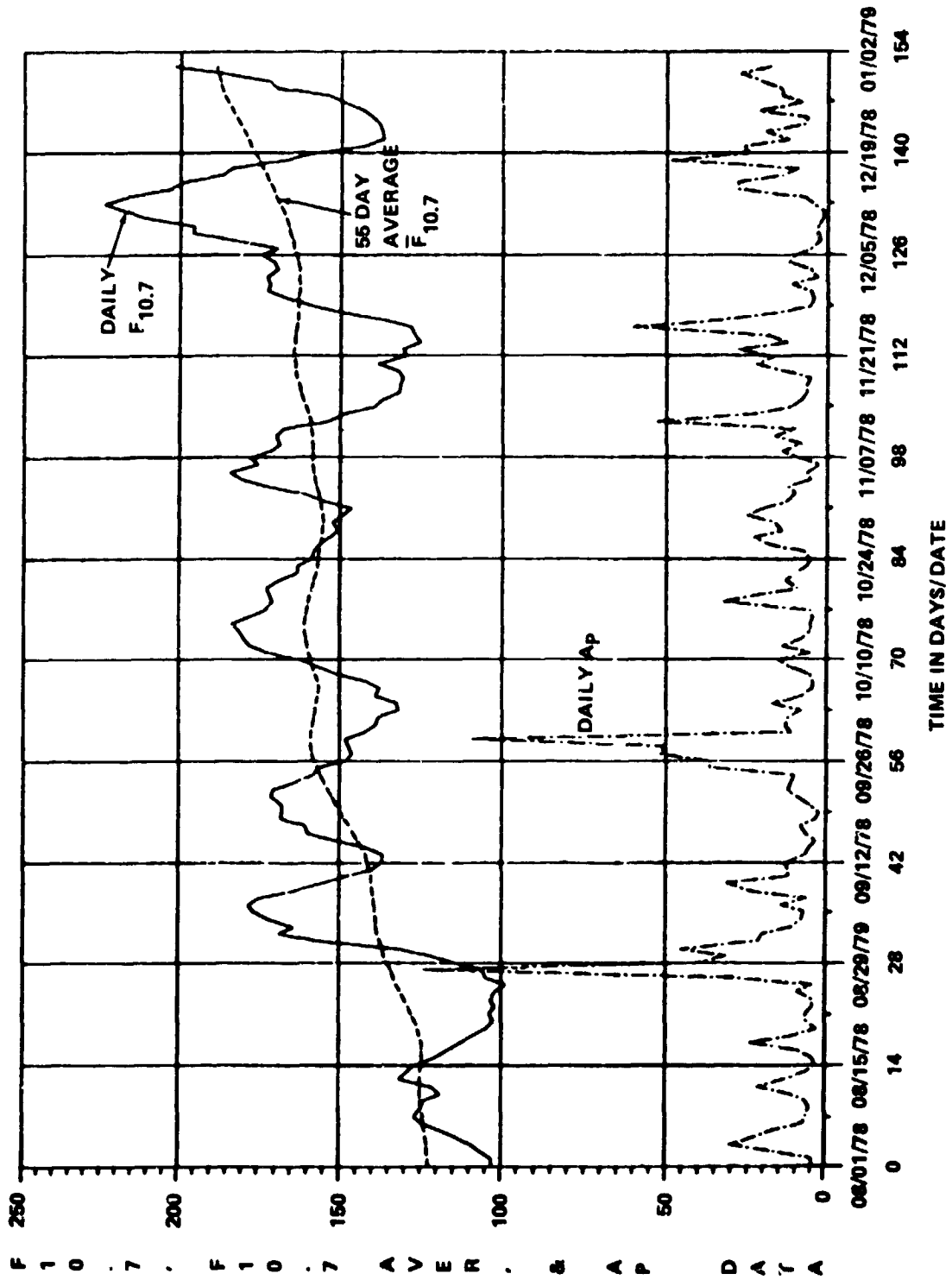


FIGURE 4.1-3 ACTUAL SOLAR ACTIVITY DATA

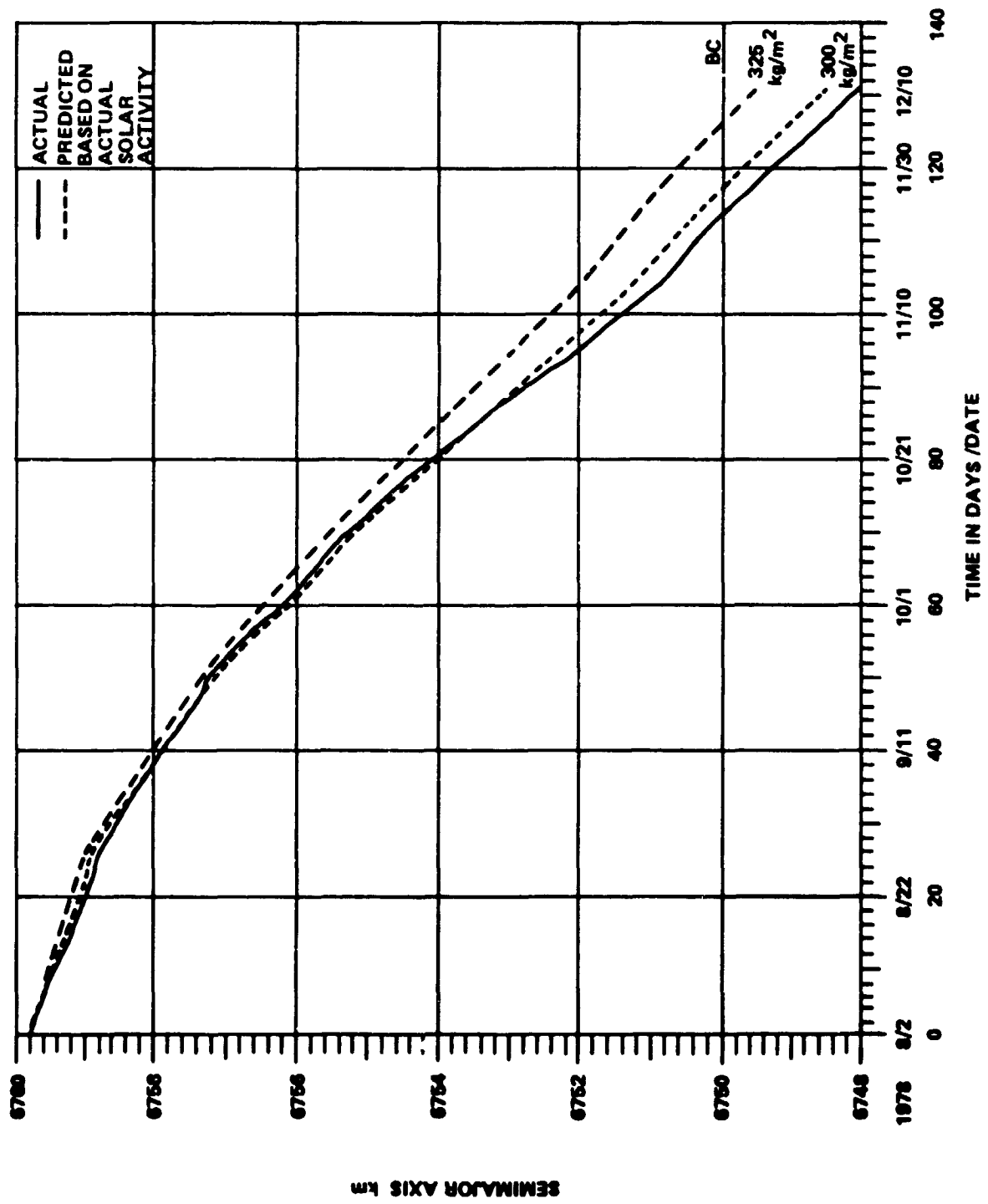


FIGURE 4.1-4 EOVV DECAY COMPARISON FOR AVERAGED BALLISTIC COEFFICIENT

300 and a BC of 325 kg/m². The BC of 300 kg/m² fit the actual decay much better than the BC of 325 kg/m², but a more detailed modeling of the Skylab BC was required.

Since the long axis of the vehicle was essentially in the orbit plane and the vehicle roll angle was a function of the beta angle (angle between earth-sun line and orbital plane), it was possible to derive a time history of the theoretical BC as a function of beta angle. Figure 4.1-5 shows the beta angle history for the entire EOVV time period from June 9, 1978 to January 25, 1979. Figure 4.1-6 shows the theoretical BC history for this time period. The BC during the EOVV mode varied from 303 to 333 kg/m². Figure 4.1-7 shows the actual decay and predicted decay for a BC of 325 kg/m² (constant) and a BC varying with beta angle.

After the fact, when the actual 162-day average $\bar{F}_{10.7}$ was known, another BC fit was made. Figure 4.1-8 shows the daily $F_{10.7}$, the 162-day average $\bar{F}_{10.7}$, and predicted nominal and $+2\sigma$ $\bar{F}_{10.7}$. Two sets of predicted $\bar{F}_{10.7}$ are shown: August 1978, and December 1978. However, using the final solar data and BC as a function of beta angle did not cause the predicted decay to match the actual decay after about two months.

This behavior is attributed in part to rapid changes in the solar activity that are not totally accounted for in the orbital atmospheric density model utilized in the orbit lifetime prediction program. This phenomenon was verified in house and in discussions with SAO (Smithsonian Astrophysical Observatory), whose model forms the basis for Reference 4, as well as by observation and comparison with other satellites. When a 6% bias was added to the density as computed by the Jacchia density model, the predicted decay matched the actual quite well. Figure 4.1-9 shows the actual decay and the predicted decay with and without the 6% bias. Figures 4.1-10 - 4.1-13 show the predicted and actual decay rates and the ratio of the decay rates for no bias and 6% density bias respectively.

The average value of the theoretical BC (as a function of beta angle) during the EOVV period was 313 kg/m². The time spent in the EOVV attitude extended Skylab's orbital lifetime approximately 3½ months. If Skylab had remained in the EOVV attitude until impact, reentry would have occurred in January 1980.

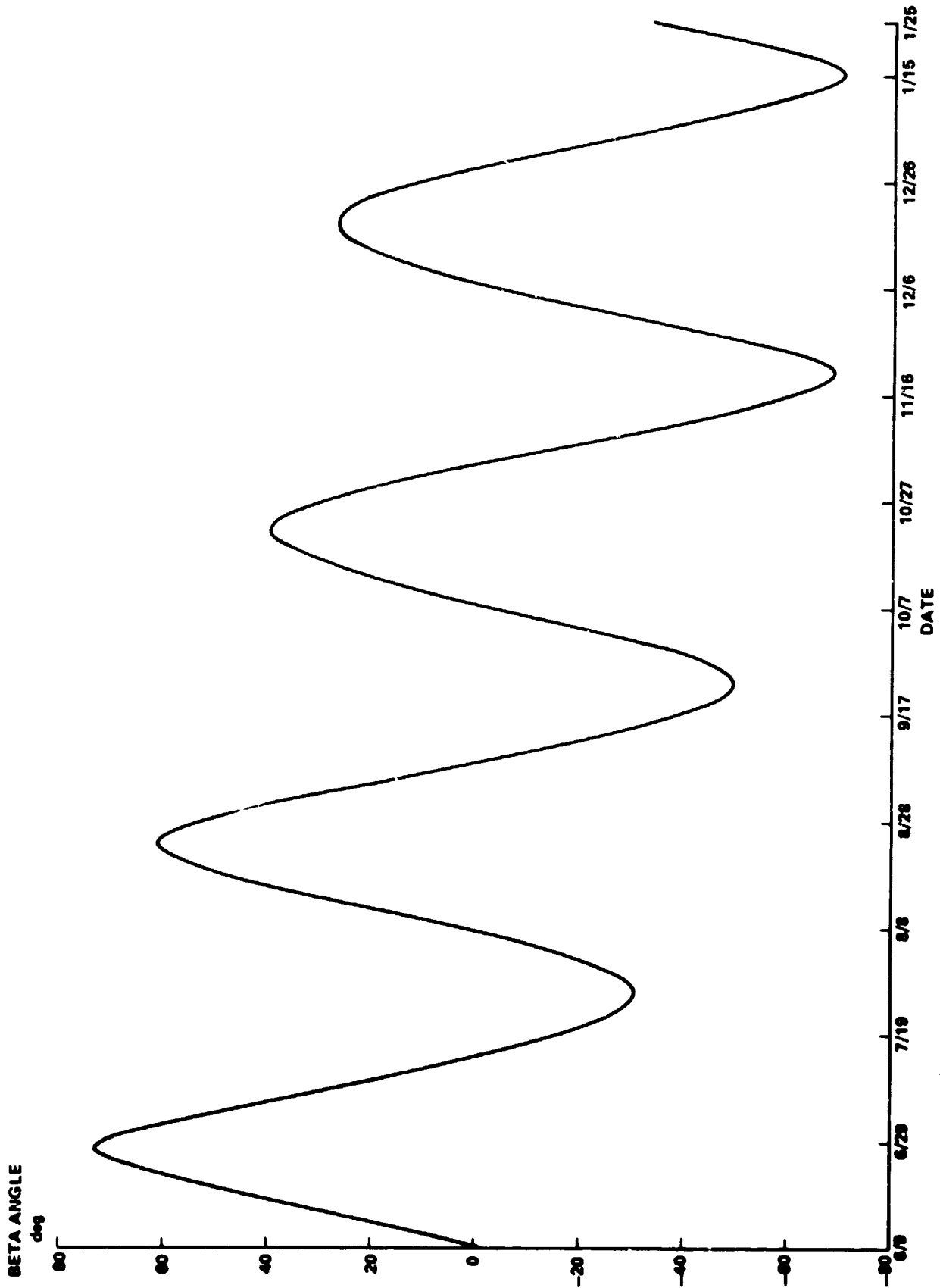


FIGURE 4.1-5 BETA ANGLE DURING THE EOVS PERIOD (JUNE 9, 1978 TO JAN 25, 1979)

BALLISTIC COEFFICIENT **

kg/m²

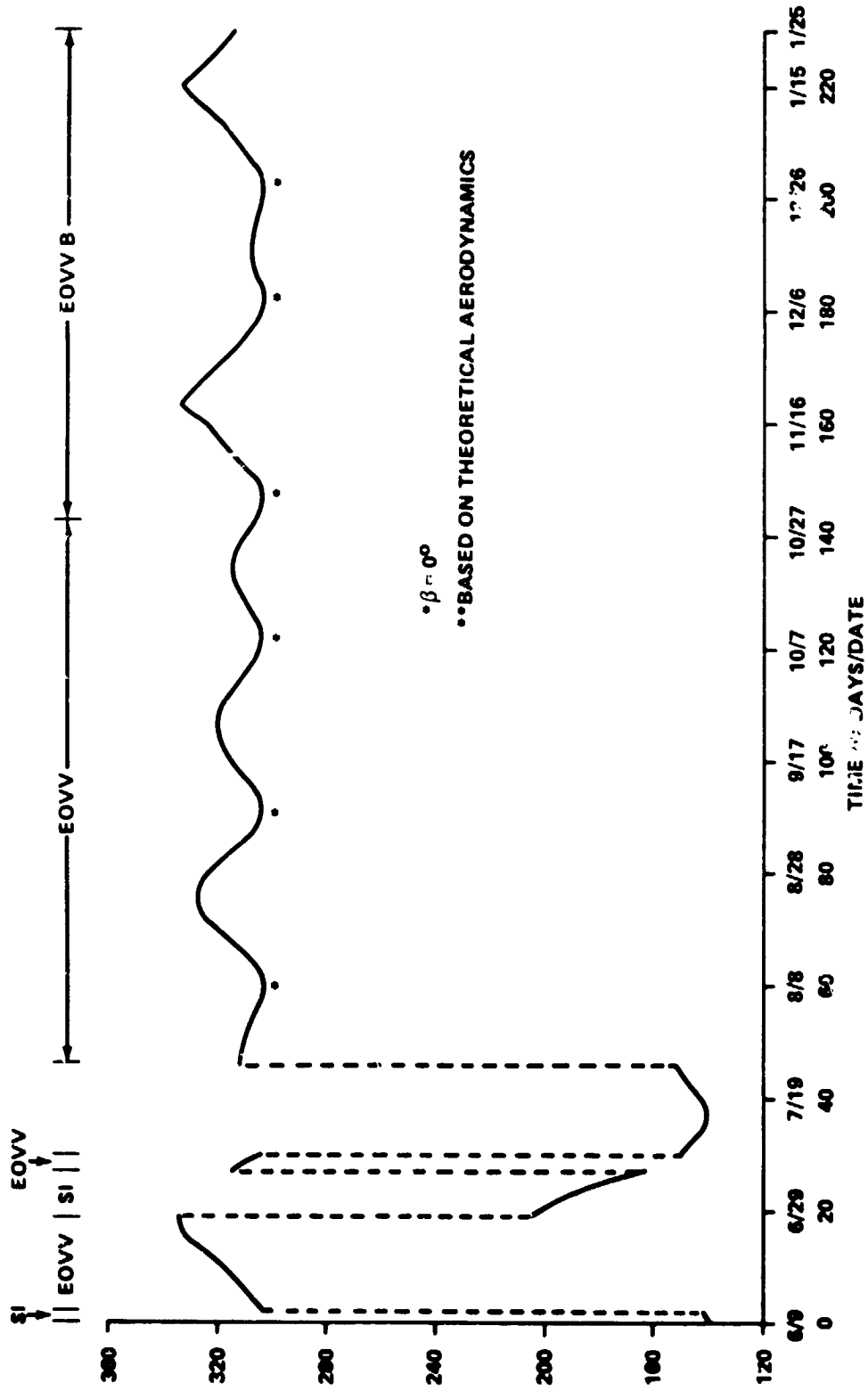


FIGURE 4.1-6 BALLISTIC COEFFICIENT FROM JUNE 9, 1978 TO JAN 25, 1979

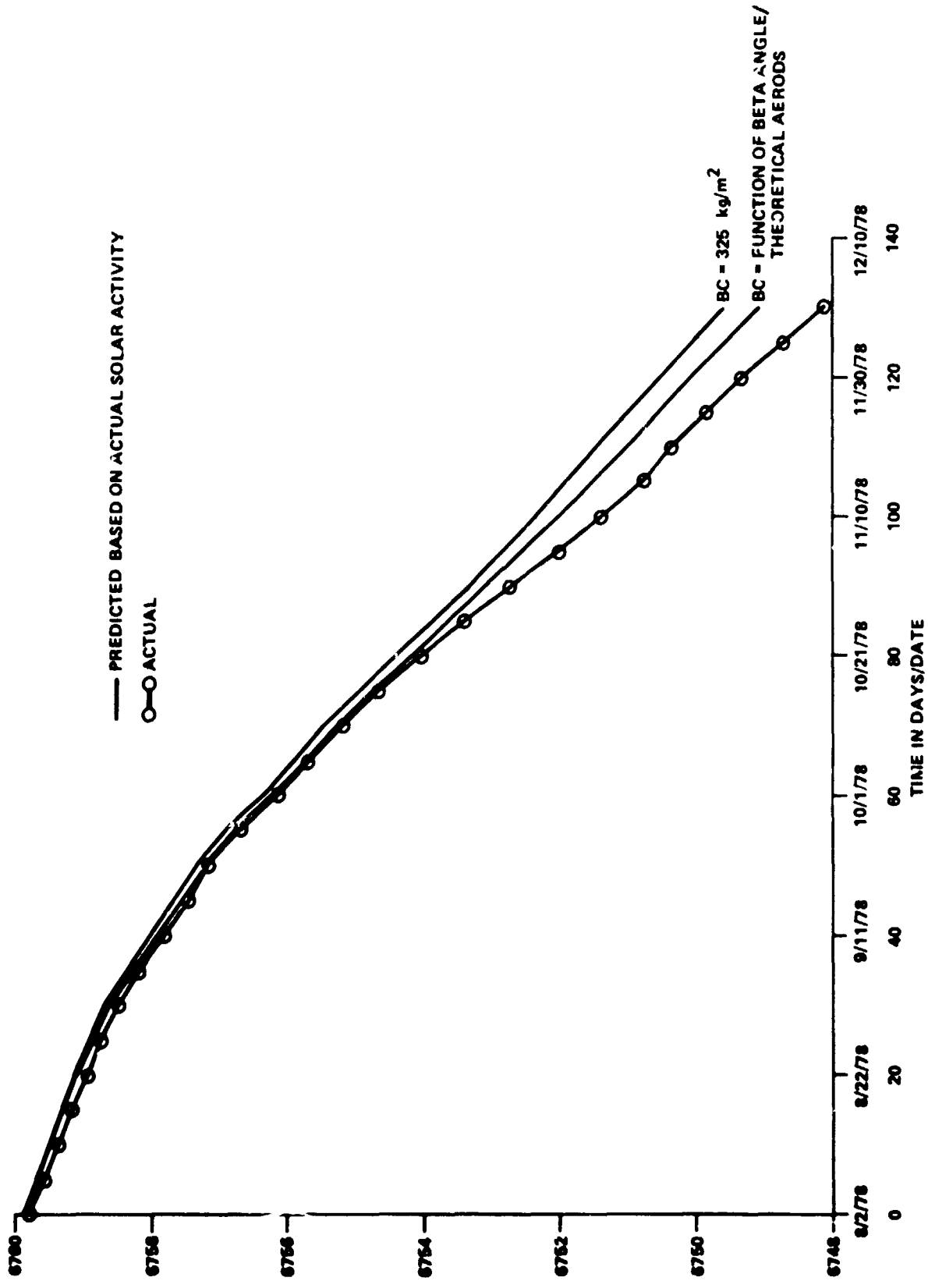


FIGURE 4.1-7 EOVV DECAY COMPARISON

EMMAJON AXIS km

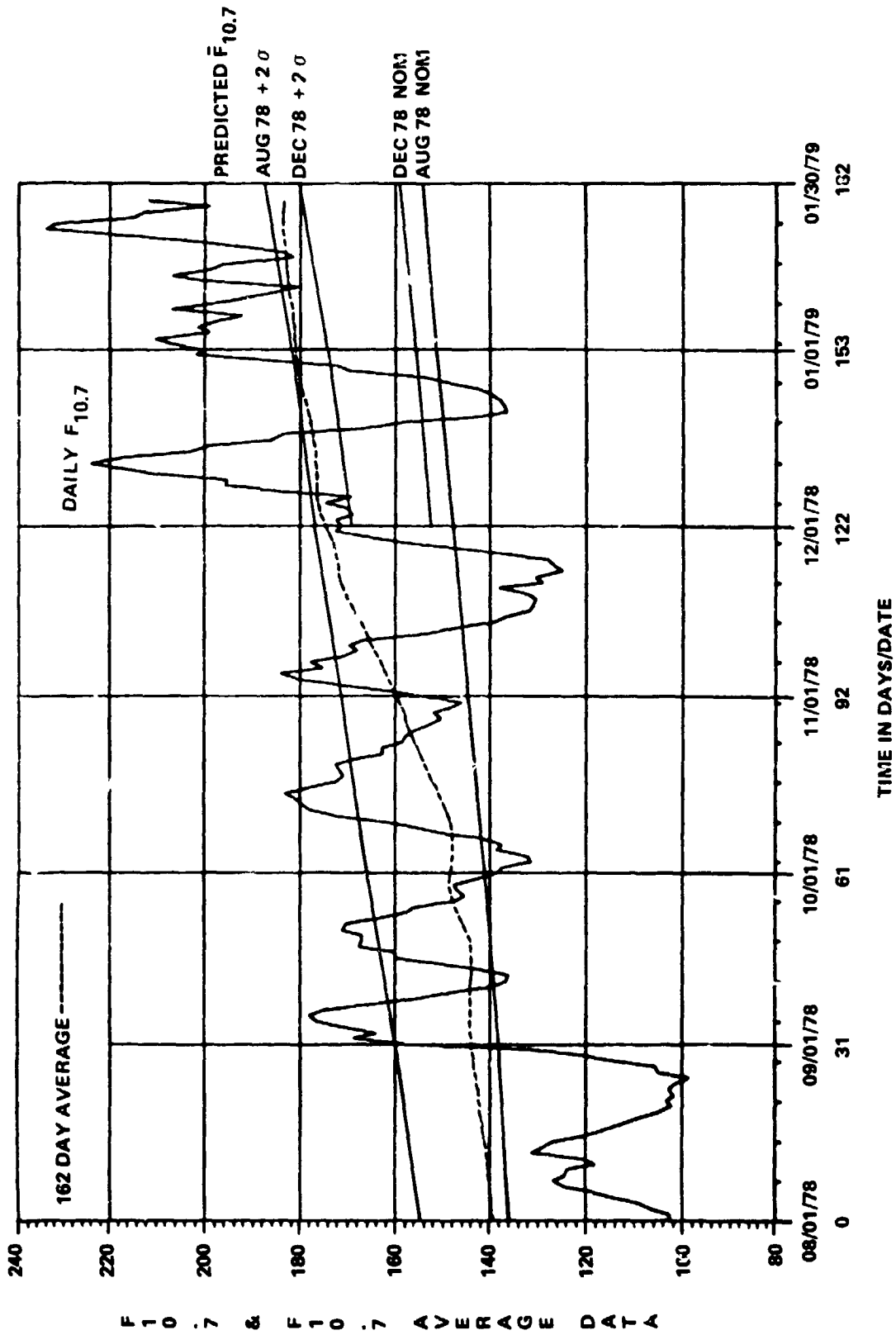


FIGURE 4.1-8 SOLAR ACTIVITY - ACTUAL AND PREDICTED

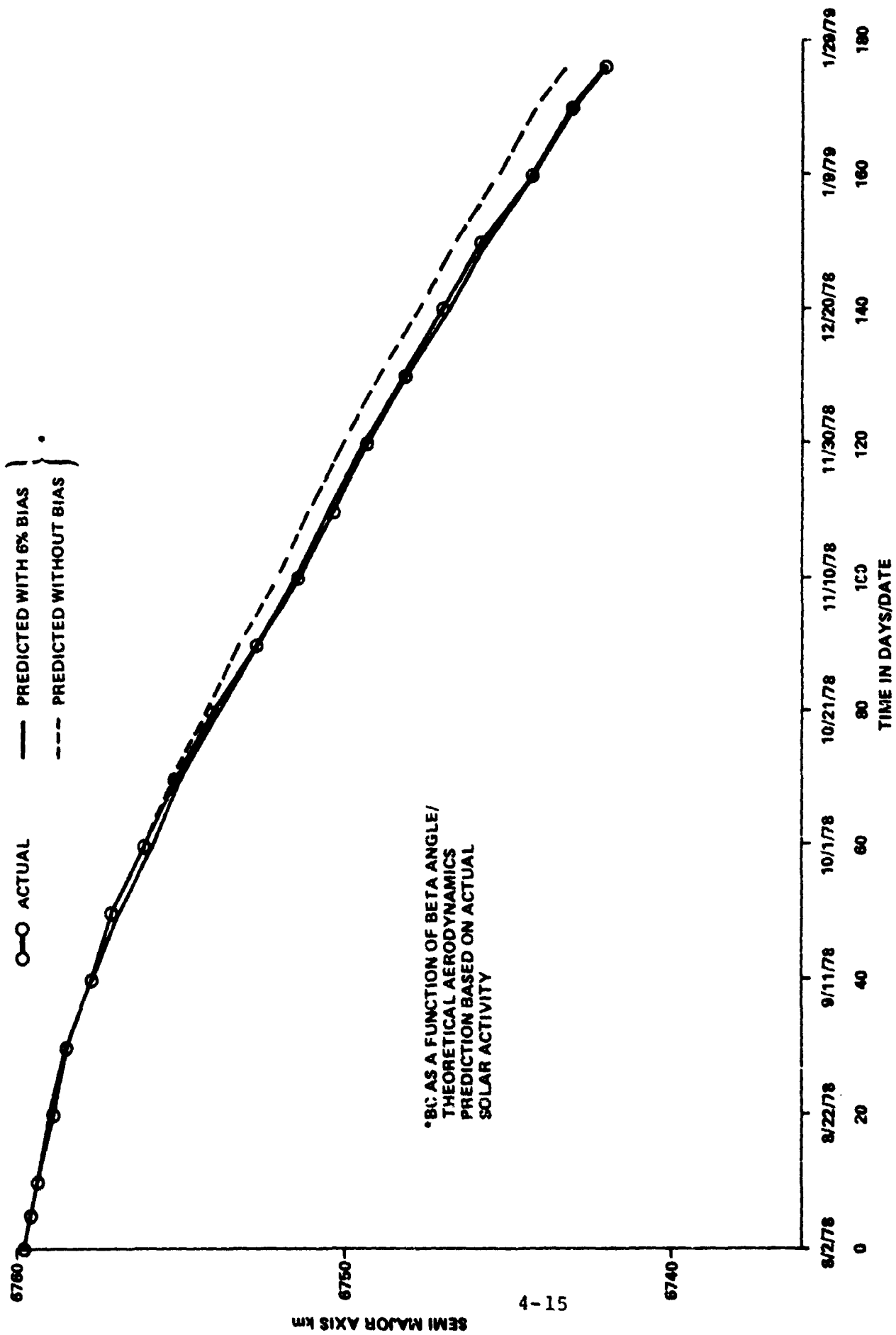


FIGURE 4.1-9 EO/VV DECAY COMPARISON USING THEORETICAL BC

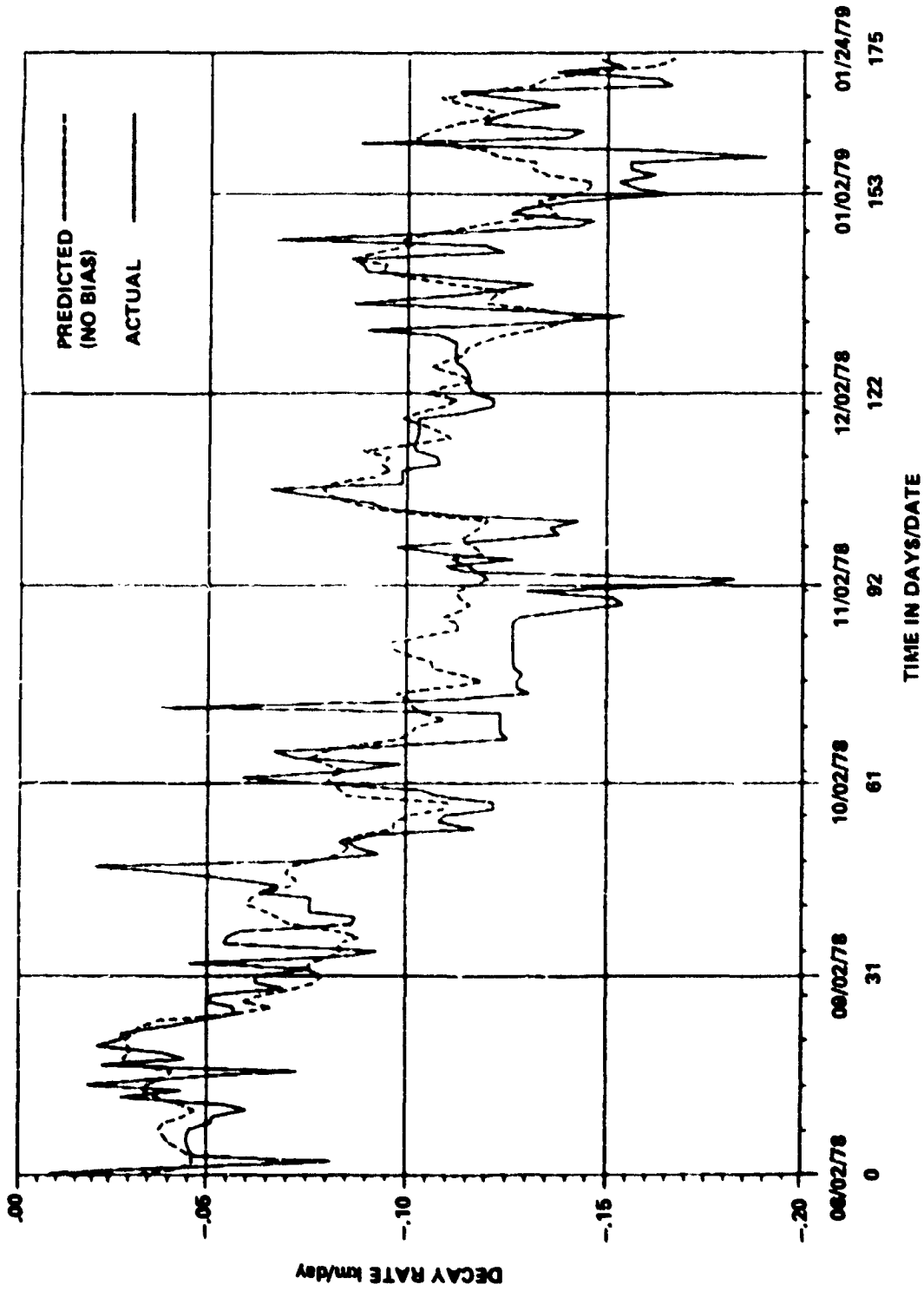


FIGURE 4.1-10 EOVV PREDICTED AND ACTUAL DECAY RATES USING THEORETICAL BC

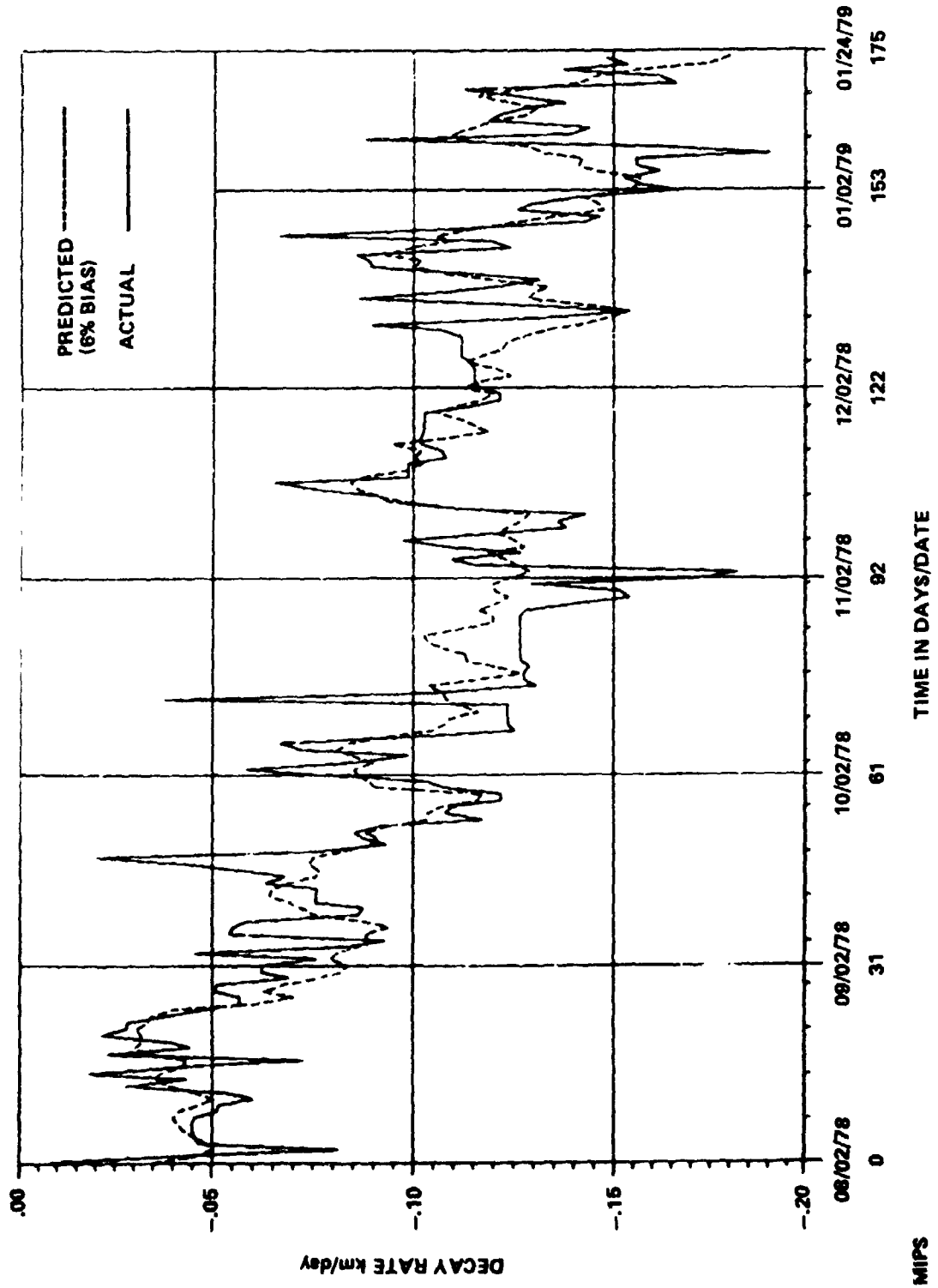


FIGURE 4.1-11 PREDICTED AND ACTUAL DECAY RATES DURING EOVV USING THEORETICAL BC

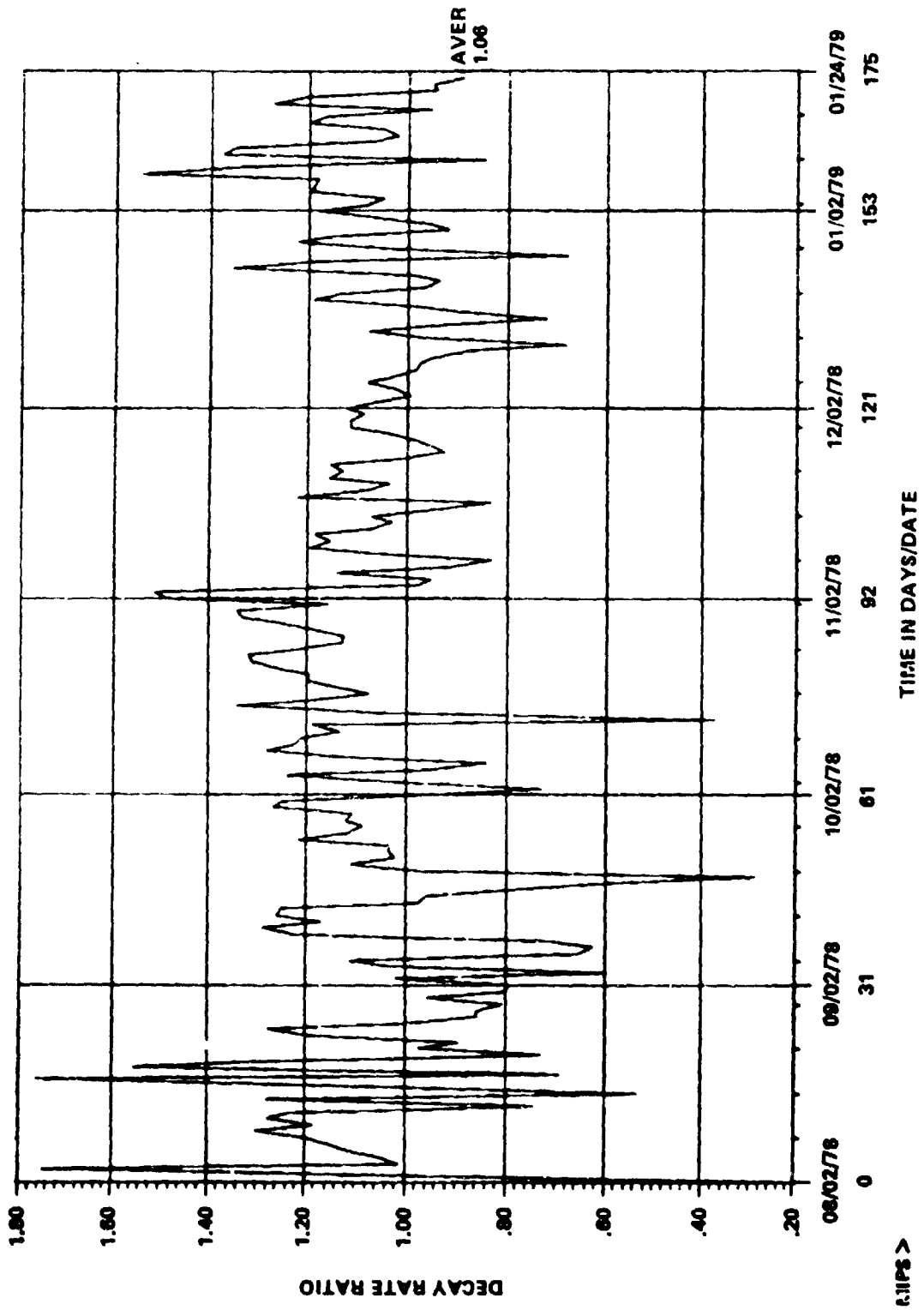


FIGURE 4.1-12 RATIO OF ACTUAL TO PREDICTED (NO BIAS) DECAY RATE DURING EOVV USING THEORETICAL BC

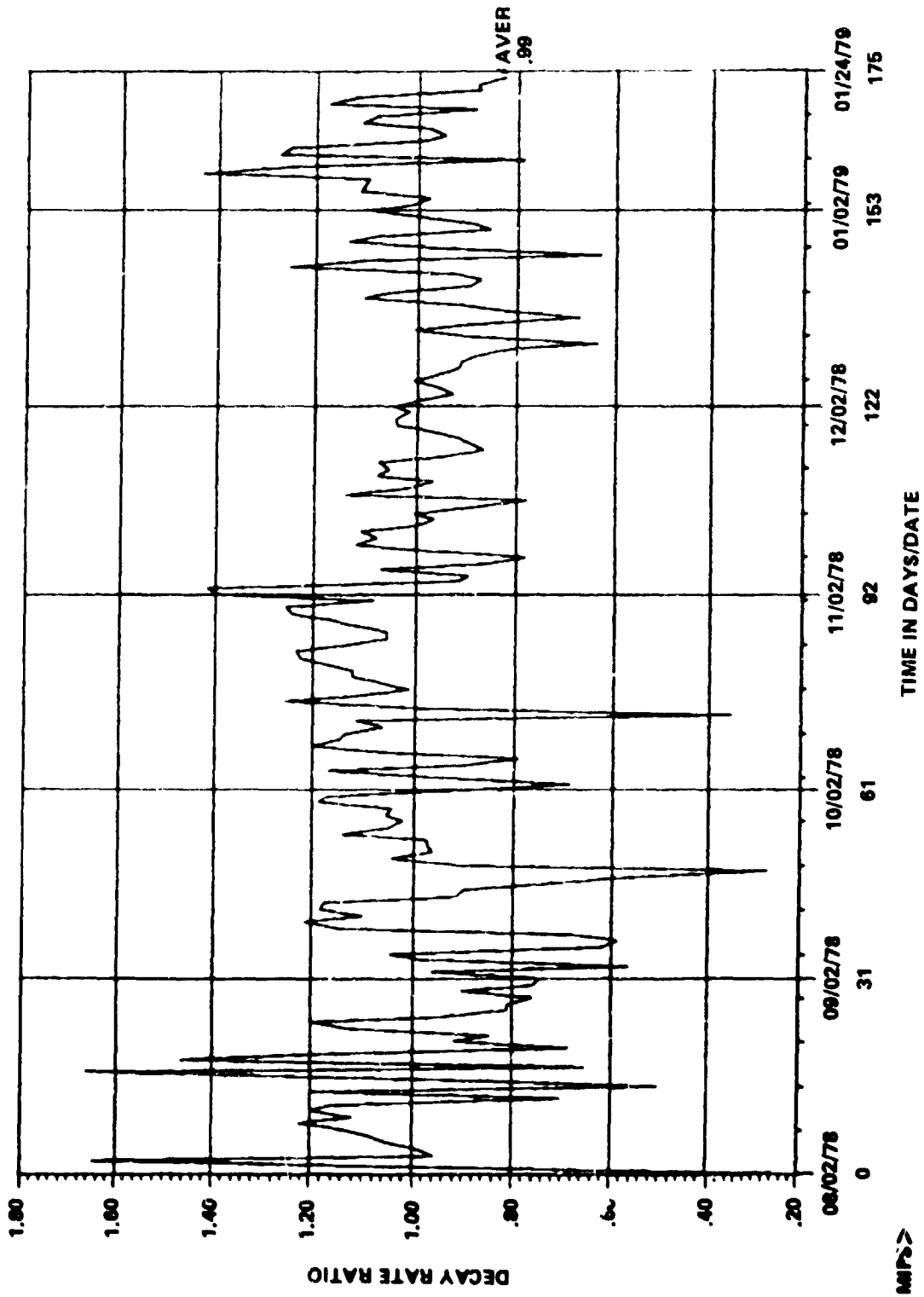


FIGURE 4.1-13 RATIO OF ACTUAL TO PREDICTED (6% BIAS) DECAY RATE DURING EOVV USING THEORETICAL BC

4.2 ORBITAL DECAY DURING THE SI PERIOD (January 25, 1979 - June 21, 1979)

Prior to the decision in December of 1978 to terminate efforts to attempt a controlled reboost or deorbit of Skylab with an orbital retrieval system, every effort possible was made to keep Skylab in orbit as long as possible. After this decision, extending Skylab's orbital lifetime was no longer an objective. Skylab was placed in the SI control attitude on January 25, 1979, to reduce the operational maintenance required; and attention was directed to the remaining orbital lifetime, considering the SI attitude. Skylab was in the SI attitude until June 20, 1979.

Precise derivation of the ballistic coefficient (BC) for this attitude was necessary. Since the SI attitude places the plane of the solar arrays perpendicular to the earth/sun line, Skylab's orientation relative to the velocity vector and the resulting BC were continually changing. It was necessary to take this into account in predicting the ballistic coefficient. Knowing that the long axis of the vehicle (X-axis) was essentially in the orbit plane and that the vehicle roll angle was a function of the beta angle, it was possible to derive a time history of BC as a function of beta. Figure 4.2-1 shows the beta angle for the SI period. Figure 4.2-2 shows the resulting BC, based on theoretical aerodynamics for the SI period. The BC varied from a minimum of 140 to a maximum 220 kg/m².

During the time Skylab was in the SI attitude, several uncertainties compounded the task of predicting Skylab's lifetime. First, to what minimum altitude could Skylab be controlled in the SI attitude? Second, in what attitude could Skylab be controlled to a lower altitude? Third, what would be the ballistic coefficient for this attitude? Fourth, when would the attitude change occur? Finally, the date and altitude that tumble would occur were unknown. In order to make the best possible lifetime prediction for Skylab, these questions had to be answered. They were eventually answered and reflected in the lifetime prediction strategy. Operational limitations of the LTIME program further complicated the task because the program could not model the BC vs. beta angle and TEA together. Until these questions were answered, it was necessary to maintain several strategies in predicting Skylab's lifetime and adjust as new information became available.

Early in the SI period, a constant BC of 150 kg/m² was used as the primary strategy. This value was near the average for the SI attitude for BC as a function of beta over the expected time (January 25 - May 24) to be in the SI attitude.

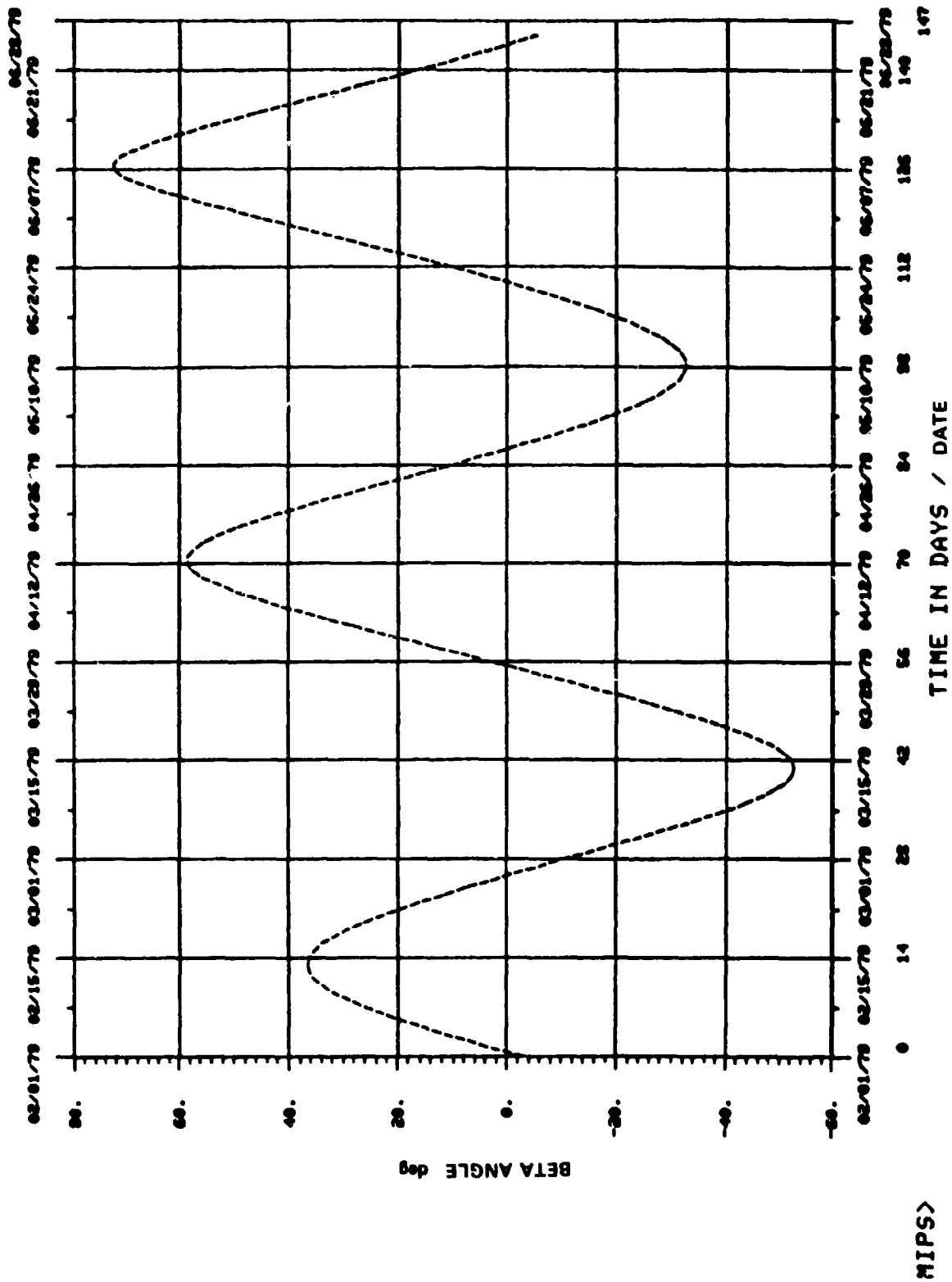


FIGURE 4.2-1 BETA ANGLE VS DATE

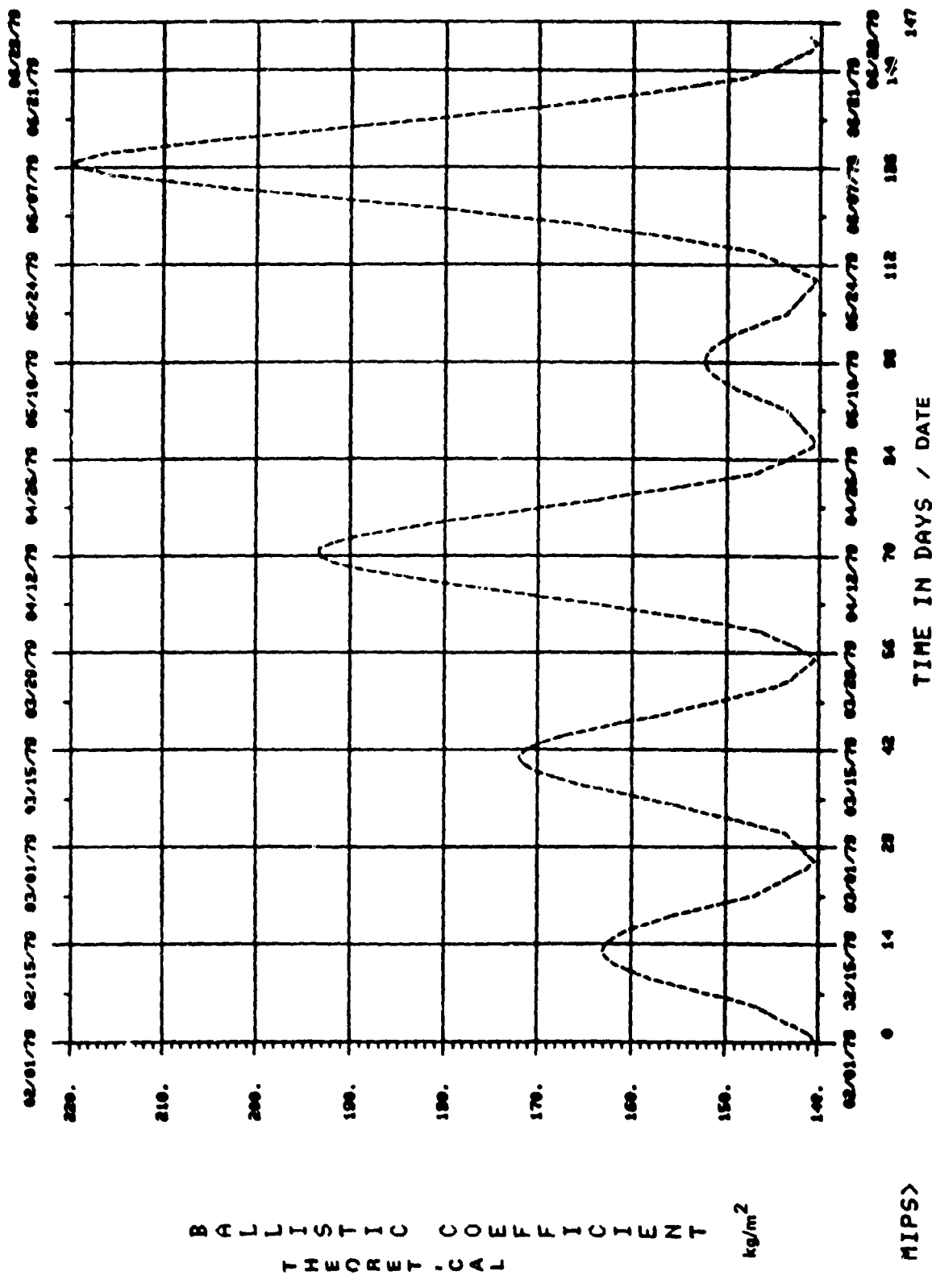


FIGURE 4.2-2 BALLISTIC COEFFICIENT VS DATE DURING SI ATTITUDE

BALLISTIC COEFFICIENT
THEORETICAL kg/m²

MIPS>

Although somewhat fortuitous, dynamic analysis for Skylab in a random tumble indicated a BC range of 135 to 160 kg/m², with the average being 150 kg/m². Initially, this strategy provided the best prediction of Skylab's lifetime. Predictions based upon this strategy were maintained throughout the SI period to provide a consistent lifetime prediction data base to evaluate daily solar activity effects upon Skylab's decay. The 6% bias determined in the EOVV period was also used. Table 4.2-1 summarizes the lifetime predictions made for this strategy.

As the expected time to end the SI attitude shifted to a later date, a variable BC as a function of beta (See Figure 4.2-2) was used to 150 nmi. Skylab was expected to go out of control in the SI attitude at 150 nmi and tumble afterwards to impact. The TEA attitude capability was uncertain at this time. The lifetime predictions included the variable BC for SI and 150 kg/m² for the tumble.

As new information became available, the strategy changed to holding SI to impact. The projected date to go to the TEA attitude was uncertain but expected to be later. The SI control limit was lowered to 140 nmi, and the BC as a function of beta was approximately 150 toward the end of Skylab's expected lifetime.

Finally, the projected date to go to the TEA attitude, the expected BC for the TEA attitude, and the minimum control altitude (70-80 nmi) were determined. This information led to the final strategy of making lifetime predictions by modeling the SI versus beta angle, plus the TEA attitude BC profile and tumble at 75 nmi. By this time, due to the short remaining lifetime, it was feasible to model the BC changes by table input for all three attitudes. Table 4.2-2 summarizes the results of these lifetime predictions.

The actual solar activity data was used with the BC as a function of beta angle (from Figure 4.2-2) to determine the density bias by reconstruction, if any, that would be needed to fit the actual decay. The predicted decay did not match the actual decay very well without a bias. Figure 4.2-3 compares the actual decay with the predicted decay for a zero, 6%, and 18% bias. During most of the SI period (February 1, 1979 to June 7, 1979), a bias of 18% was needed to match the actual decay. Figures 4.2-4 and 4.2-5 show the predicted and actual decay rates and the ratio of the decay rates, respectively, for the 18% bias. This bias, as stated earlier, is quite sensitive to rapid changes in solar activity, especially when decay comparisons are made over a relatively

TABLE 4.2-1 PREDICTED IMPACT DATES
FOR CONSTANT BC*

| Vector Date | Date of Solar Activity Prediction | Impact Date | |
|-------------|-----------------------------------|-------------|------------|
| | | Nominal | 2 σ |
| 1/25/79 | January, 1979 | 8/12/79 | 7/4/79 |
| 2/1/79 | January, 1979 | 8/1/79 | 6/28/79 |
| 2/12/79 | February, 1979 | 7/28/79 | 6/27/79 |
| 2/22/79 | February, 1979 | 7/24/79 | 6/26/79 |
| 2/28/79 | February, 1979 | 7/20/79 | 6/24/79 |
| 3/1/79 | February, 1979 | 7/12/79 | 6/20/79 |
| 3/16/79 | March, 1979 | 7/10/79 | 6/22/79 |
| 4/2/79 | March, 1979 | 7/4/79 | 6/21/79 |
| 4/16/79 | April, 1979 | 7/3/79 | 6/23/79 |
| 5/1/79 | May, 1979 | 7/3/79 | 6/25/79 |
| 5/15/79 | May, 1979 | 7/5/79 | 6/29/79 |
| 5/25/79 | May, 1979 | 7/8/79 | 7/3/79 |
| 5/29/79 | May, 1979 | 7/8/79 | 7/6/79 |
| 5/30/79 | May, 1979 | 7/9/79 | 7/4/79 |
| 5/31/79 | May, 1979 | 7/9/79 | 7/4/79 |
| 6/4/79 | June, 1979 | 7/10/79 | 7/6/79 |
| 6/5/79 | June, 1979 | 7/10/79 | 7/6/79 |
| 6/6/79 | June, 1979 | 7/11/79 | 7/7/79 |
| 6/7/79 | June, 1979 | 7/11/79 | 7/7/79 |
| 6/8/79 | June, 1979 | 7/11/79 | 7/8/79 |
| 6/11/79 | June, 1979 | 7/12/79 | 7/9/79 |
| 6/12/79 | June, 1979 | 7/12/79 | 7/9/79 |
| 6/13/79 | June, 1979 | 7/12/79 | 7/9/79 |
| 6/14/79 | June, 1979 | 7/12/79 | 7/10/79 |
| 6/15/79 | June, 1979 | 7/13/79 | 7/10/79 |
| 6/18/79 | June, 1979 | 7/13/79 | 7/10/79 |
| 6/19/79 | June, 1979 | 7/13/79 | 7/11/79 |
| 6/20/79 | June, 1979 | 7/13/79 | 7/11/79 |
| 6/21/79 | June, 1979 | 7/13/79 | 7/11/79 |
| 6/22/79 | June, 1979 | 7/13/79 | 7/11/79 |
| 6/25/79 | June, 1979 | 7/13/79 | 7/11/79 |

*150 kg/m² with 6% Bias

TABLE 4.2-2 PREDICTED IMPACT DATES FOR
SI AND TEA ATTITUDES

| Vector | Date of Solar Activity Prediction | Impact Date | | BC Conditions |
|---------|--------------------------------------|-------------|----------------|-----------------------------------------------|
| | | (Nom) | (+2 σ) | |
| 3/23/79 | April, 1979 | 7/13/79 | 6/28/79 | SI to Impact (function of β angle) |
| 4/4/79 | April, 1979 | 7/10/79 | 6/27/79 | SI to Impact (function of β angle) |
| 5/16/79 | May, 1979 | 6/28/79 | 6/23/79 | SI (function of β) + TEA on 5/24/79 |
| 5/18/79 | May, 1979 | 6/28/79 | 6/23/79 | SI (function of β) + TEA on 5/24/79 |
| 5/21/79 | May, 1979 | 6/28/79 | 6/23/79 | SI (function of β) + TEA on 5/24/79 |
| 5/23/79 | May, 1979 | 7/9/79 | 7/4/79 | SI (function of β) TEA on 6/21/79 |
| 5/30/79 | May, 1979 | 7/10/79 | 7/6/79 | SI (function of β) + TEA on 6/21/79 |
| 6/12/79 | June, 1979 | 7/10/79 | 7/7/79 | SI (function of β) + TEA on 6/21/79 |
| 6/22/79 | June, 1979 | 7/10/79 | 7/8/79 | SI (function of β) + TEA on 6/21/79 |

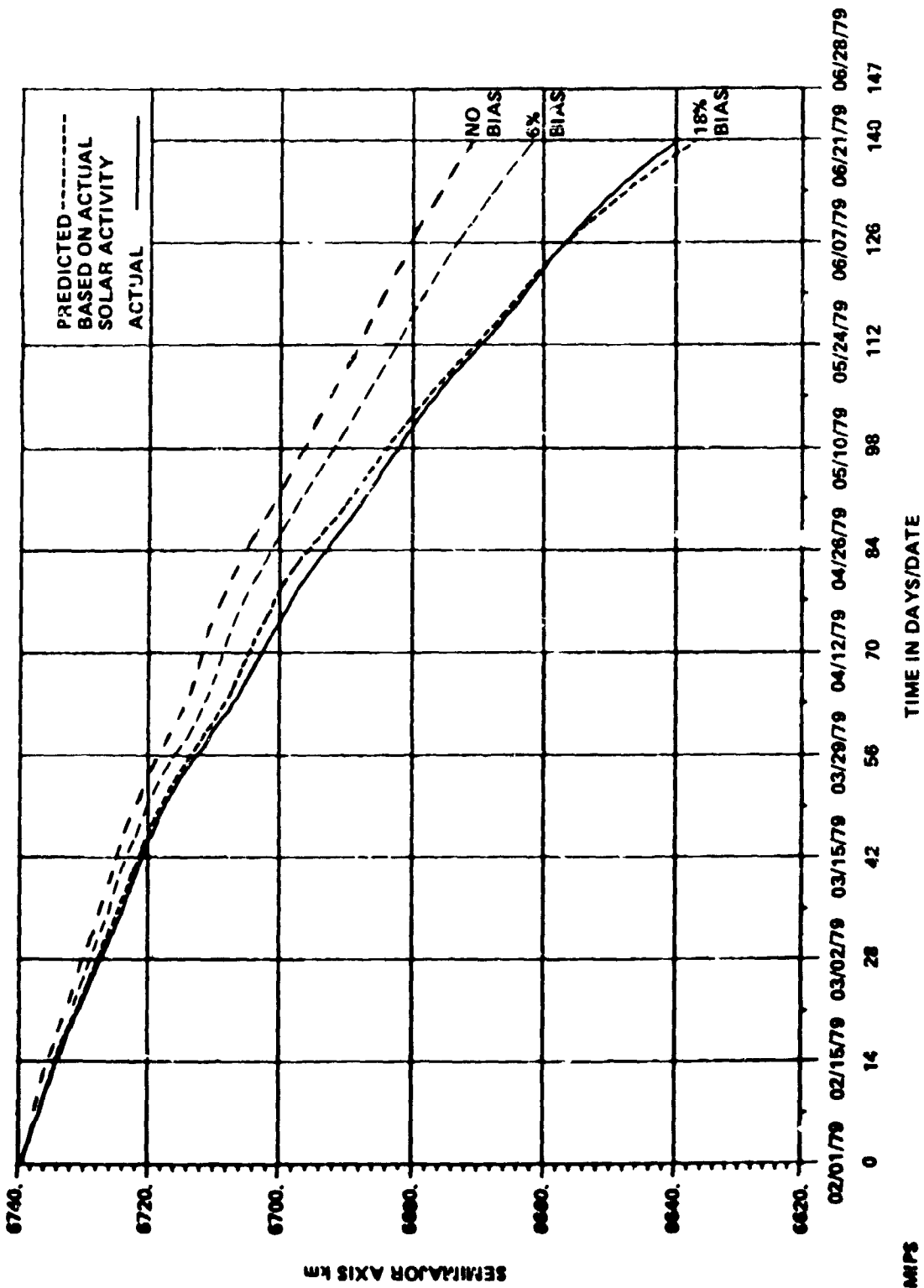


FIGURE 4.2-3 DECAY COMPARISONS DURING SI ATTITUDE

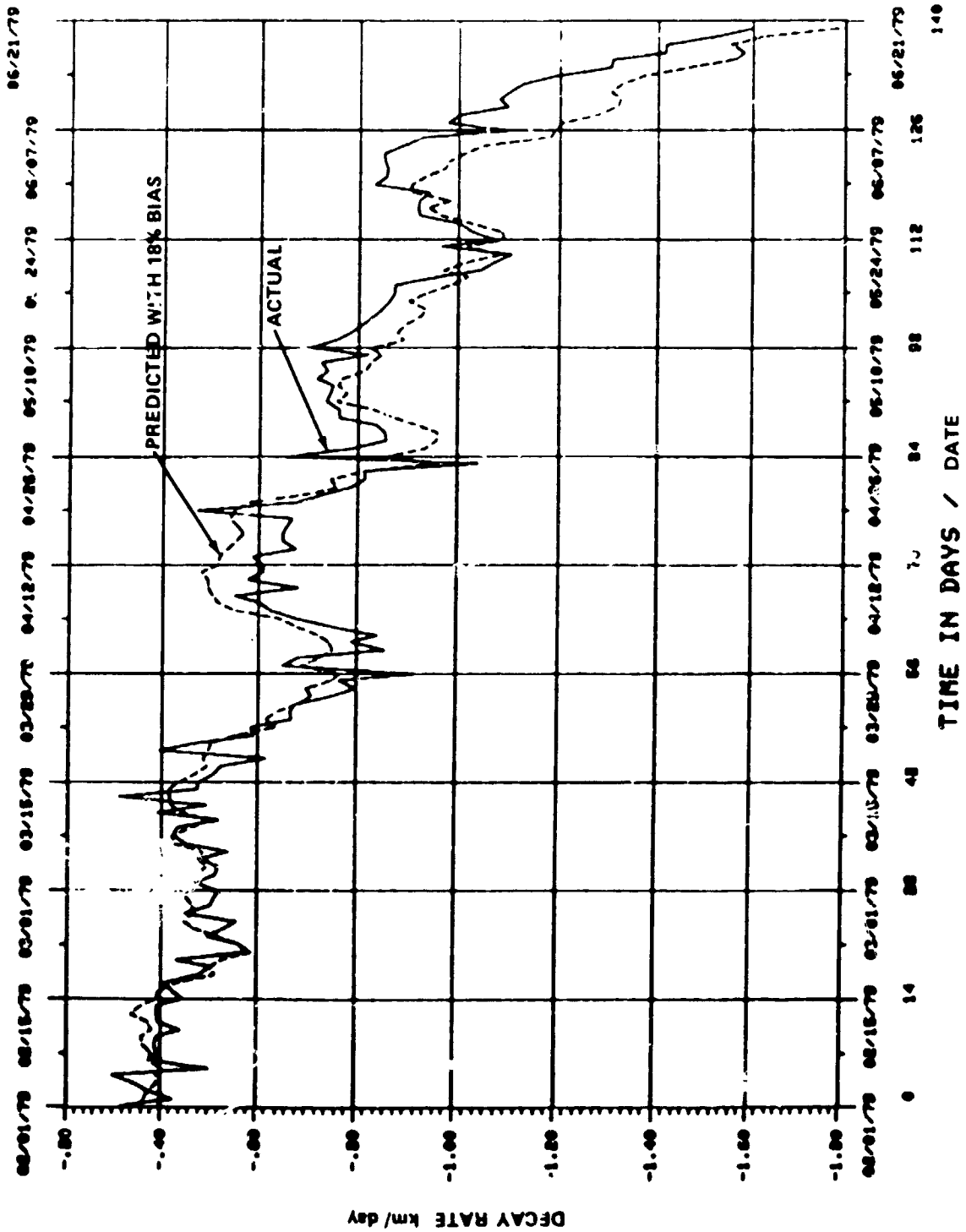


FIGURE 4.2-4 PREDICTED AND ACTUAL DECAY RATES DURING SI ATTITUDE

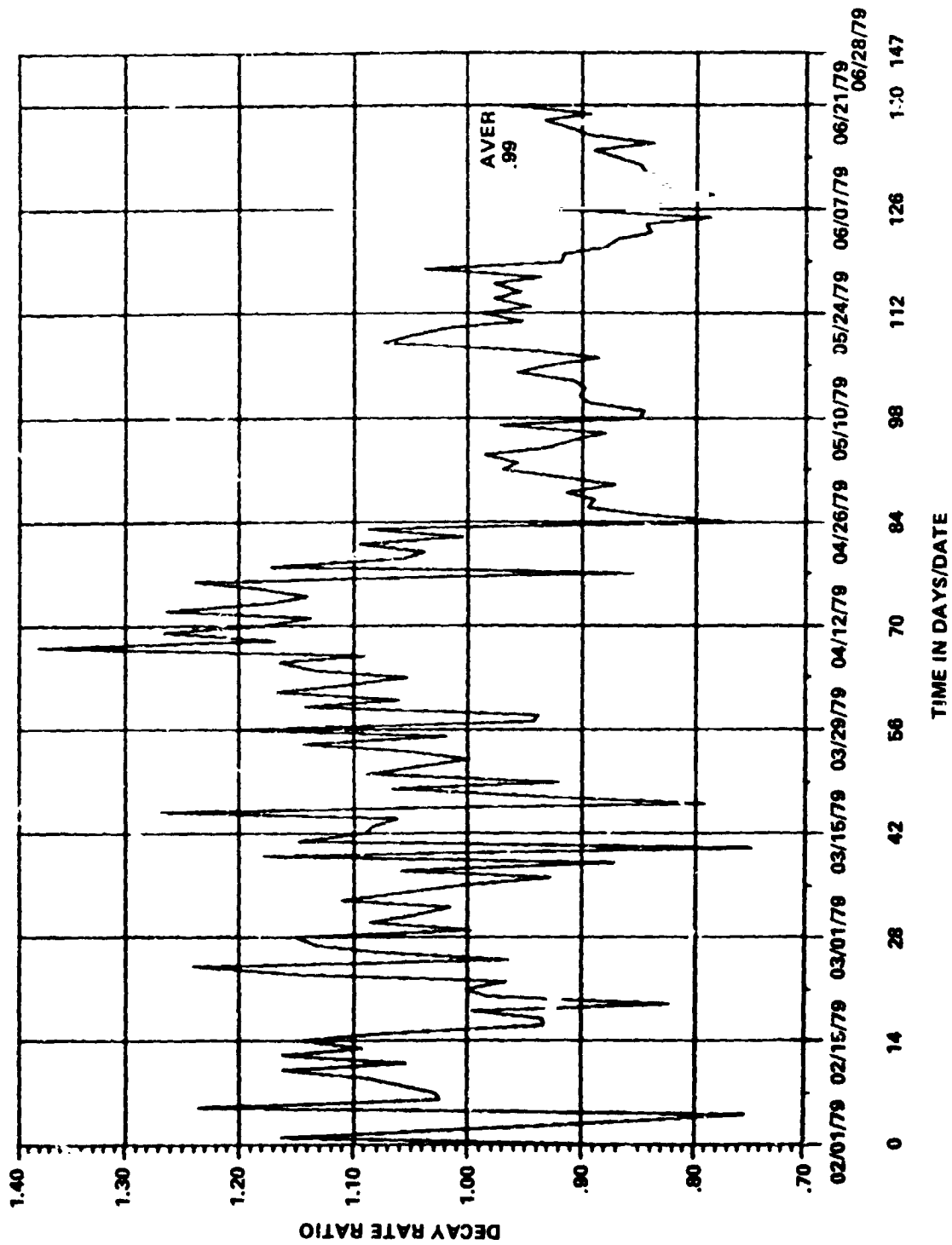


FIGURE 4.2-5 RATIO OF ACTUAL TO PREDICTED (18% BIAS) DECAY RATE

short time period. Some correlation may be observed upon comparison to the solar activity on Figure 4.2-6, which shows the $F_{10.7}$, $\bar{F}_{10.7}$, and A_p for the SI period. The 162-day average is shown for $\bar{F}_{10.7}$. Toward the end of the SI period, it was apparent that the density bias had changed. This can be seen in Figure 4.2-5. The bias change occurred around April 26, 1979. A decay reconstruction for the last month of SI was done to determine the new bias. Figures 4.2-7 through 4.2-9 show the predicted and actual decay, predicted and actual decay rates, and the ratio of the decay rates, respectively, for the time period from May 25, 1979 to June 22, 1979. At the time of the initial decay reconstruction the preliminary $F_{10.7}$ data and the 55-day average $\bar{F}_{10.7}$ were used, and a 4% density bias was required to match the actual decay. Later, when the final solar data was available, the 162-day average was used; and a 6% density bias was required to match the actual decay. This 2% difference is due to the difference between the actual and final solar data, combined with the difference between the 55-day and 162-day $\bar{F}_{10.7}$. Figure 4.2-10 shows the preliminary and final values of $F_{10.7}$, the 55-day $\bar{F}_{10.7}$, and the 162-day average $\bar{F}_{10.7}$. As stated earlier, values of $F_{10.7}$ and A_p are available in real time, but final data is not available until 1 to 2 months later. Usually, there is little change in the $F_{10.7}$ data from preliminary to final. However, this is not the case with the A_p data because the preliminary is the observed value from one observatory, and the final data is an average value for a number of observatories.

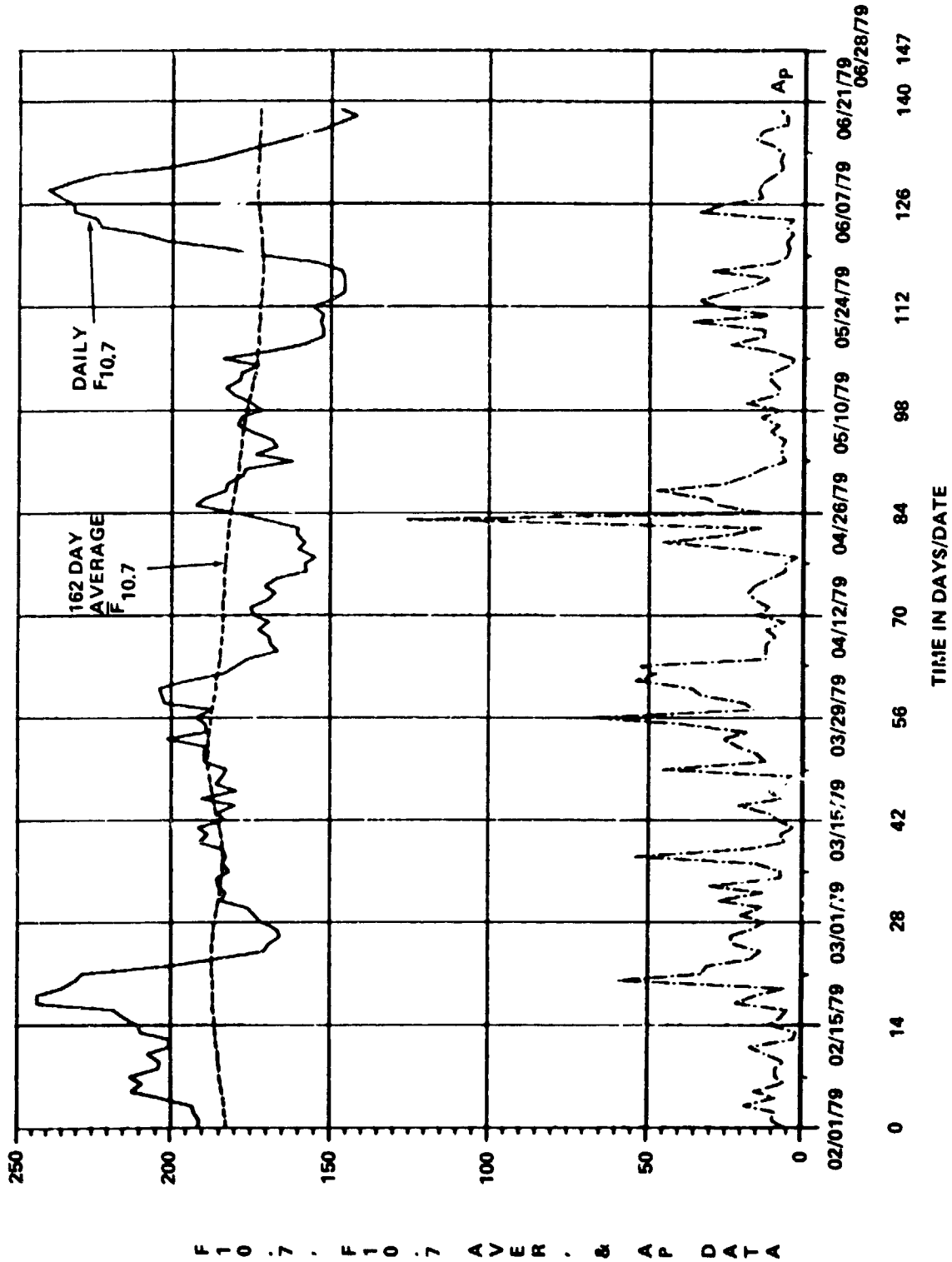


FIGURE 4.2-6 ACTUAL SOLAR ACTIVITY DATA

F 1 0 . 7 . F 1 0 . 7 A V E R . & A P D A T A

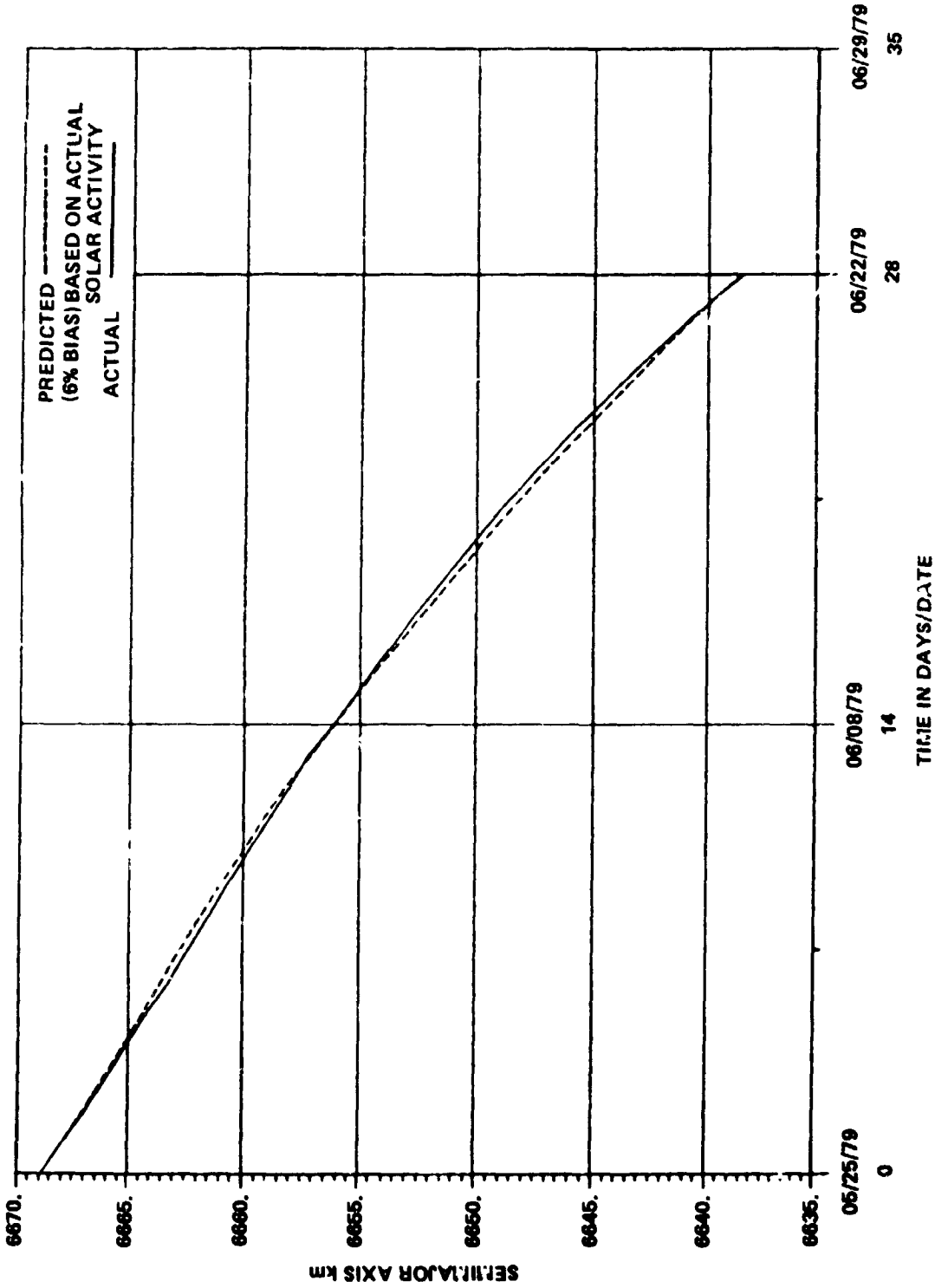


FIGURE 4.2-7 DECAY COMPARISON DURING SI ATTITUDE

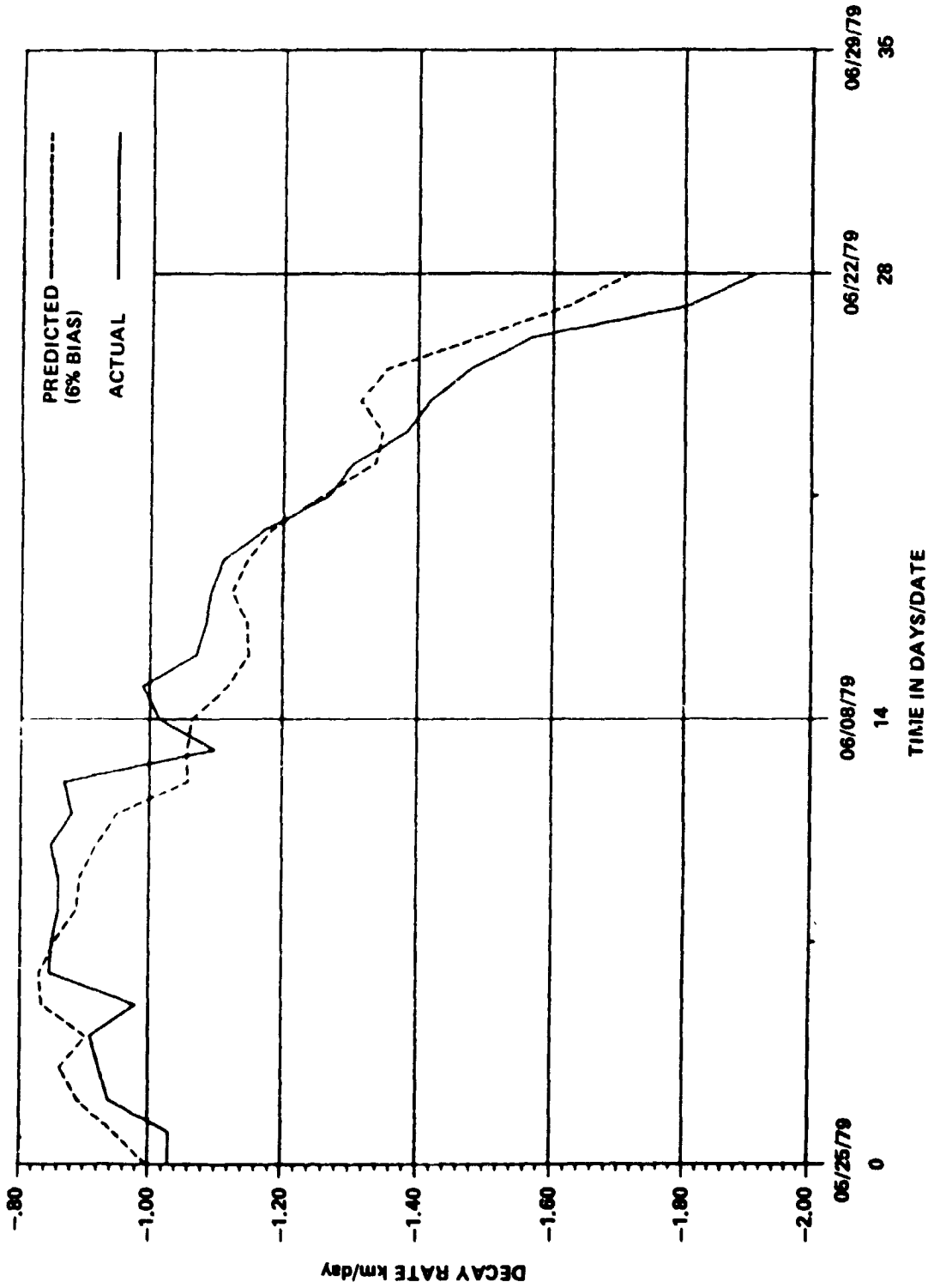


FIGURE 4.2-8 PREDICTED AND ACTUAL DECAY RATES DURING SI ATTITUDE

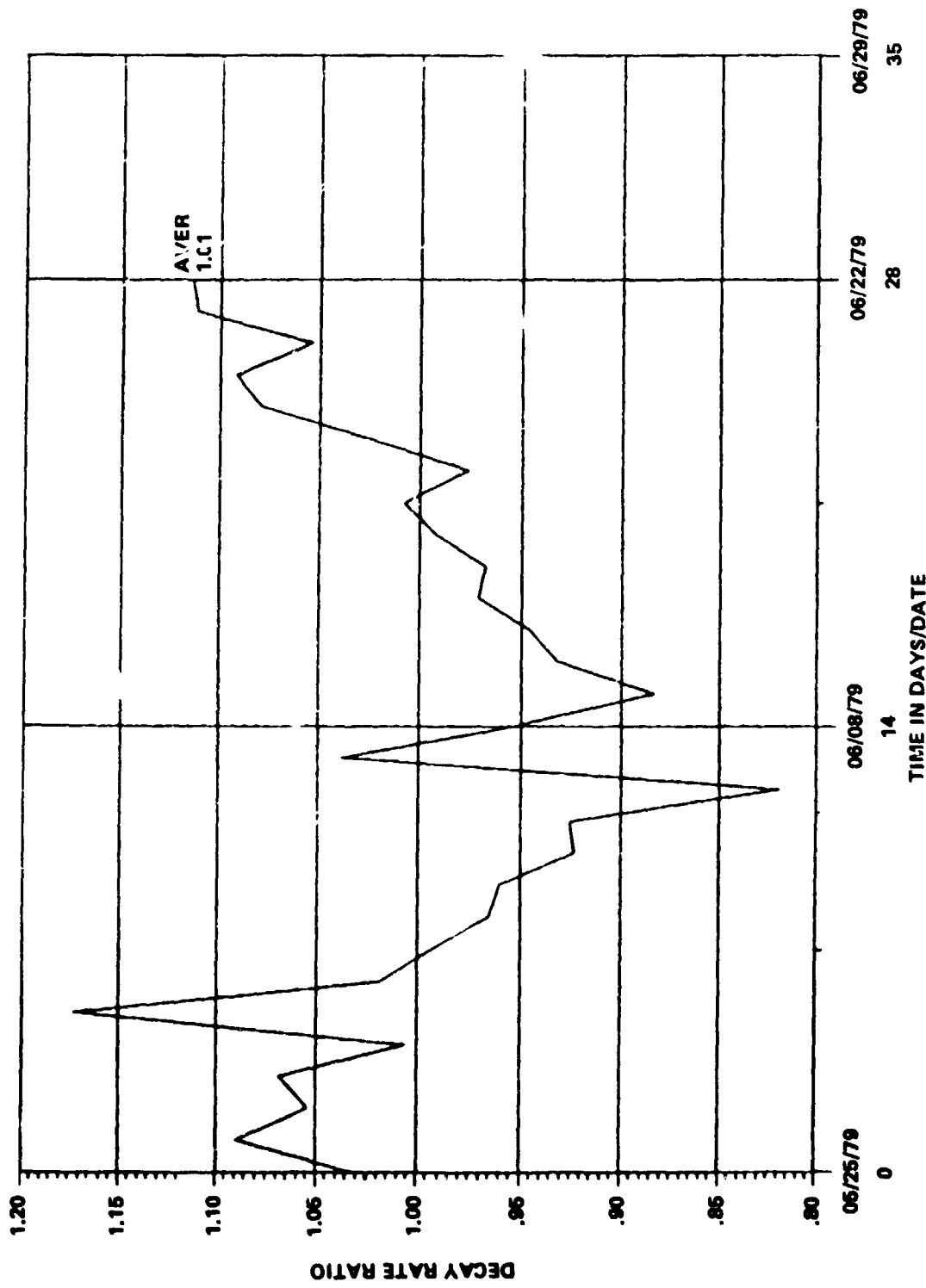


FIGURE 4.2-9 RATIO OF ACTUAL TO PREDICTED (6% BIAS) DECAY RATE

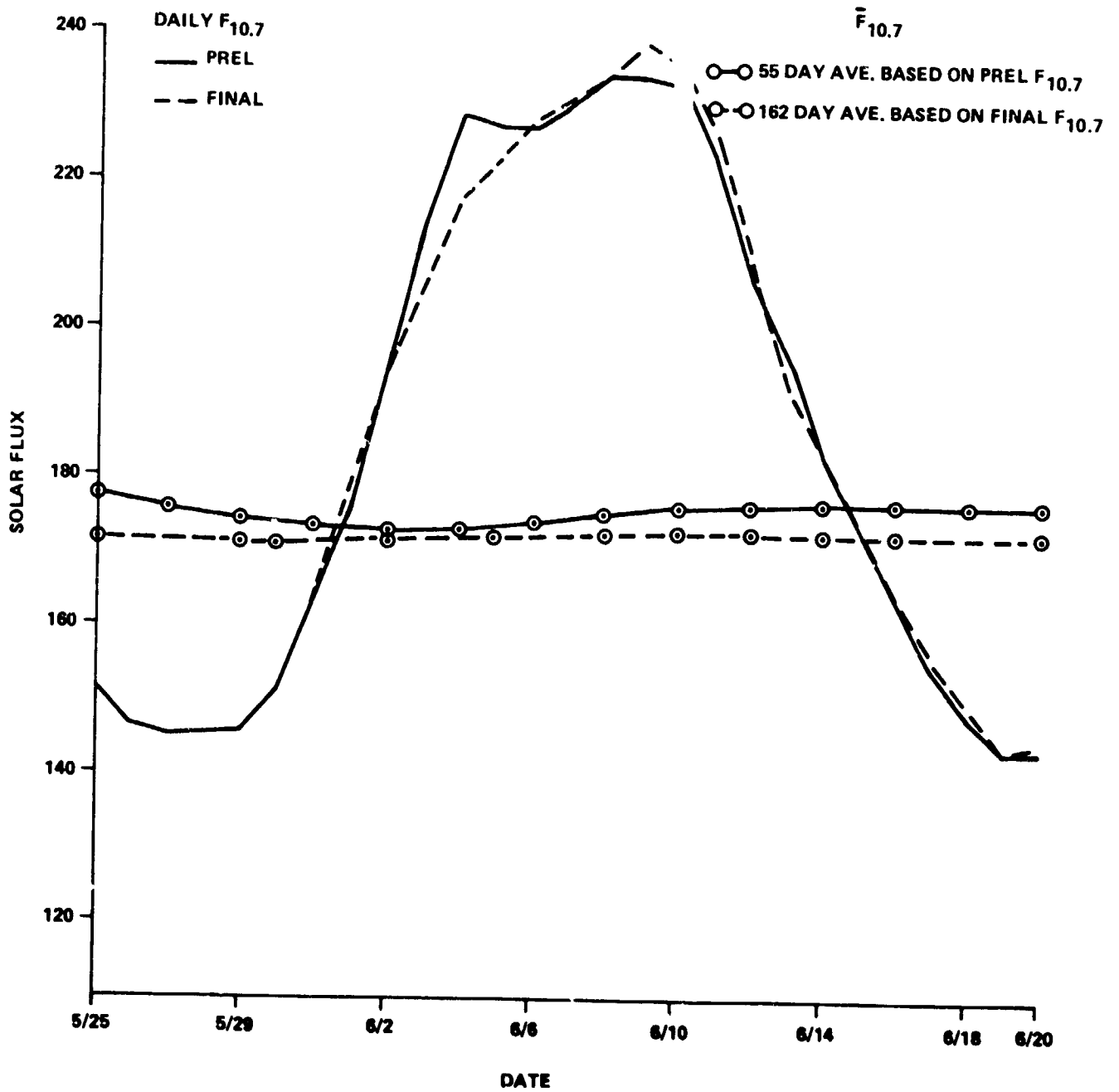


FIGURE 4.2-10 SOLAR ACTIVITY DATA

4.3 ORBITAL DECAY DURING THE TEA PERIOD (June 21, 1979 - July 11, 1979)

Development of the TEA control mode (Reference 13) resulted from a decision to try to control the impact of Skylab to a particular orbit, one which would be characterized by a low population density. Skylab was in the TEA control mode from June 21, 1979 until shortly before impact on July 11, 1979. There were essentially two constraints which determined when the TEA control scheme could be used. One of these depended upon the sun angle on the solar arrays. The other constraint was the minimum altitude (~ 140 nmi) at which Skylab could still be controlled in the SI attitude.

It thus became necessary to accurately predict both the beta angle and the altitude of Skylab such that a time (window) could be picked where sufficient power would be available during the total time Skylab would be in the high drag attitude (T121P). It was also necessary for the window to open before Skylab's altitude fell below the SI control threshold. Figure 4.3-1 shows the beta angle and altitude that were acceptable for T121P control. As can be seen, June 20, 1979 to June 23, 1979 satisfied both the power and altitude constraints for entering T121P. Based upon predictions of altitude and beta angle, June 20, 1979 was selected as the date to go to the new attitude, which corresponded to an altitude of 142 nmi. It was then necessary to derive a BC for the T121P attitude. Initial estimates were predicted by dynamics and control simulations of the vehicle in its operating environment. Final values were determined by methods developed by observing the orbital decay behavior. This method compared the decay rate of the vehicle for various BC's to that BC which gave the best fit of the actual decay rate. The method was modified by checking other satellite decay rates in order to be assured that atmospheric model variations and other factors were accounted for in the calculation of the BC.

Figure 4.3-2 shows the resulting BC for the T121P attitude. Figure 4.3-3 shows the predicted and actual decay of Skylab during the time of the T121P attitude where predicted decay is determined using the actual solar data and the predicted BC's. Figure 4.3-4 shows that a 3% density bias is required to match the actual decay. This bias included uncertainties in the vehicle attitude, the aerodynamic data, and the solar activity data. As can be seen, the predicted and observed decay curves were quite close in terms of a daily average. Lifetime predictions for this scenario (i.e., SI until June 21, 1979; T121P until 80 nmi; and tumble thereafter) are shown in Table 4.3-1. The T121P configuration was

maintained until 7:45 GMT on July 11, 1979, when the maneuver to tumble was initiated.

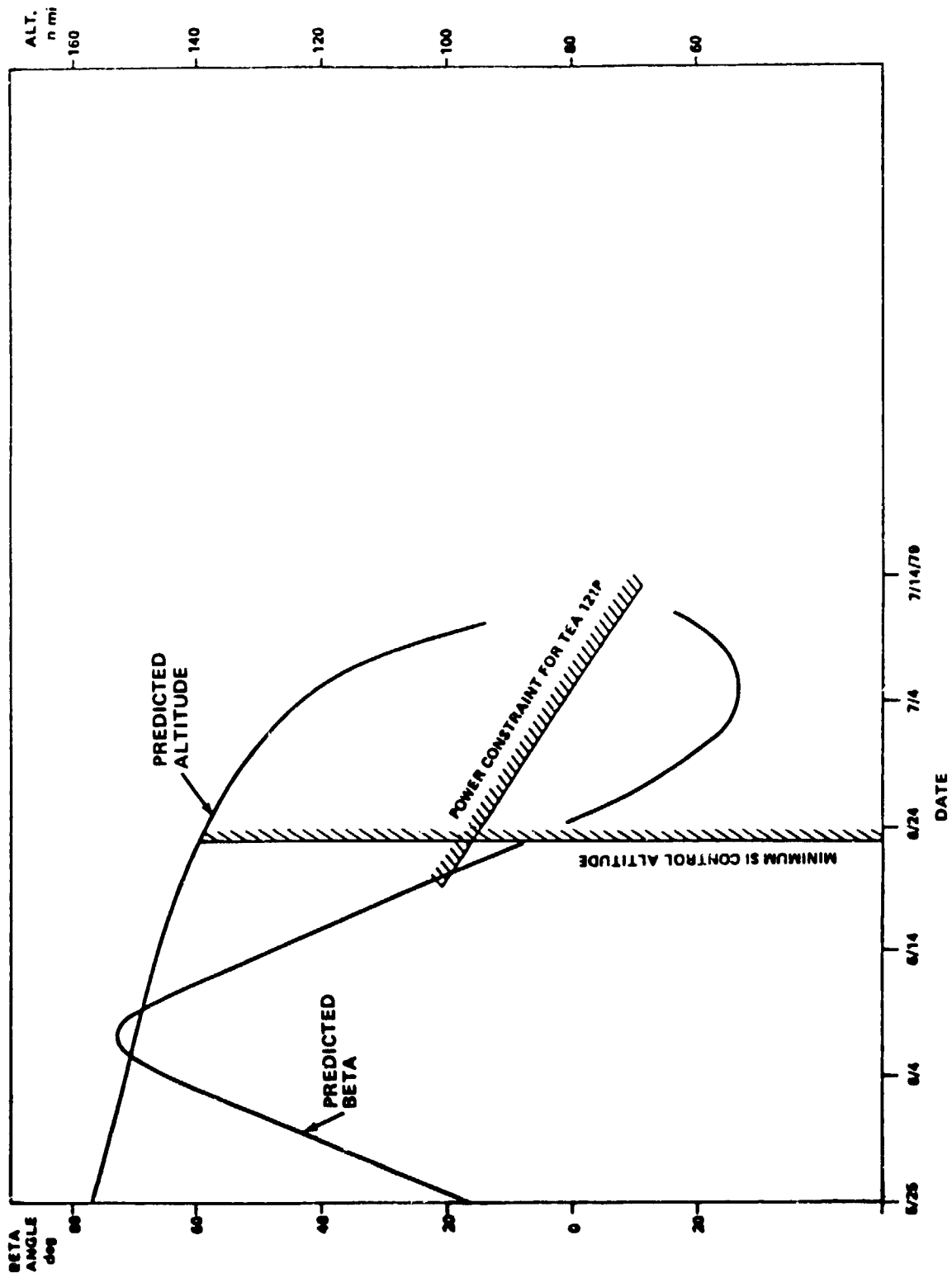
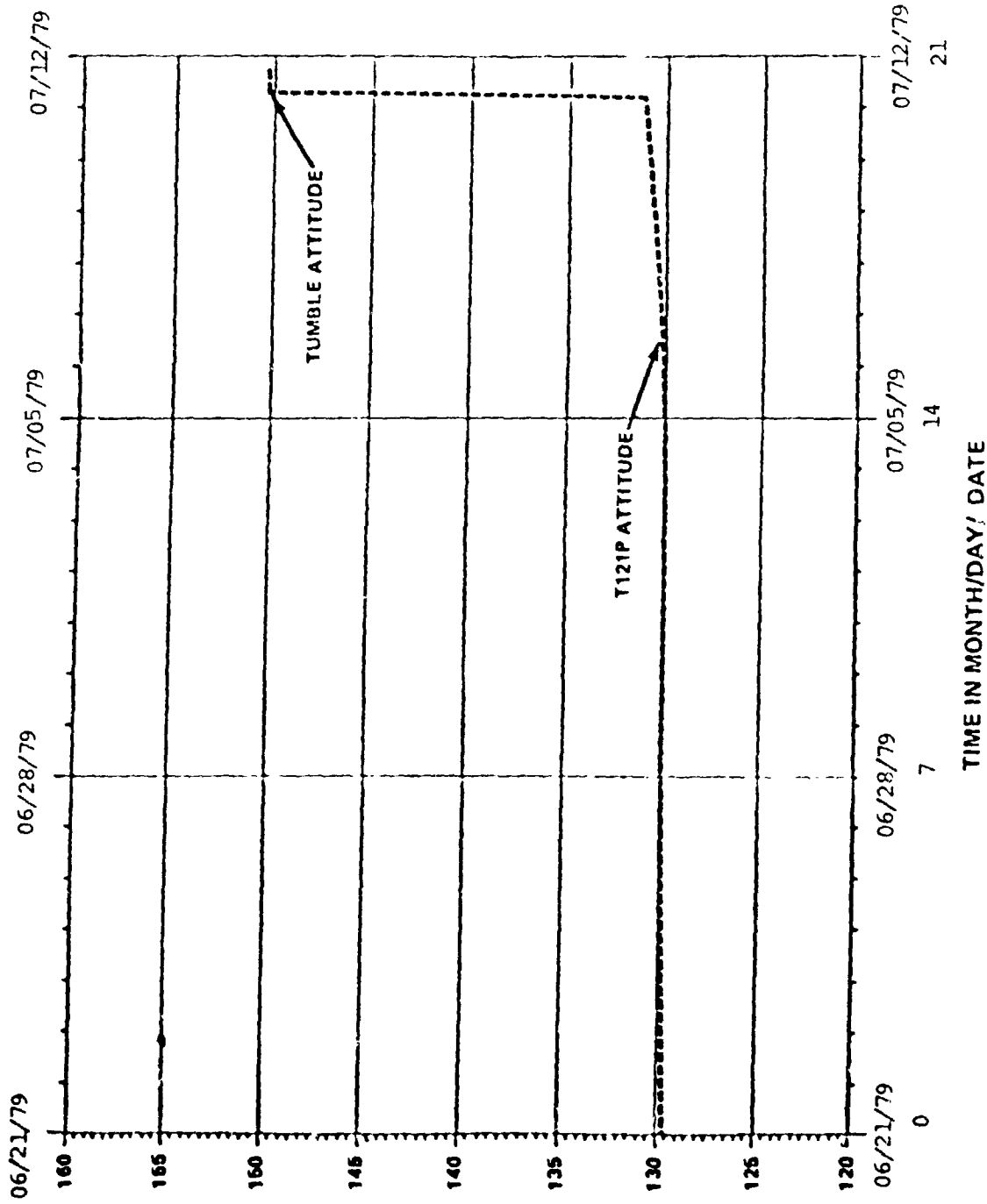
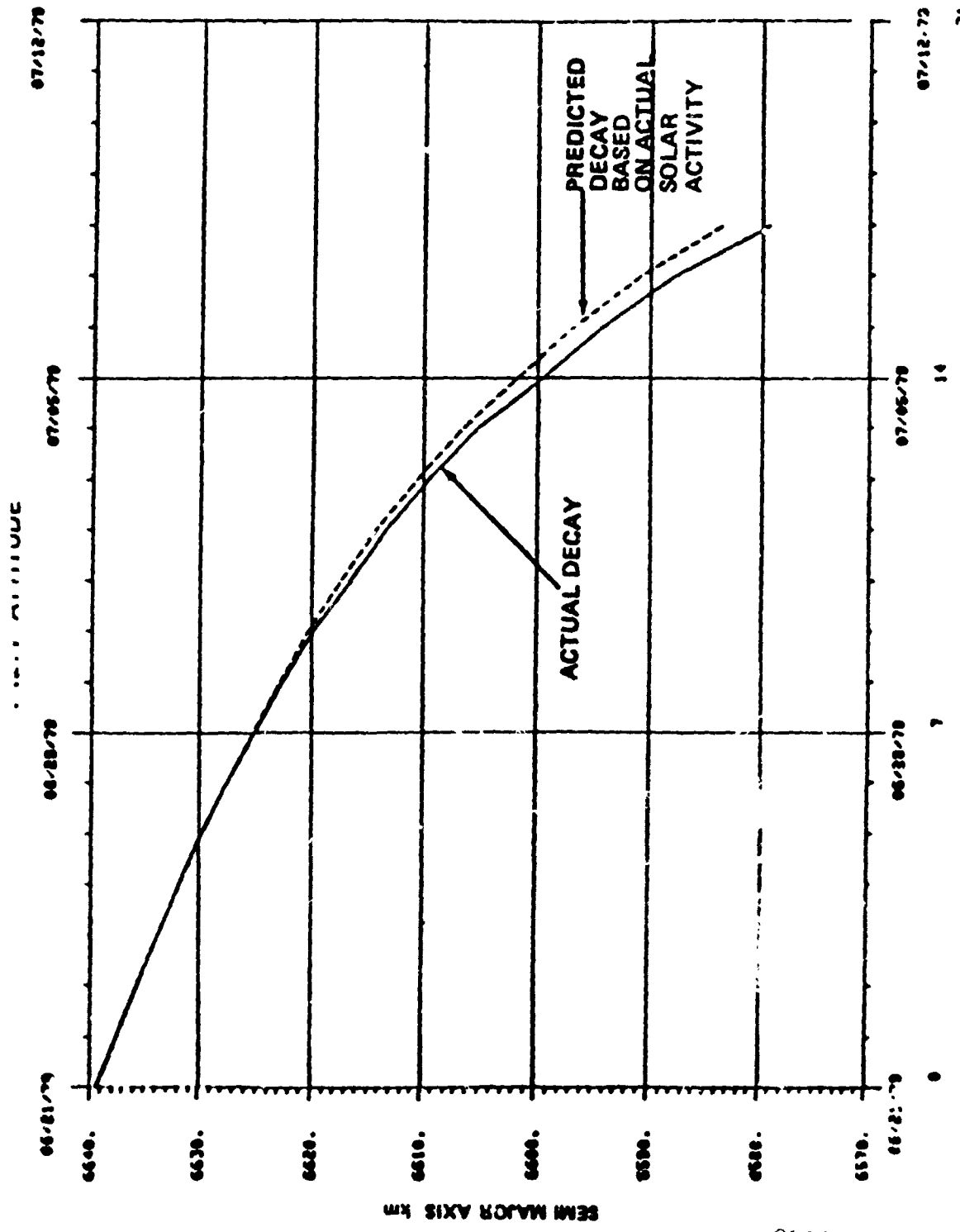


FIGURE 4.3-1 CONSTRAINTS FOR TEA ATTITUDE



T 1 2 1 : B A L L I S T I C C O E F F I C I E N T
 4-38 kg/m²

FIGURE 4.3-2
 T121 BALLISTIC COEFFICIENT VS DATE



21

NOTE: EARTH RADIUS IS ~ 6378

FIGURE 4.3-3
PREDICTED AND ACTUAL DECAY

ORIGINAL PAGE IS
OF POOR QUALITY

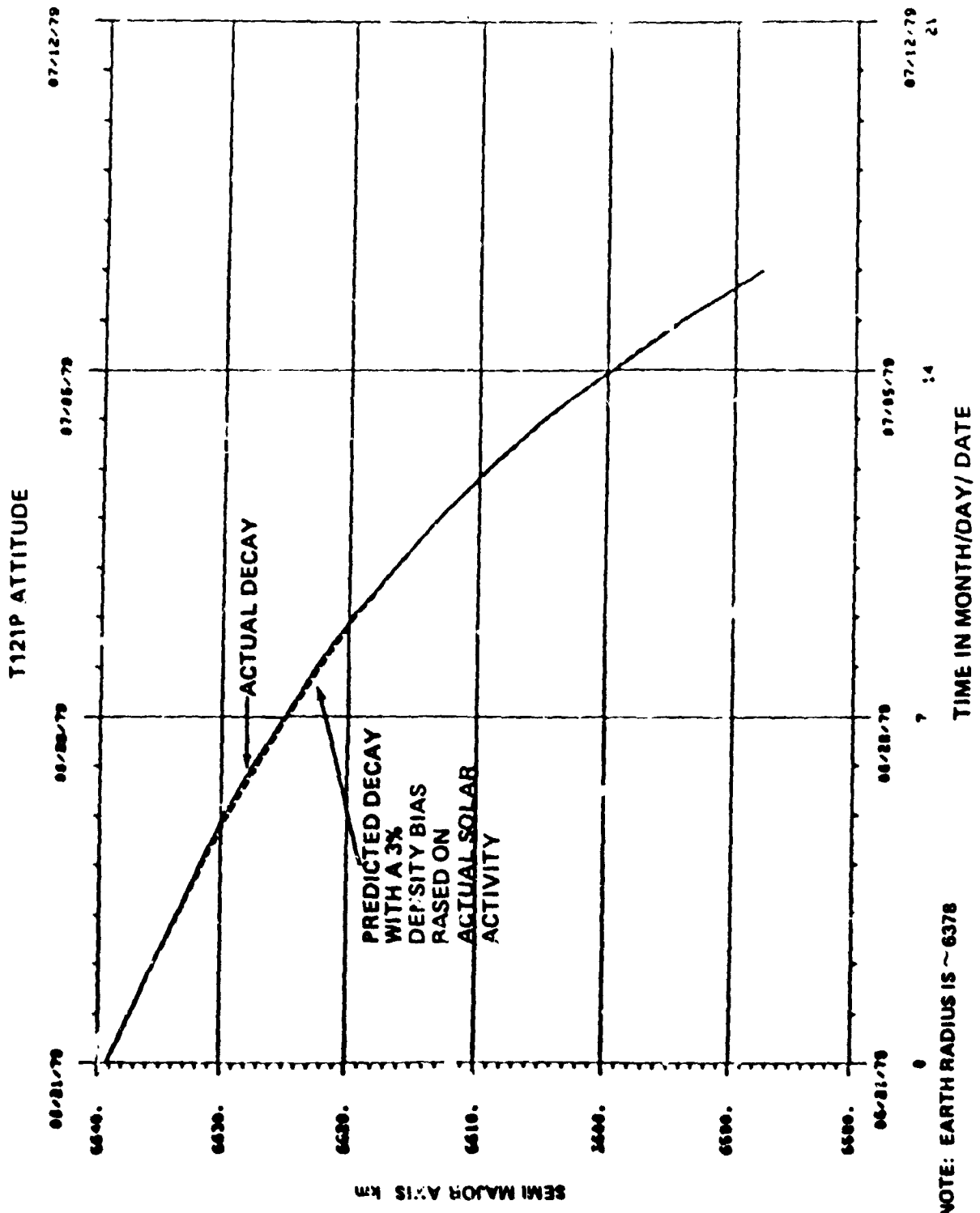


FIGURE 4.3-4 PREDICTED AND ACTUAL DECAY

TABLE 4.3-1 PREDICTED IMPACT DATES USING
SI, 121P AND TUMBLE BC *

| Vector Date | Impact Date |
|-------------|-------------|
| 5/25/79 | 7/09/79 |
| 5/29/79 | 7/09/79 |
| 5/30/79 | 7/10/79 |
| 5/31/79 | 7/10/79 |
| 6/04/79 | 7/10/79 |
| 6/05/79 | 7/10/79 |
| 6/06/79 | 7/10/79 |
| 6/07/79 | 7/10/79 |
| 6/08/79 | 7/10/79 |
| 6/11/79 | 7/10/79 |
| 6/12/79 | 7/10/79 |
| 6/13/79 | 7/09/79 |
| 6/14/79 | 7/09/79 |
| 6/15/79 | 7/09/79 |
| 6/18/79 | 7/09/79 |
| 6/19/79 | 7/10/79 |
| 6/20/79 | 7/10/79 |
| 6/21/79 | 7/10/79 |
| 6/22/79 | 7/10/79 |

*NOTE: SI until June 21, 1979, T121P until 80 nmi, and
Tumble thereafter.

5. SKYLAB REENTRY (July 11, 1979)

5.1 DRAG MODULATION TO CONTROL REENTRY

With the decision to discontinue the effort to extend Skylab's orbital lifetime, a plan evolved to maintain vehicle control in various attitudes as a function of altitude, since lower altitudes resulted in a different aerodynamic drag effect on the vehicle. By changing the vehicle's attitude at pre-selected times, its orbital decay rate could be increased or decreased as necessary to insure that the reentry of Skylab occurred on an orbit characterized by a low population density. For example (1) if it was desired to extend vehicle lifetime a multiple number of revolutions, the vehicle could be maneuvered from the high drag TEA attitude to the low drag TEA attitude reducing the drag approximately 50% (holding the low drag attitude for 12 revolutions resulted in a lifetime extension of approximately 6 revolutions); (2) a maneuver to effect a tumble during the terminal phase of decay (below about 85 nmi to 75 nmi) reduced the drag by approximately 15% for a lifetime extension of up to one revolution; and (3) continued control in a high drag attitude in conjunction with a tumble (approximately 70 nmi) reduced orbital lifetime by up to one revolution. In the actual mission, option (2) was successfully executed at about 81 nmi.

5.1.1 PROCEDURES

The procedures used in real time were: first, determine the predicted longitude of the ascending node, time, and impact position of the reentry orbit; second, estimate the uncertainty in this impact point and time and the associated population hazard; and third, apply previously established mission rules to help establish a NASA Headquarters' "veto" or approval of any proposed maneuver. Decisions were to be based largely on the initial values of the population hazard, on the predicted revolution of impact, and the reduction of that hazard afforded by implementing a maneuver to alter the aerodynamic drag on the vehicle and thus shifting the revolution of impact. Ground rules for implementing the maneuver were: (1) if the revolution of impact was such that a substantial reduction of risk to the world population occurred, the planned maneuver would be implemented unless vetoed within a preset time; (2) if the impact orbit population hazard was low but the impact point (and its associated footprint) endangered a populated area, approval was required to implement a maneuver to shift the impact footprint. Technically, the procedures varied slightly depending on the maneuver selected. For the low drag attitude multiple revolution shift maneuver, the plan was to determine the number of revolutions

required to reduce the population hazard without danger of shifting the impact revolution to one of high population density. With this accomplished, it was then desirable to place the predicted impact point over the maximum amount of water on the impact revolution such that the nominal center of the footprint (heavy pieces at the front end of the footprint) was centered in water. This established the preliminary maneuver time and duration. Final calculations precisely determined the maneuver time and duration. A final recommendation was then to be made to implement the maneuver which would be done automatically unless overruled by NASA Headquarters. For the tumble maneuver, only a small specified population area was to be protected by shifting the predicted impact point and its nominal footprint to an ocean impact. To implement this plan required NASA Headquarters' approval. In the actual situation, this was the procedure used.

The decision criteria for determining what data should be used to plan and implement the final maneuver went as follows. Based on historical NORAD statistical data, the state vector which appeared to correlate most solidly with the actual determination of final impact was the T-24 hour vector. Less satisfactory fits resulted with the T-12 hour vector. With the data available from Skylab decay history since 1974, the vehicle drag coefficients and associated ballistic terms for the uncontrolled tumble, end-on-velocity-vector (EOVV), solar inertial (SI), and torque equilibrium (TEA) attitudes were determined. Also based on the results of a simulation performed during the decay of object #5644 (NORAD numbering system), the significance of the phenomena of transition from free molecular to continuous aerodynamics as altitude decreased was established. The phenomena was significant for Skylab reentry determination. Figure 5-1 shows the reduction (ratio) of the drag coefficient as altitude decreases. The ratio is for C_D with transitional aerodynamic effects considered to C_D without considering transition aerodynamics. The transition from free molecular aerodynamics was predicted to start at 90 nmi and to be continuous aerodynamics by 60 nmi. This effect gradually increased the BC by 20%, with the major effect occurring before 65 nmi, and extended predicted impact time by as much as 1 hour and 10 minutes.

The impact time results from the T-18 and T-12 hour vectors as compared to the T-24 hour vector established an uncertainty of impact of ± 25 min ($\pm 1/4$ revolution). Based on these results, the time to initiate the tumble was selected to place the predicted impact point plus the $\pm 1/4$ revolution

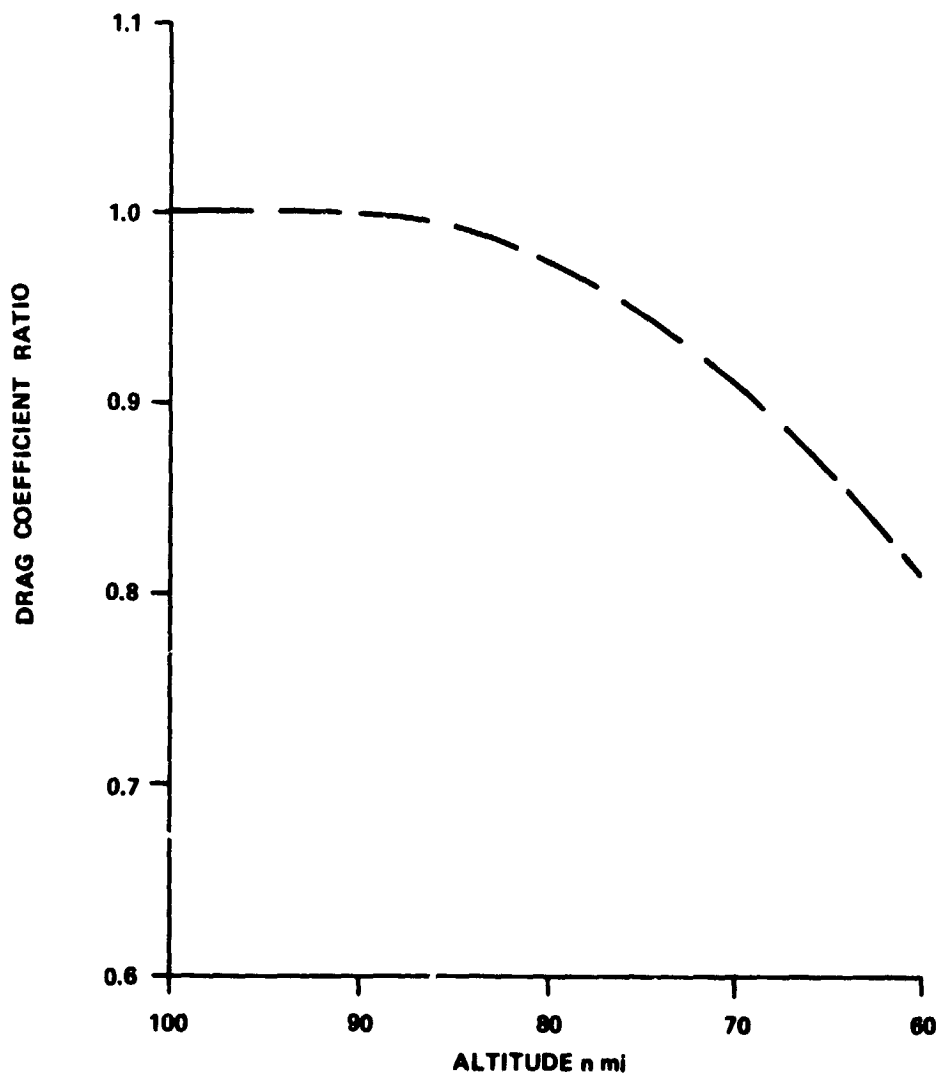


FIGURE 5-1 TRANSITION AERODYNAMICS

uncertainty in the South Atlantic, based on the T-24 hour vector. The time selected was 7:45 GMT July 11, 1979.

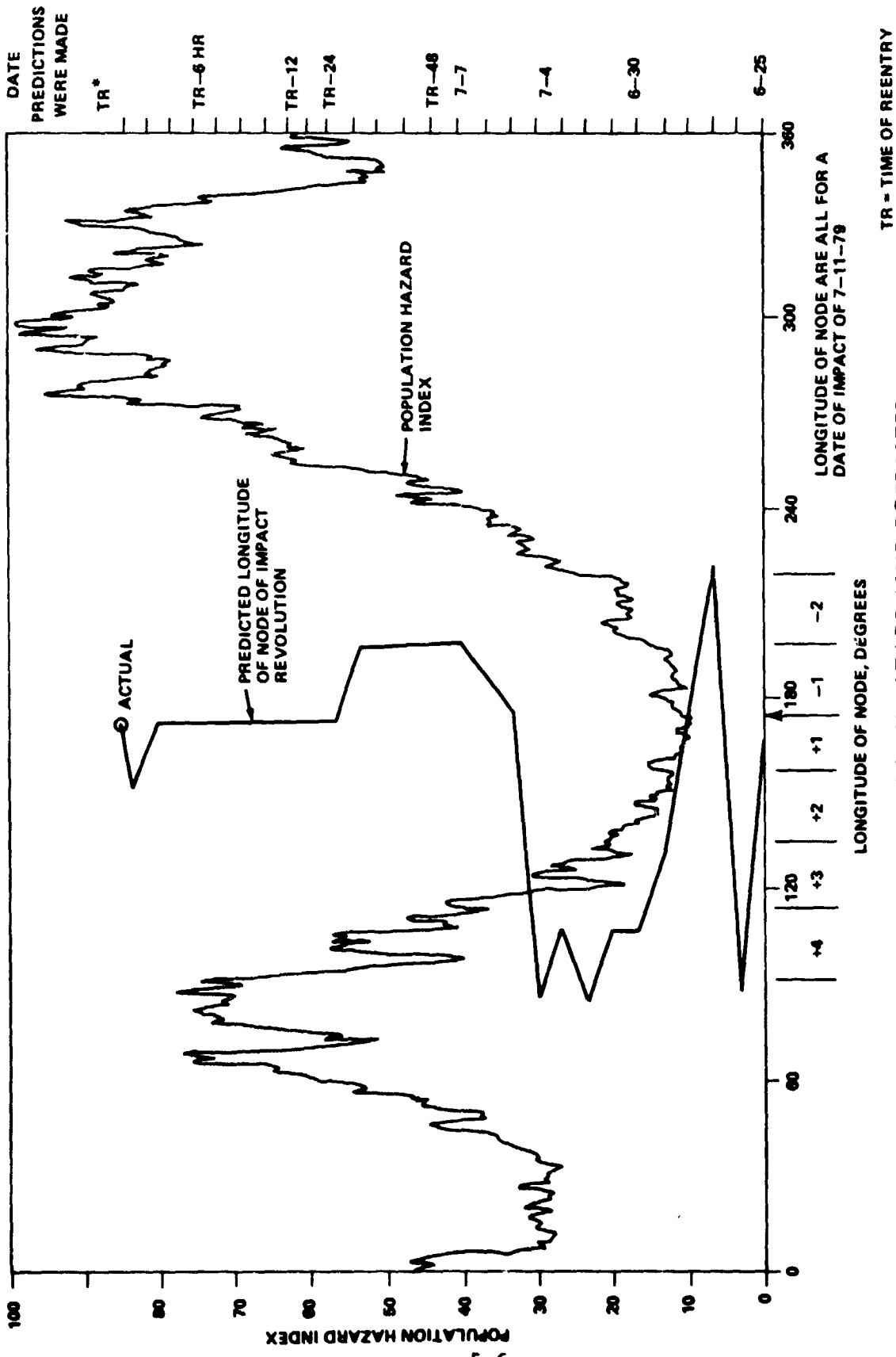
5.1.2 RESULTS

Table 5-1 shows a summary of the projected times, latitude, and longitude of impact (approximately the forward end of the footprint) from 72 hours prior to impact until 1 hour prior to impact. Figure 5-2 shows the population hazard versus the longitude of the ascending node for the revolution of impact. To evaluate this data, note that a 22.2 degree delta in node results in a shift of one revolution or about 88 minutes. On the right is shown the date that the predictions were made starting with June 25, 1979. All cases predicted the impact revolution to be on July 11, 1979 but varied from +4 to -2 revolutions until the predictions made on July 5 and subsequent at which time they were within ± 1 revolution. The impact prediction was essentially on the correct revolution from T-24 hours on. This corresponded to the "best" possible revolution of impact denoted by a low hazard index. The hazard index is the ratio of the total population beneath a certain orbit to that lying beneath the revolution of maximum population.

Figure 5-3 shows the impact predictions based on the baseline 75 nmi tumble and the predictions that resulted from the decision to tumble early (81 nmi) for the T-24 hour, T-18 hour, and T-12 hour vectors. As shown in Figure 5-3, the predicted impact points for the baseline 75 nmi tumble (with uncertainty) trended toward the United States and Canada. These data points are indicated by circles and spread from the Pacific Ocean (10 min from the west coast) to points just off the east coast (about 5 min from the east coast). Taking into account the debris footprint (3500 nmi behind these points), this indicated a relatively large population area had a high probability of being impacted by Skylab debris. After the planned maneuver, the impact area (shown by dots) was shifted to the Indian Ocean (T-24, T-18, T-12) with a slight probability of an Australian impact. Additionally, the population density over that portion of Australia was very low indicating that if an overshoot occurred, there would be very little risk to the population.

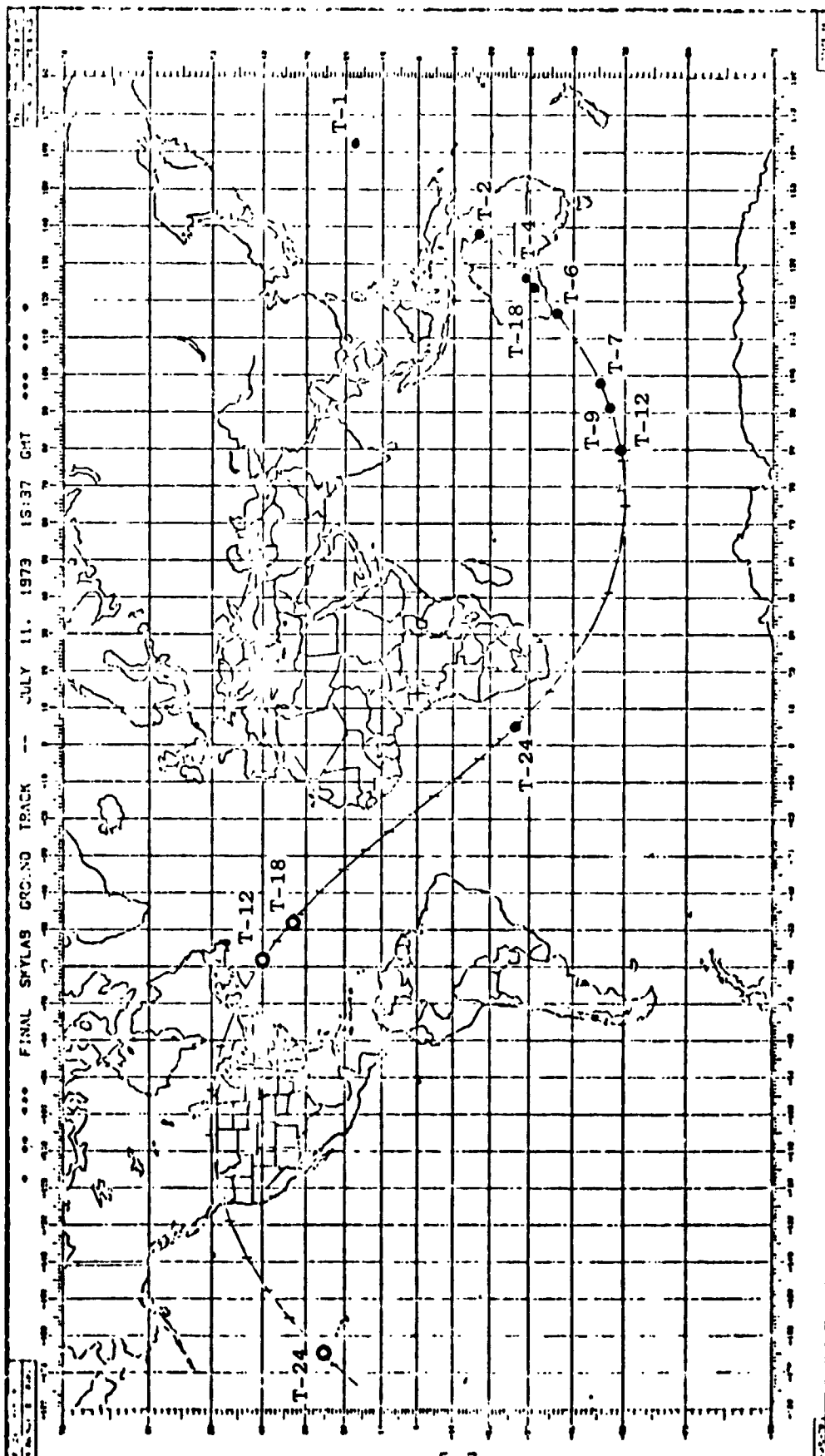
TABLE 5-1 IMPACT PREDICTIONS FOR JULY 11, 1979

| Date of Vector | Time of Vector (GMT) | Time of Estimate (Hours) | Impact Time (GMT) | Impact Location | |
|----------------|----------------------|--------------------------|-------------------|-----------------|------------|
| | | | | LAT (Deg) | LONG (Deg) |
| 7/7 | 13:16:56 | T-72 | 15:06:51 | 37.0 S | 139.5 E |
| 7/8 | 16:30:52 | T-48 | 13:53:20 | 4.5 N | 201.1 E |
| 7/8 | 20:31:19 | T-42 | 13:55:01 | 10.0 N | 205.3 E |
| 7/10 | 3:02:54 | T-36 | 15:06:49 | 37.8 S | 138.2 E |
| 7/9 | 15:33:04 | T-30 | 14:49:50 | 40.3 S | 47.9 E |
| 7/10 | 14:42:06 | T-24 | 15:27:30 | 23.2 N | 194.3 E |
| 7/10 | 19:31:12 | T-18 | 15:52:15 | 34.6 N | 311.8 E |
| 7/11 | 2:53:40 | T-12 | 15:50:12 | 39.5 N | 304.1 E |
| 7/11 | 4:27:53 | T-9 | 16:31:28 | 44.2 S | 102.7 E |
| 7/11 | 6:53:25 | T-7 | 16:33:03 | 41.0 S | 110.0 E |
| 7/11 | 10:03:49 | T-6 | 16:35:04 | 36.4 S | 118.1 E |
| 7/11 | 11:24:35 | T-4 | 16:37:39 | 29.6 S | 127.2 E |
| 7/11 | 12:45:43 | T-2 | 16:42:16 | 16.1 S | 140.4 E |
| 7/11 | 14:16:45 | T-1 | 16:52:44 | 16.7 N | 166.2 E |



TR - TIME OF REENTRY

FIGURE 5-2 POPULATION HAZARD (AND PREDICTED LONGITUDE OF ASCENDING NODES)



- PREDICTIONS ASSUMING TUMBLE AT 75 nmi (INDUCED TUMBLE AT 11:35 GMT) BEFORE DECISION TO TUMBLE AT 7:45 GMT
- PREDICTIONS AFTER DECISION TO TUMBLE AT 7:45 HRS GMT (81 nmi)

FIGURE 5-3
 MAP OF REAL TIME RESULTS
 OF IMPACT PREDICTION

5.2 POSTFLIGHT ANALYSIS

5.2.1 RECONSTRUCTION PROCEDURES

Data has been analyzed to reconstruct a best estimate of what actually occurred, based on observations after the decision was made to tumble at 81 nmi and what possibly would have occurred if the tumble had been postponed until the 75 nmi altitude had been reached. The reconstruction procedure for Skylab decay was complex due to the extreme sensitivity that very small deviations in the observed data has on moving the impact point by a large amount. The data (and uncertainty) and sources used for this analysis were as follows:

- o Actual Solar Flux Data ($\pm 25\%$) NOAA
- o State Vectors Based on Tracking (± 2 nmi) NORAD
- o Special Altitude/Time Observations NORAD
- o Range/Elevation, Telemetry (± 2 nmi) Ascension Tracking Site
- o Time of Tumble NASA
- o Predicted Aerodynamics and Breakup Sequence NASA

Small uncertainties were associated with the preceding data. For example, the actual solar flux data was an estimate provided by NOAA of the final solar flux data which was not available at the time the analysis was done. If the data changed by 5%, a three to five-minute change in the impact time could occur. Another example would be to consider the state vector as being off slightly (2 nmi) in altitude. Then up to a 10-minute variation in impact time could occur. Similarly, with the special observation and range/elevation data. Further, in the case of the T-24 hour prediction, a 1% variation in predicted aerodynamics or breakup altitude could easily change the impact point by up to 10 minutes. Finally, it was impossible to separate these errors; therefore, no single data base will give the same impact points when run from each of the different state vectors. The analysis was based on the following assumptions;

- o Use of estimated solar flux data
- o The altitude history as observed should fit reasonably well with the reconstructed predictions.

- o All orbital workshop (OWS) solar array system (SAS) arrays were intact at Bermuda.
- o The OWS SAS arrays were broken before acquisition of signal at Ascension

The assumed Skylab breakup scenario was as follows:

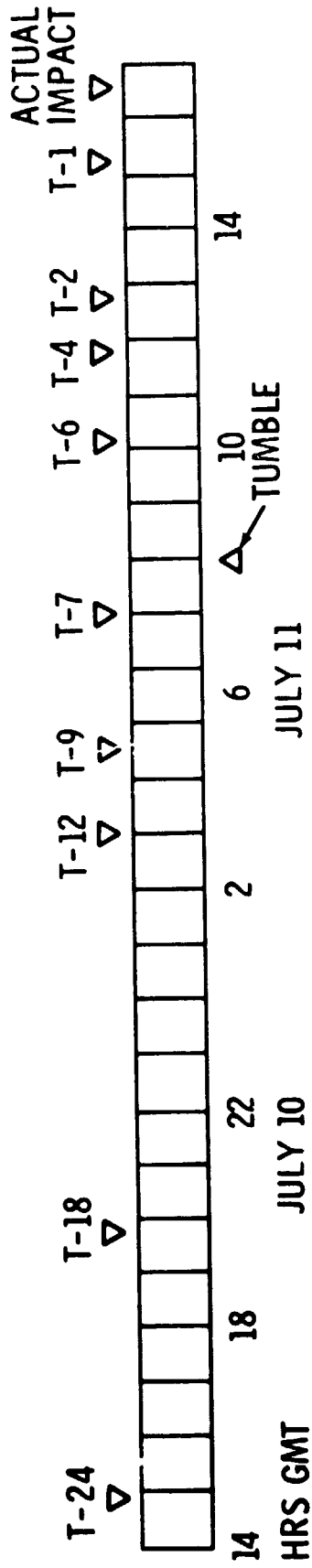
- o The OWS SAS array (aerodynamically) off at 62 nmi.
- o The ATM separates from the remaining OWS at 54 nmi.
- o ATM SAS arrays separate from the vehicle between 54 to 50 nmi.
- o ATM and OWS break up at 42 nmi.

5.2.2 RECONSTRUCTION ANALYSIS

An analysis was conducted to determine the drag and related BC of each of the attitude configuration "nominal" impact points required to match the observed data. First, however, the effect of the revised breakup sequence was evaluated. Figure 5-4 depicts the rationale for this analysis. The upper portion is the timeline showing the times when the NORAD vectors were obtained. There were three attitude configurations which had to be considered: high drag, T121P, tumble, and breakup. Any time/impact predictions based on vectors from T-24 to T-9 required BC's for all three configurations. However, from T-7 to T-1, only tumble and breakup needed to be considered. The T-7 hour case was selected and the effect of the revised breakup sequence was determined; this moved the impact point uprange. The tumble drag coefficient was varied to adjust the T-7 hour impact point to the actual impact point. This required a reduction in the tumble drag coefficient of about 4%. To check the breakup sequence further, these results were used for the sequence and the drag coefficient assumptions for each element. The results of these cases are shown in Figure 5-5 denoted by solid dots. As expected, these two cases moved closer to each other than had been estimated from real time results (Figure 5-3). The T-7 hour vector moved downrange from the Indian Ocean to close to the actual impact point, and the T-1 hour vector moved uprange from an impact north of the equator to the northeast tip of Australia. This indicated that the revised estimate of the tumble drag coefficient and the revised breakup sequence fit quite well.

Having dealt with the tumble and breakup sequence, all that remained was to adjust the T121P high drag coefficient.

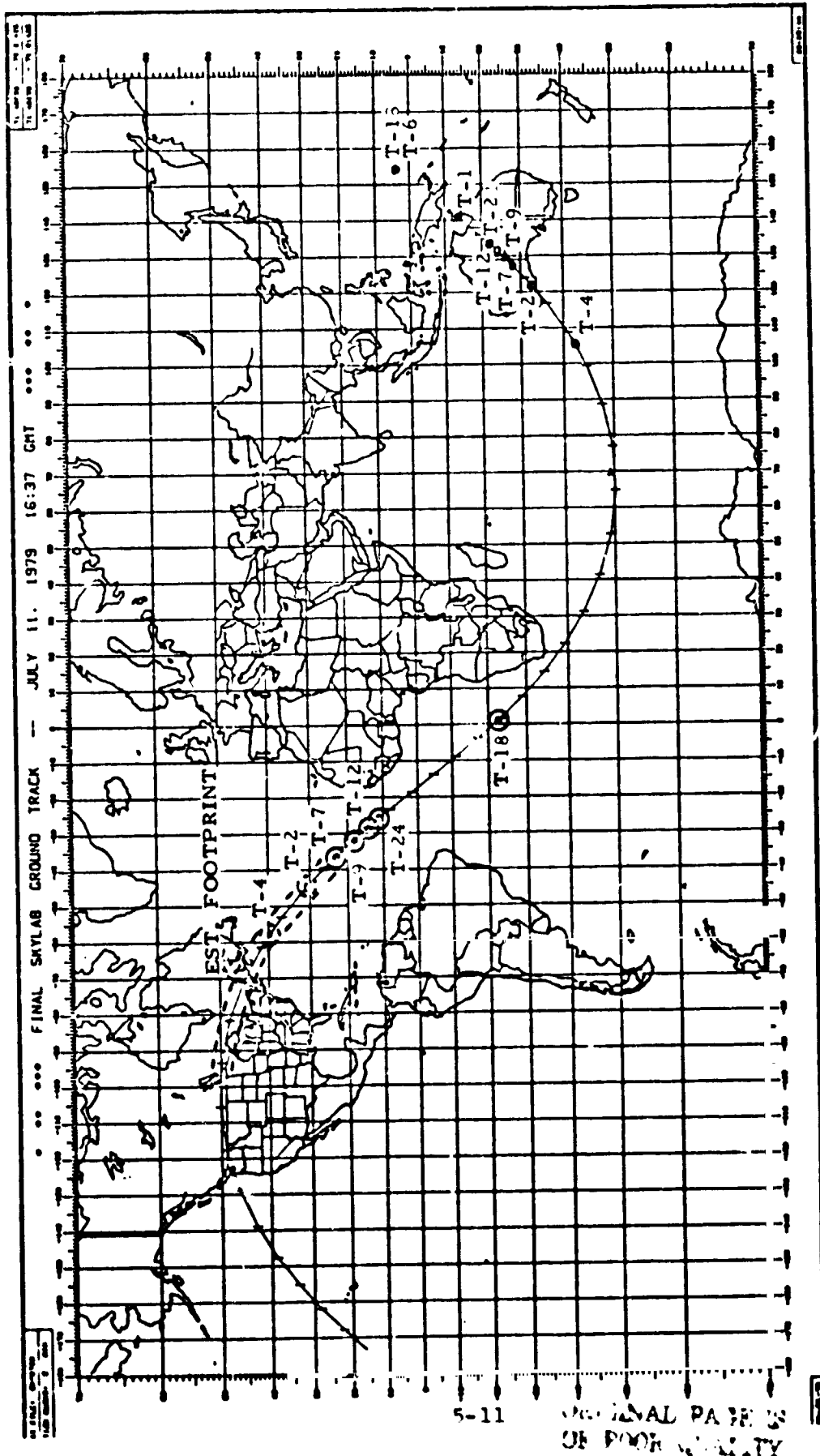
NORAD VECTOR DESIGNATIONS



| | |
|------------------|---------------------------------------------------|
| DRAG IN TEA 12IP | PREDICTED BC = 128.5 REVISED BC = 129.2 (+.5%) |
| DRAG IN TUMBLE | PRED BC = 150 REV BC = 156 (+4%) |

DRAG CONFIGURATIONS

FIGURE 5-4
DRAG/ATTITUDE TIMELINE



- TUMBLE AT 7:45 GMT (81 nmi)
- TUMBLE AT 11:36 GMT (75 nmi)
- ⊗ ESTIMATED RECONSTRUCTION AT 11:36 GMT (75 nmi)

POST FLIGHT RECONSTRUCTION
 FIGURE 5-5
 MAP OF POST FLIGHT RESULTS RECONSTRUCTED IMPACTS

Using the T-12 hour vector, the drag coefficient was reduced by 1/2%. These results are shown in Figure 5-5 again resulting in an impact extremely close to the actual impact point for the T-12 hour vector and comparing favorably with all other vectors. The effects of these analyses can be compared with the real time results shown in Figure 5-3. Since the T-7 hour vector prediction provided the best correlation of the analysis to the observed data, the baseline impact point was derived with the T-7 hour vector resulting in the following:

| | MSFC | NORAD |
|----------------|----------------|--------------|
| Time of Impact | - 16:37:37 GMT | 16:37:30 GMT |
| Latitude | - 30 Deg South | 32 Deg South |
| Longitude | - 127 Deg East | 124 Deg East |

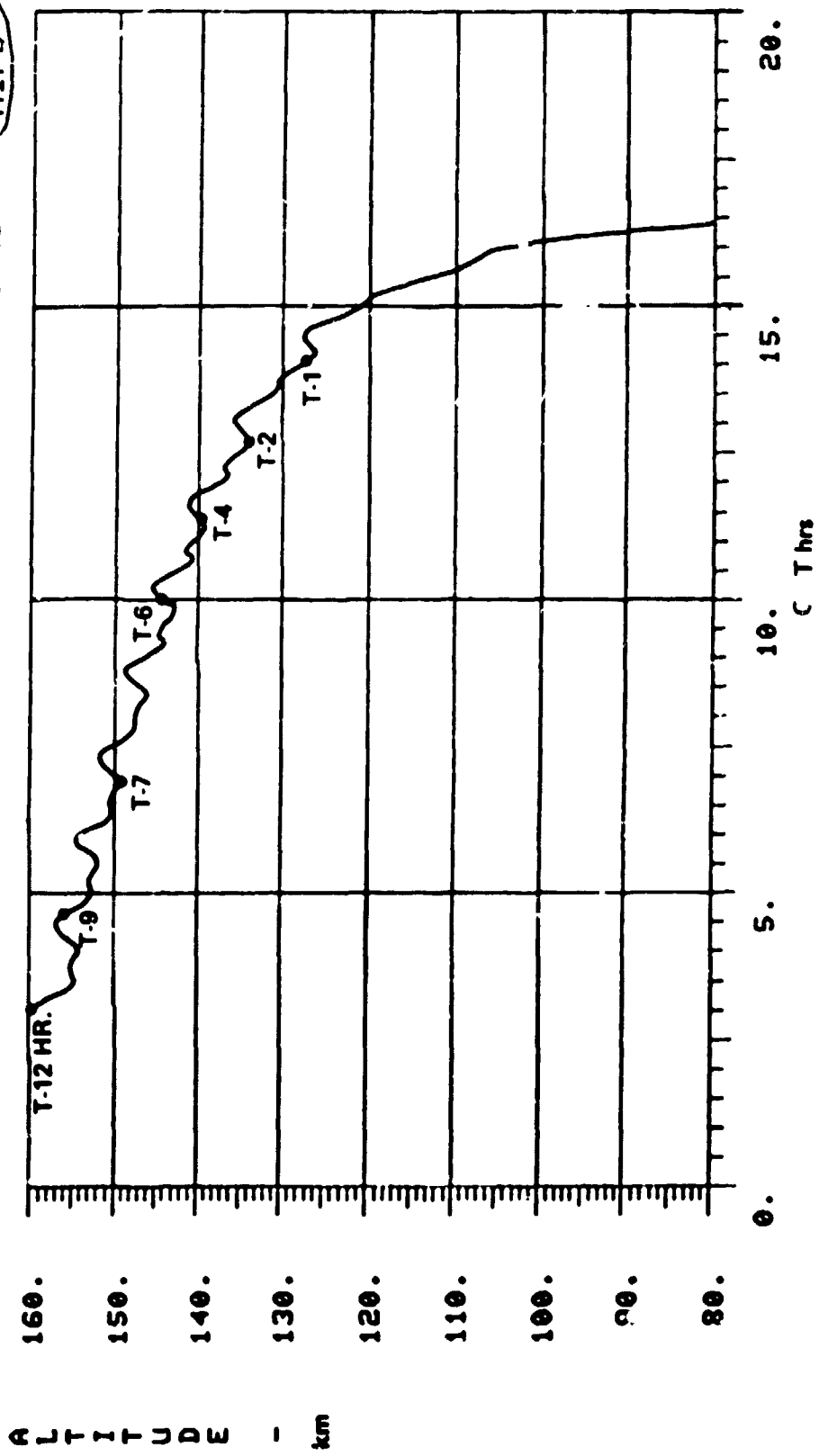
The final NORAD impact point is shown for comparison.

As is seen from Figure 5-5 denoted by solid dots, the entire set of reconstructed predictions fall within a quarter revolution of each other. The altitude fit is shown in Figure 5-6 for several vectors, from T-12 to T-1. The data was very close to the observed altitude.

The last set of data generated shows where the impact points would have been for the T-24, T-12, and T-9 state vectors if the baseline 75 nmi (11:35 GMT) tumble had been initiated. These results are shown as clear circles on the ground track in Figure 5-5. These reconstructions of the planned 75 nmi tumble now appear to center about a latitude of approximately 18 degrees north. Also shown are estimates of where the T-2, T-4 hour impact predictions would have been. As can be seen, the predictions are as far uprange as about 46 degrees north latitude. With the extrapolation of the debris footprint, this shows that a significant probability of a United States/Canadian impact still existed after the reconstruction. The reconstructed T-7 hour impact prediction and the estimated T-2 and T-4 hour cases all show significant amounts of debris in the United States and Canada. These results are all well within the estimated uncertainty of $\pm 1/4$ of a revolution. The primary cause of Skylab impacting down range from the nominal impact point was due to the less than expected drag experienced by the vehicle (4% less) during its tumble phase. The lack of this knowledge resulted in the planned time to tumble being earlier than required. In real time it was felt that drag predictions should be accurate to within $\pm 5\%$. In the actual case the drag was predicted to be within 4% of what it actually was. Based on real time data, the decision to tumble at 81 nmi in lieu of waiting until 75 nmi was correct when the accuracy of the data used in making the decision was considered.

MIPS

08/10/79 10:26:49



• NORAD VECTORS AT T-12, T-9,
T-7, T-6, T-4, T-1

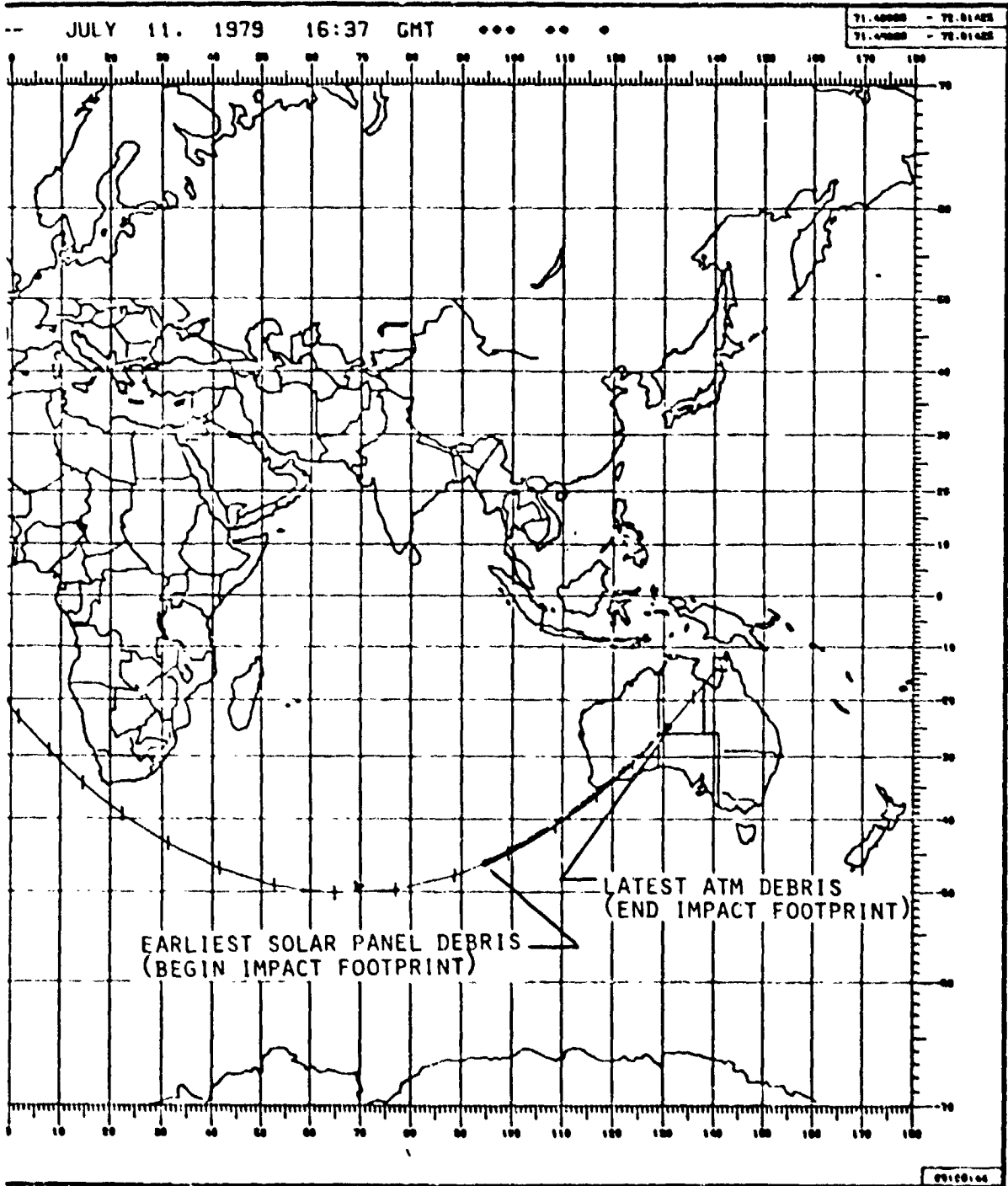
FIGURE 5-6 RECONSTRUCTED ALTITUDE PROFILE

5.3 IMPACT FOOTPRINT ANALYSIS

Figures 5-7 and 5-8 show a summary of the results of the footprint analysis of Skylab debris. A more detailed analysis is presented in Reference 14. This analysis was based on the following data:

1. Special Perturbations Vector at T-2 hr.
2. Altitude at Ascension overflight = 57 nmi
(derived from elevation and range)
3. OWS arrays still attached but aerodynamically off (i.e., folded back or dangling at 62 nmi all arrays off at 54 nmi)
4. Special altitude observations by NORAD
5. Location of pieces in Australia
 - a. Oxygen Tanks at 31.15 degrees South, 125.3 degrees East.
 - b. Water Tanks at 33.8 degrees South, 122.05 degrees East.
 - c. Heat Exchangers at 33.75 degrees South, 122.1 degrees East

As shown in Figure 5-7, this footprint extends from 46.9 degrees South 94.4 degrees East to 26.0 degrees South, 131.2 degrees East (about 2140 nmi). Figure 5-8 provides additional detail of the footprint showing the location of pieces which were found and identifying where major elements are predicted to be located. The OWS/Cluster and AM pieces are centered around 32 degrees South, 124 degrees East, and the ATM pieces are predicted to be centered around 28.5 degrees South, 128.5 degrees East. The observed impact footprint compared favorably to that predicted at the T-2 and T-4 hour impact prediction times and was within $\pm 1/4$ orbit of all predictions made from 18 hours to one hour prior to impact. The overall best impact prediction (T-7) and the NORAD final impact point are denoted.



46.90S, 94.40E TO 260S, 131.10E
 2100 NMI (2450 STATUTE MI)
 ARRAYS OFF AT 54 NMI

MAP OF FOOTPRINT

FIGURE 5-7

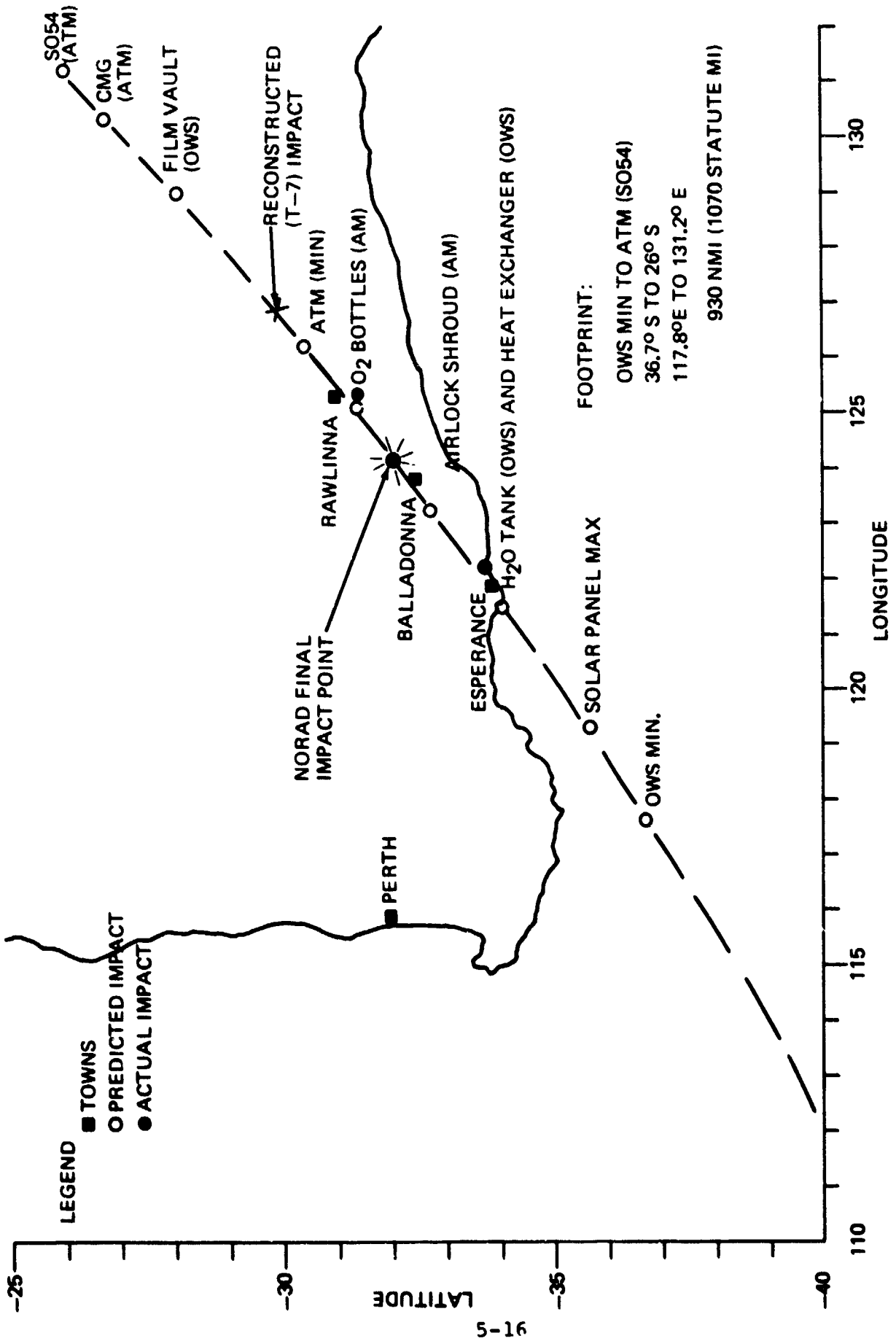


FIGURE 5-8 DETAILED MAP OF FOOTPRINT

6. SUMMARY AND CONCLUSIONS

The last preflight prediction showed a range of the time of impact from November 1977, for a $+2\sigma$ atmospheric density, to June 1982, for a -2σ atmospheric density, with the nominal being October 1979. Considering the many changes during Skylab's orbital life, this prediction made 7 years earlier was very close to the July 11, 1979 impact.

One of the primary factors influencing orbital lifetime is the solar activity prediction. This is the reason ranges based on statistical data are given, rather than an answer. This approach is usually adequate unless a Skylab comes along, and then we would conclude that much additional work should be done on short (<1 year) to intermediate (1 to 5 years) solar activity predictions.

Skylab's reactivation and reentry control planning demanded a degree of accuracy in orbital lifetime predictions which was beyond the state-of-the-art. Prediction of Skylab's lifetime was a complex and non-determinate task which continually required updating as new data was available. However, Skylab provided a unique opportunity to develop, confirm, and check out procedures and computer programs which were used to predict lifetime and reentry, as well as influence its orbital decay and final reentry time and location.

It also provided verification of aerodynamic environment which had been predicted in several aerodynamic configurations. This, in turn, provided excellent data on the atmospheric density model's reaction to rapidly changing Solar Flux over relatively short periods of time and how to better account for this in future predictions. A summary of this is shown here;

| | <u>Reconstructed BC</u> | <u>Theoretical BC</u> |
|-----------------------------------------|----------------------------------|--------------------------|
| Passive Period (2/74 - 6/9/78) | | (Dynamic Simulation) |
| (8/74-1/77 Near GG) | 130 | 101-114 |
| (1/77-11/77 Transition) | 130 | N/A |
| (11/77-6/78 Tumble) | 130 | 150 average (135-160) |
| Various Attitudes (6/9/78 - 7/25/78) | N/A | See Figure 4.1-6 |
| EOVV (7/25/78 - 1/25/79) | 294 average (6% density bias) | 313 average (303-333) |

Reconstructed BC Theoretical BC

SI (1/25/79 - 6/20/79)

(1/25/79 - 5/24/79)

127 average
(18% density
bias)

155 average
(140-220)

As can be seen, generally the predicted aerodynamics were quite good.

The density bias that causes an apparent change in the BC seems to vary with the solar activity. This is under further study and will be covered in Reference 10.

Attitude control in the EOVV attitude effectively reduced the orbit decay such that Skylab remained in orbit 3½ months longer than if the EOVV attitude had not been utilized. This verified predictions made during the planning for the extension of Skylab's lifetime. It is further estimated that Skylab would have remained in orbit 6 - 9 months longer had the EOVV attitude been maintained to or near impact.

Finally, procedures for modulating the Skylab's drag to impact with minimum risk to the earth's population were developed and successfully executed, moving the actual impact point by approximately half a revolution.

LIST OF ACRONYMS

| | |
|-------|-------------------------------------------------|
| AM | Airlock Module |
| AR | Array Rotated |
| ASO | Array Solar Oriented |
| ATM | Apollo Telescope Mount |
| BC | Ballistic Coefficient |
| EOVV | End-On-Velocity Vector |
| GG | Gravity Gradient |
| GMT | Greenwich Mean Time |
| LM | Lunar Module |
| LTIME | Orbital Lifetime Prediction Program |
| NOAA | National Oceanic and Atmospheric Administration |
| NORAD | North American Air Defense Command |
| OWS | Orbital Workshop |
| SAO | Smithsonian Astrophysical Observatory |
| SAS | Solar Array System |
| SI | Solar Inertial |
| TEA | Torque Equilibrium Attitude |
| T121P | A High Drag TEA with 121 BC |

REFERENCES

1. Liu, J. J.; A Second-Order Theory of an Artificial Satellite Under the Influence of the Oblateness of Earth. Northrop - Huntsville M-240-1203, January 1973.
2. Alford, R. L. and Liu, J. J.; The Orbital Decay and Lifetime Prediction Program. Northrop - Huntsville M-240-1278, May 1974.
3. The U.S. Standard Atmosphere, 1962, December 1962.
4. Jacchia, L. G.; New Static Models of the Thermosphere and Exosphere with Empirical Temperature Profiles. Smithsonian Astrophysical Observatory Special Report No. 313, 1970.
5. Models of Earth Atmosphere (90 to 2500 km). NASA SP-8021, March 1973.
6. Johnson, J. D.; Orbital Aerodynamic Data for the AAP Configuration Consisting of the OWS with the Docked LM/ATM and the OWS Panels Aligned Parallel to the OWS Longitudinal Axis. S&E-AERO-AD-69-21, April 1969.
7. Johnson, J. D.; Orbital Aerodynamic Data for the Skylab Cluster Configuration With and Without the Docked CSM. S&E-AERO-AA-70-21, March 1970.
8. Johnson, J. D.; In-Orbit Aerodynamic Data for the Skylab Orbital Assembly Configuration With and Without the Docked CSM. S&E-AERO-AA-71-25, March 1971.
9. Grahame, W. E.; Orbital Aerodynamic Data for the Updated Skylab I In-Orbit Configuration. Northrop - Huntsville M-9230-73-197, July 1973.
10. Little, R. P. and Dreher, P. E.; Orbital Decay and Density Analysis (unpublished).
11. Buchanan, H.; Hopkins, M.; and Galaboff, Z; Uncontrolled Dynamics of the Skylab Vehicle, AIAA Paper January 1980.
12. MSFC, SAIL, Skylab Reactivation Mission Report, March 1980.
13. Glaese, J. R. and Kennel, H. F.; Torque Equilibrium Control for Skylab Reentry, NASA TM 78252, November 1979.
14. Varnado, L.; Skylab Reentry and Impact Footprint Reconstruction (unpublished).